

Random Features for Kernel Approximation: A Survey in Algorithms, Theory, and Beyond

Fanghui Liu, Xiaolin Huang, Yudong Chen, Johan A.K. Suykens

Abstract—Random features is one of the most sought-after research topics in statistical machine learning to speed up kernel methods in large-scale situations. Related works have won the NeurIPS test-of-time award in 2017 and the ICML best paper finalist in 2019. However, comprehensive studies on this topic seem to be missing, which results in different, sometimes conflicting, statements. In this survey, we attempt to throughout and systematically review the past ten years work on random features regarding to algorithmic and theoretical aspects. First, the fundamental characteristics, primary motivations, and contributions of representative random features based algorithms are summarized according to their sampling scheme, learning procedure, variance reduction, and exploitation of training data. Second, we review theoretical results of random features to answer the key question: how many random features are needed to ensure a high approximation quality or no loss of empirical risk and expected risk in a learning estimator. Third, popular random features based algorithms are comprehensively evaluated on several large scale benchmark datasets on the approximation quality and the prediction performance for classification and regression. Last, we link random features to current over-parameterized deep neural networks (DNNs) by investigating their relationships, the usage of random features to analysis over-parameterized networks, and the gap in the current theoretical results. As a result, this survey could be a gentle use guide for practitioners to follow this topic, apply representative algorithms, and grasp theoretical results under various technical assumptions. We think that this survey helps to facilitate a discussion on ongoing issues for this topic, and specifically, it sheds light on promising research directions.

Index Terms—random features, kernel approximation, generalization properties, over-parameterized neural networks

1 INTRODUCTION

KERNEL methods [1], [2], [3] are one of the most powerful techniques to tackle nonlinear learning problems in statistical machine learning, including classification [4], regression [5], dimension reduction [6], and clustering [7]. In kernel methods, given any two samples $\mathbf{x}, \mathbf{x}' \in \mathcal{X} \subseteq \mathbb{R}^d$, the inner product of these two mapping vectors in a high-dimensional (or even infinite-dimensional) feature space can be computed by a kernel function $k(\cdot, \cdot) : \mathbb{R}^d \times \mathbb{R}^d \rightarrow \mathbb{R}$ such that

$$k(\mathbf{x}, \mathbf{x}') = \langle \phi(\mathbf{x}), \phi(\mathbf{x}') \rangle_{\mathcal{H}},$$

where $\phi : \mathcal{X} \rightarrow \mathcal{H}$ is a non-linear feature map transforming elements in \mathcal{X} into a reproducing kernel Hilbert space (RKHS) \mathcal{H} . In practice, this inner product is given by the introducing kernel k , a.k.a *kernel trick*, instead of obtaining the explicit formulation of ϕ . Albeit effective, kernel methods often suffer from scalability issues in large-scale problems due to high space and time complexities. For instance, given n samples in the original d -dimensional space \mathcal{X} , kernel ridge regression (KRR) requires $\mathcal{O}(n^3)$ training time and

$\mathcal{O}(n^2)$ space to store the kernel matrix, which appears intractable when n is large.

One of the most popular approaches to scale up kernel methods is random Fourier features (RFF) [8], mainly for shift-invariant kernels satisfying $k(\mathbf{x}, \mathbf{x}') = k(\mathbf{x} - \mathbf{x}')$. By virtue of the correspondence between a shift-invariant kernel (also termed as “stationary”) and its Fourier spectral density, the kernel can be approximated by $k(\mathbf{x}, \mathbf{x}') \approx \langle \varphi(\mathbf{x}), \varphi(\mathbf{x}') \rangle$, where the random Fourier feature mapping $\varphi : \mathbb{R}^d \rightarrow \mathbb{R}^s$ is obtained by sampling from a distribution defined by the inverse Fourier transform of k . Generally, s is larger than d but is much smaller than n . This approximation strategy hence allows us to train an efficient linear predictor in the transformed space \mathbb{R}^s while retaining the power of kernel methods. With s random features, this approximation applied to KRR only requires $\mathcal{O}(ns^2)$ time and $\mathcal{O}(ns)$ memory, and thus achieving a substantial computational saving when $s \ll n$. Therefore, RFF exhibits promising performance on scaling up kernel methods in classification including support vector machines (SVM) [9], regression [10], nonlinear component analysis [11], [12]. More importantly, the random features model can be viewed as a class of two-layer neural networks with fixed weights in the first layer. One hand, it exhibits some “abnormal” phenomena in *over-parameterized* deep neural networks (DNNs) if $s \geq n$, e.g., a good fitness of random labels [13] and double curve descent [14], and thus we can extend theoretical results of random features to analysis two-layer *over-parameterized* neural networks. On the other hand, the random features method serves as an effective implementation way for neural tangent kernel (NTK) [15] associated with an infinite wide neural network in practical uses. Besides, graph neural networks (GNNs) [16] and network pruning, e.g., the lottery ticket hypothesis [17] also utilize random features to support their findings. Hence, random features are powerful in experimental and theoretical aspects to investigate the generalization property of

This work was supported in part by the European Research Council under the European Union’s Horizon 2020 research and innovation program / ERC Advanced Grant E-DUALITY (787960), in part by the National Natural Science Foundation of China 61977046, in part by the National Key Research and Development Project (No. 2018AAA0100702), in part by National Science Foundation grants CCF-1657420 and CCF-1704828. This paper reflects only the authors’ views and the Union is not liable for any use that may be made of the contained information; Research Council KUL C14/18/068; Flemish Government FWO project GOA4917N; Onderzoeksprogramma Artificieel Intelligentie (AI) Vlaanderen programme.

F. Liu and J.A.K. Suykens are with the Department of Electrical Engineering (ESAT-STADIUS), KU Leuven, B-3001 Leuven, Belgium (email: {fanghui.liu;johan.suykens}@esat.kuleuven.be).

X. Huang is with Institute of Image Processing and Pattern Recognition, and also with Institute of Medical Robotics, Shanghai Jiao Tong University, Shanghai 200240, P.R. China (e-mail: xiaolinhuang@sjtu.edu.cn).

Y. Chen is with School of Operations Research and Information Engineering, Cornell University, Ithaca, NY 14850 USA (e-mail: yudong.chen@cornell.edu).

over-parameterized neural networks [18], [19]. According to its remarkable repercussions, on the *Thirty-first Advances in Neural Information Processing Systems* (NeurIPS2017), Rahimi and Recht won the test-of-time award for their seminal work on RFF [8].

RFF spawns the new direction on kernel approximation with a flurry of research papers over the past ten years. In algorithmic aspect, the subsequent works attempt to decrease the kernel approximation error [29], [45], reduce the time and space complexities [33], [34], and improve the predict performance [9], [10], [46]. In theoretical aspect, a series of works aim to mainly address the following two questions:

- 1) how many random features are needed to ensure high quality estimation in kernel approximation?
- 2) how many random features are needed to incur no loss of empirical risk and expected risk in a learning estimator?

Here “no loss” denotes that, if we use an exact kernel estimator, e.g., KRR, as a natural baseline: how large should s be for KRR equipped with s random features to be almost as good as the exact KRR estimator? Many references therein attempt to answer the above questions on kernel approximation error (the first question) [8], [39], or studying the risk and generalization properties (the second question) [9], [10] with more and more refined results. On the *thirty-six International Conference on Machine Learning* (ICML2019), Li et al. [10] won the ICML Honorable Mentions (i.e., the best paper finalist) for their unified theoretical analysis results on RFF.

Although RFF have demonstrated success in numerous tasks and a series of subsequent works are proposed to improve it in algorithm and theory, comprehensive studies on this topic seem to be missing. A lack of comprehensive overview may result in different, sometimes conflicting, statements regarding the effectiveness of various random features methods on real-world problems and the presented theoretical results with some technical/unattainable assumptions. To this end, we need to throughout review the past ten years works on random features in terms of algorithmic and theoretical aspects. Figure 1 presents a brief history of the development of random features in recent years. These works have distinct characteristics such as exploitation of training data, sampling scheme, learning procedure, the used assumptions, asymptotical properties, and so forth. The main contributions of this survey include

- 1) We provide a comprehensive study of a wide range of random features based algorithms in a unifying description framework.
- 2) We throughout summarize a series of theoretical results on approximation error in various metrics, empirical risk and generalization risk of kernel estimators. Specifically, the used assumptions in these results are discussed in details.
- 3) We systematically evaluate and compare representative random features based algorithms under different experimental settings.
- 4) We further discuss random features in over-parameterized neural networks regarding to the relationship, the usage, and the current gap in theoretical analysis. It sheds light on promising research directions.

The remainder is structured as follows. After a presentation of preliminaries in Section 2, we introduce our taxonomy of random features, and review *data-independent* algorithms in Section 3 and *data-dependent* approaches in Section 4. In Section 5, we compare

the theoretical results regarding to uniform approximation and generalization properties in details. Experimental comparisons of the representative random features based methods are performed in Section 6. In Section 7, we give an overview of results on random features extended to neural networks in the over-parameterized regime. We think that it would be a promising research topic for random features. Finally, Section 8 summarizes the conclusions and further directions.

2 PRELIMINARIES AND STRUCTURE

2.1 Notation

In this paper, we denote vectors as boldface lowercase letters, e.g., \mathbf{a} , and matrices as boldface capital letters, e.g., \mathbf{A} , of which elements are a_i and A_{ij} , respectively. The set is denoted by Euler script letters, i.e., \mathcal{A} , and specifically, the set $\{1, 2, \dots, n\}$ is short for $[n]$. Denote \mathbf{I}_n as the $n \times n$ identity matrix, $\mathbf{0}$ as a zero matrix or vector with the appropriate size, and $\mathbf{1}_n$ as the n -dimensional vector of all ones. A d -dimensional sphere is defined as $\mathbb{S}^d := \{\mathbf{x} \in \mathbb{R}^{d+1} \mid \|\mathbf{x}\|_2 = 1\}$.

2.2 Problem settings

In supervised learning, denote $\mathcal{X} \subseteq \mathbb{R}^d$ as a compact metric space of features, and $\mathcal{Y} = \{-1, 1\}$ (in classification) or $\mathcal{Y} \subseteq \mathbb{R}$ (in regression) as the label space, we assume that a sample set $\mathcal{Z} = \{(x_i, y_i)\}_{i=1}^n$ is drawn from a non-degenerate Borel probability measure ρ on $\mathcal{X} \times \mathcal{Y}$. Let $k(\cdot, \cdot)$ be a positive definite kernel function endowed in the Reproducing Kernel Hilbert Space \mathcal{H} , and $\mathbf{K} = [k(\mathbf{x}_i, \mathbf{x}_j)]_{n \times n}$ be the kernel matrix sampled from \mathcal{Z} . The *target function* of ρ is defined by $f_\rho(\mathbf{x}) = \int_{\mathcal{Y}} y d\rho(y|\mathbf{x})$, $\mathbf{x} \in \mathcal{X}$, where $\rho(\cdot|\mathbf{x})$ is the conditional distribution of ρ at $\mathbf{x} \in \mathcal{X}$. In this paper, we consider a learning algorithm generated by a regularization scheme in a RKHS associated with the reproducing kernel k , i.e.

$$f_{\mathbf{z}, \lambda} := \operatorname{argmin}_{f \in \mathcal{H}} \left\{ \frac{1}{n} \sum_{i=1}^n \ell(y_i, f(\mathbf{x}_i)) + \lambda \|f\|_{\mathcal{H}}^2 \right\}, \quad (1)$$

where $\lambda > 0$ is a regularization parameter, which depends on the sample size in learning theory, i.e. $\lambda := \lambda(n)$ with $\lim_{n \rightarrow \infty} \lambda(n) = 0$. Mathematically, we assume $\lambda = n^{-\alpha}$ with $\alpha \in (0, 1]$. Different selections for λ lead to different convergence rates. For example, Li et al. [10] choose $\lambda := n^{-1/2}$ in KRR and $\lambda := 1/n$ in SVM to ensure $\mathcal{O}(n^{-1/2})$ learning rates. The convex loss $\ell : \mathcal{Y} \times \mathcal{Y} \rightarrow \mathbb{R}$ quantifies the merit of the evaluation $f(\mathbf{x})$ at $\mathbf{x} \in \mathcal{X}$, which can be chosen as the squared loss in KRR, i.e., $\ell(y, f(\mathbf{x})) = (y - f(\mathbf{x}))^2$, the hinge loss in SVM, i.e., $\ell(y, f(\mathbf{x})) = \max(0, 1 - yf(\mathbf{x}))$, etc. Accordingly, the empirical risk functional is defined on the sample set, i.e., $\mathcal{E}_{\mathbf{z}}(f) = \frac{1}{n} \sum_{i=1}^n \ell(y_i, f(\mathbf{x}_i))$, and the expected risk is defined as $\mathcal{E}(f) = \int_{\mathcal{X} \times \mathcal{Y}} \ell(y, f(\mathbf{x})) d\rho$. So the goal of a supervised learning task aims to find a good approximation of f_ρ by $f_{\mathbf{z}, \lambda}$ by some delicate algorithms. And in the theoretical aspect, a series works attempt to study the generalization properties by giving the upper bound of $\mathcal{E}(f_{\mathbf{z}, \lambda}) - \mathcal{E}(f_\rho)$, or $\|f_{\mathbf{z}, \lambda} - f_\rho\|$ in some metric spaces.

When using random features, the kernel function $k(\mathbf{x}, \mathbf{x}')$ can be approximated by $k(\mathbf{x}, \mathbf{x}') \approx \tilde{k}(\mathbf{x}, \mathbf{x}') = \langle \varphi(\mathbf{x}), \varphi(\mathbf{x}') \rangle$ with an explicit feature mapping $\varphi : \mathbb{R}^d \rightarrow \mathbb{R}^s$. In this case, the approximated kernel $\tilde{k}(\cdot, \cdot)$ is associated with a RKHS $\tilde{\mathcal{H}}$ (not

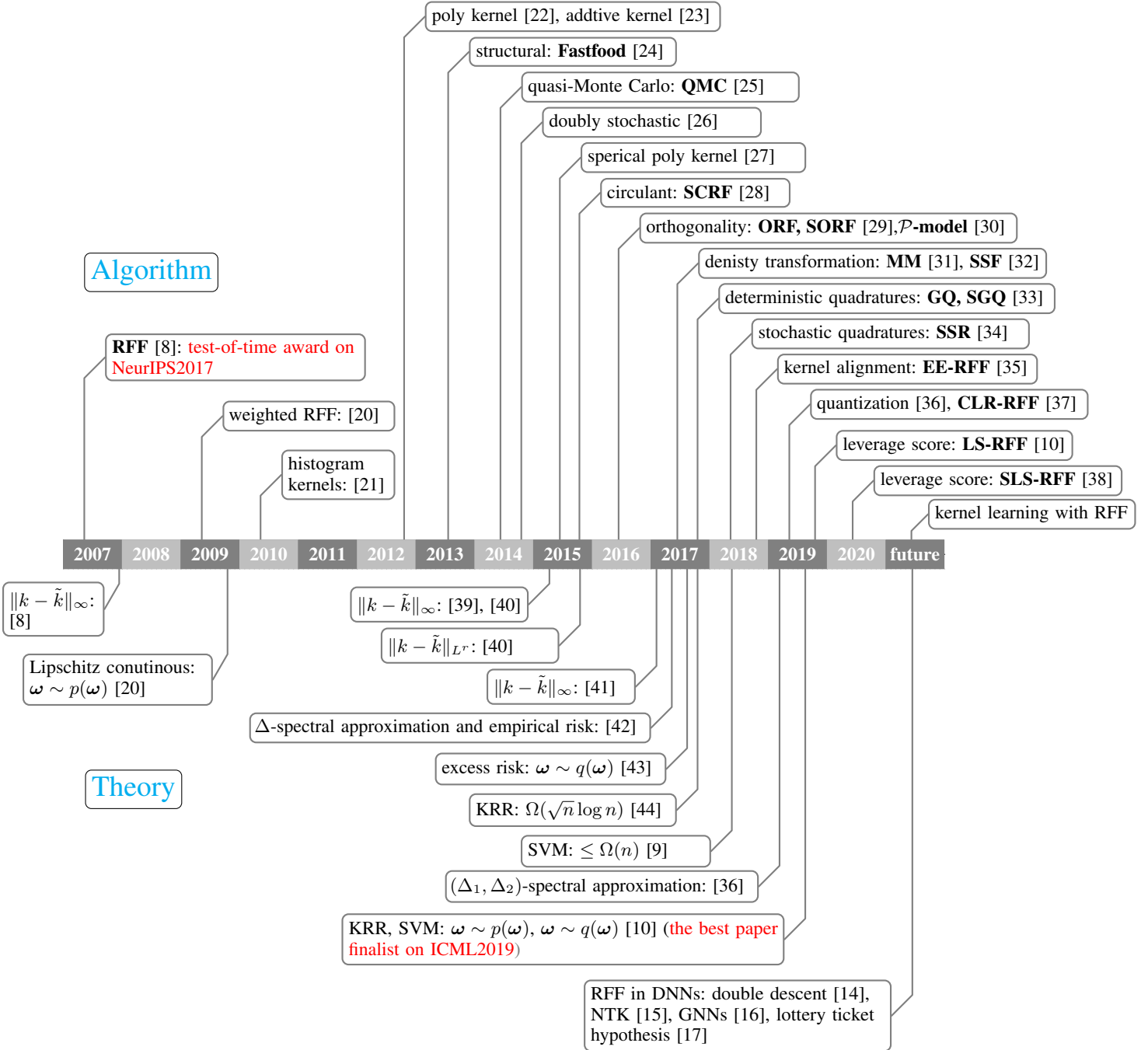


Figure 1. Timeline of representative random features in algorithmic and theoretical aspects.

necessarily contained in \mathcal{H} corresponding to the kernel function k). Using random features, problem (1) can be reformulated as

$$\widetilde{f_{z,\lambda}} := \operatorname{argmin}_{f \in \widetilde{\mathcal{H}}} \left\{ \frac{1}{n} \sum_{i=1}^n \ell(y_i, f(\mathbf{x}_i)) + \lambda \|f\|_{\widetilde{\mathcal{H}}}^2 \right\}. \quad (2)$$

By virtue of the representer theorem [1], problem (2) can be formulated as an empirical risk minimization problem. Here we take the least squares regression problem as example

$$\beta_\lambda := \operatorname{argmin}_{\beta \in \mathbb{R}^s} \frac{1}{n} \|\mathbf{y} - \mathbf{Z}\beta\|_2^2 + \lambda \|\beta\|_2^2, \quad (3)$$

where the label vector is $\mathbf{y} = [y_1, y_2, \dots, y_n]^\top$ and the feature matrix is $\mathbf{Z} = [\varphi(\mathbf{x}_1), \dots, \varphi(\mathbf{x}_n)]^\top \in \mathbb{R}^{n \times s}$. This is a linear

ridge regression problem in the space spanned by random features and the optimal hypothesis is given by $\widetilde{f_{z,\lambda}} = \mathbf{Z}\beta_\lambda$, with $\beta_\lambda = (\mathbf{Z}^\top \mathbf{Z} + n\lambda \mathbf{I})^{-1} \mathbf{Z}^\top \mathbf{y}$. For classification, we use the sign function to output the binary classification label.

2.3 The used kernels

Random features based algorithms often consider the following kernels:

i) the Gaussian kernel: it is the most notable member of stationary kernels with

$$k(\mathbf{x}, \mathbf{x}') = \exp\left(-\frac{\|\mathbf{x} - \mathbf{x}'\|_2^2}{2\sigma^2}\right),$$

where σ is the kernel width. The associated density of the Gaussian kernel is again Gaussian $\boldsymbol{\omega} \sim \mathcal{N}(0, \sigma^{-2} \mathbf{I}_d)$.

ii) arc-cosine kernels: they belong to rotation-invariant but not shift-invariant kernels. As discussed in [47], the b -order arc-cosine kernel admits

$$k(\mathbf{x}, \mathbf{x}') = \frac{1}{\pi} \|\mathbf{x}\|_2^b \|\mathbf{x}'\|_2^b J_b(\theta),$$

where $\theta = \cos^{-1} \left(\frac{\mathbf{x}^\top \mathbf{x}'}{\|\mathbf{x}\|_2 \|\mathbf{x}'\|_2} \right)$ and $J_b(\theta)$ is defined as

$$J_b(\theta) = (-1)^b (\sin \theta)^{2b+1} \left(\frac{1}{\sin \theta} \frac{\partial}{\partial \theta} \right)^b \left(\frac{\pi - \theta}{\sin \theta} \right).$$

In practice, the common used arc-cosine kernels are the zero-th and first order kernels with $b = 0$ or $b = 1$. The zero-order arc-cosine kernel is formulated as

$$k(\mathbf{x}, \mathbf{x}') = 1 - \frac{\theta}{\pi},$$

and the first-order arc-cosine kernel is

$$k(\mathbf{x}, \mathbf{x}') = \frac{1}{\pi} \|\mathbf{x}\|_2 \|\mathbf{x}'\|_2 (\sin \theta + (\pi - \theta) \cos \theta).$$

iii) the polynomial kernel: it is also a widely-used non-stationary kernel with

$$k(\mathbf{x}, \mathbf{x}') = (1 + \langle \mathbf{x}, \mathbf{x}' \rangle)^b,$$

where b is the order. Apart from the above-mentioned kernels, some research works focus on random features approximation for additive kernels [48], polynomial kernels on the unit sphere [27], indefinite (real, symmetric, but not positive definite) kernels [49].

2.4 Theoretical foundation of random features

The theoretical foundation of RFF relies on Bochner's celebrated characterization of positive definite functions.

Theorem 1. (Bochner's theorem [50]) *A continuous and shift-invariant function $k : \mathbb{R}^d \times \mathbb{R}^d \rightarrow \mathbb{R}$ is positive definite if and only if it can be represented as*

$$k(\mathbf{x} - \mathbf{x}') = \int_{\mathbb{R}^d} \exp(i\boldsymbol{\omega}^\top (\mathbf{x} - \mathbf{x}')) \mu_k(d\boldsymbol{\omega}),$$

where μ_k is a positive finite measure on frequencies $\boldsymbol{\omega}$.

According to Bochner's theorem, the spectral distribution μ_k of a stationary kernel is the finite measure induced by a Fourier transform. That means, there exists a finite Borel measure $p(\boldsymbol{\omega})$ (the Fourier transform associated with k) such that

$$\begin{aligned} k(\mathbf{x} - \mathbf{x}') &= \int_{\mathbb{R}^d} p(\boldsymbol{\omega}) \exp(i\boldsymbol{\omega}^\top (\mathbf{x} - \mathbf{x}')) d\boldsymbol{\omega} \\ &= \mathbb{E}_{\boldsymbol{\omega} \sim p} [\exp(i\boldsymbol{\omega}^\top \mathbf{x}) \exp(i\boldsymbol{\omega}^\top \mathbf{x}')^*], \end{aligned} \quad (4)$$

where the symbol \mathbf{x}^* denotes the complex conjugate of \mathbf{x} , and $p(\boldsymbol{\omega})$ can be scaled to a normalized density by setting $k(0) = 1$. Typically, the kernel in practical uses is real-valued and thus the imaginary part in Eq. (4) can be discarded. RFF applies the standard Monte Carlo sampling scheme to approximate $k(\mathbf{x}, \mathbf{x}')$ such that $k(\mathbf{x}, \mathbf{x}') = \mathbb{E}_{\boldsymbol{\omega} \sim p} [\varphi_p(\boldsymbol{\omega})^\top \varphi_p(\boldsymbol{\omega}')] \approx \tilde{k}_p(\mathbf{x}, \mathbf{x}') = \varphi_p(\boldsymbol{\omega})^\top \varphi_p(\boldsymbol{\omega}')$ with the explicit mapping¹

$$\varphi_p(\boldsymbol{\omega}) := \frac{1}{\sqrt{s}} [\exp(-i\boldsymbol{\omega}_1^\top \mathbf{x}), \dots, \exp(-i\boldsymbol{\omega}_s^\top \mathbf{x})]^\top, \quad (5)$$

1. The subscript p in \tilde{k}_p and φ_p denotes the sampling distribution $p(\boldsymbol{\omega})$.

where $\{\boldsymbol{\omega}_i\}_{i=1}^s$ are sampled from $p(\boldsymbol{\omega})$ independently of the training set. Also, we denote $z_p(\boldsymbol{\omega}_i, \mathbf{x}_j) := \exp(-i\boldsymbol{\omega}_i^\top \mathbf{x}_j)$ such that $\varphi_p(\boldsymbol{\omega}) = 1/\sqrt{s} [z_p(\boldsymbol{\omega}_1, \mathbf{x}), \dots, z_p(\boldsymbol{\omega}_s, \mathbf{x})]^\top$. In this case, $\tilde{k}_p(\mathbf{x}, \mathbf{x}')$ are reformulated as

$$\tilde{k}_p(\mathbf{x}, \mathbf{x}') = \frac{1}{s} \sum_{i=1}^s z_p(\boldsymbol{\omega}_i, \mathbf{x}) z_p(\boldsymbol{\omega}_i, \mathbf{x}').$$

Consequently, the original kernel matrix $\mathbf{K} = [k(\mathbf{x}_i, \mathbf{x}_j)]_{n \times n}$ can be approximated by $\mathbf{K} \approx \tilde{\mathbf{K}}_p = \mathbf{Z}_p \mathbf{Z}_p^\top$ with $\mathbf{Z}_p = [\varphi_p(\mathbf{x}_1), \dots, \varphi_p(\mathbf{x}_n)]^\top \in \mathbb{R}^{n \times s}$. Actually, the above principle in Eq. (4) can be further generalized by considering the class of kernel functions [43] which can be decomposed as

$$k(\mathbf{x} - \mathbf{x}') = \int_{\mathbb{R}^d} z(\boldsymbol{\omega}, \mathbf{x}) z(\boldsymbol{\omega}, \mathbf{x}') p(\boldsymbol{\omega}) d\boldsymbol{\omega}, \quad (6)$$

where $z(\boldsymbol{\omega}, \mathbf{x})$ is a continuous and bounded function.

It can be noticed that, Bochner's theorem requires the shift-invariant property of kernels on $\mathcal{X} = \mathbb{R}^d$ that depends on $\mathbf{x} - \mathbf{x}'$. Instead, as one of the most general family of kernels, rotation-invariant kernels [47], [51], [52], e.g., the above mentioned arc-cosine kernels, violate the stationary condition of Bochner's theorem. They are defined on the hypersphere $\mathcal{X} = \mathbb{S}^{d-1}$, and actually determined by $\langle \mathbf{x}, \mathbf{x}' \rangle$. Accordingly, to make Bochner's theorem feasible to rotation-invariant kernels, an improvement is conducted on the Fourier basis functions by *spherical harmonics*. They are a countably infinite family of complex polynomials which form an orthogonal basis for square-integrable functions $\mathcal{X} \rightarrow \mathbb{C}$.

Theorem 2. ([53], [54]) *A rotation-invariant continuous function $k : \mathbb{S}^{d-1} \times \mathbb{S}^{d-1} \rightarrow \mathbb{R}$ is positive definite if and only if it has a symmetric non-negative expansion into spherical harmonics $Y_{\ell, m}^d$*

$$k(\langle \mathbf{x}, \mathbf{x}' \rangle) = \sum_{j=0}^{\infty} \sum_{l=1}^{N(d, \ell)} p(\ell, m) Y_{\ell, m}^d(\mathbf{x}) \overline{Y_{\ell, m}^d(\mathbf{x}')}, \quad (7)$$

for some $p(\boldsymbol{\omega}) \geq 0$ satisfying $p(\boldsymbol{\omega}) = p(-\boldsymbol{\omega})$ for all valid index pairs $\boldsymbol{\omega} = (\ell, m) \in \mathbb{S}^{d-1} \times \mathbb{S}^{d-1}$. Here we use $N(d, \ell) = \binom{d-1+\ell}{\ell} - \binom{d-1+\ell}{\ell-2}$ and $\int_{\mathbb{S}^{d-1}} |Y_{\ell, m}^d(\mathbf{x})|^2 d\mathbf{x} = 1$.

In this case, both of the above mentioned Gaussian kernel and arc-cosine kernels admit the following unified integration representation [32], [34]

$$k(\mathbf{x}, \mathbf{x}') := \int_{\mathbb{R}^d} \mathcal{N}(\mathbf{0}, \mathbf{I}_d) g(\boldsymbol{\omega}) d\boldsymbol{\omega}, \quad (8)$$

where the integrand is $g(\boldsymbol{\omega}) = \phi(\boldsymbol{\omega}^\top \mathbf{x})^\top \phi(\boldsymbol{\omega}^\top \mathbf{x}')$. The Gaussian kernel corresponds to $\phi(x) = [\cos(x), \sin(x)]^\top$; and the arc-cosine kernels correspond to $\phi(x) = \Phi(x)$ in the zero-order case, where $\Phi(x) = \frac{1}{2}(1 + \text{sign}(x))$ is the Heaviside step function, and $\phi(x) = \max\{0, x\}$ in the first-order case.

2.5 Taxonomy of random features based algorithms

Random features based algorithms focus on constructing the mapping

$$\varphi(\mathbf{x}) := \frac{1}{\sqrt{s}} [a_1 \exp(-i\boldsymbol{\omega}_1^\top \mathbf{x}), \dots, a_s \exp(-i\boldsymbol{\omega}_s^\top \mathbf{x})]^\top. \quad (9)$$

The key question is how to select the points $\boldsymbol{\omega}_i$ and weights a_i so as to uniformly approximate the integral in Eq. (4). Figure 2 presents the taxonomy of some representative random features

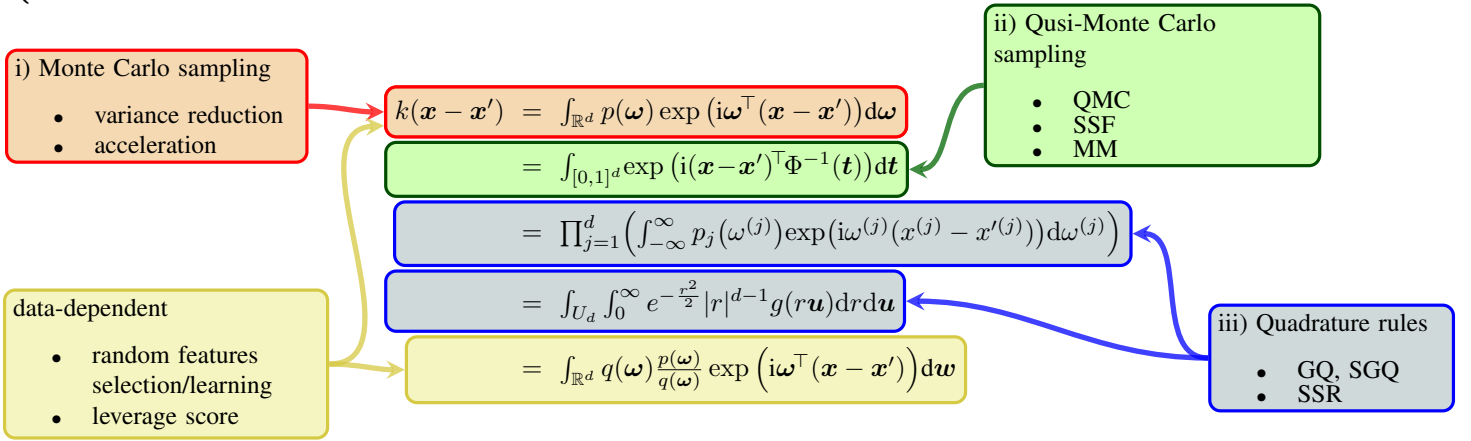
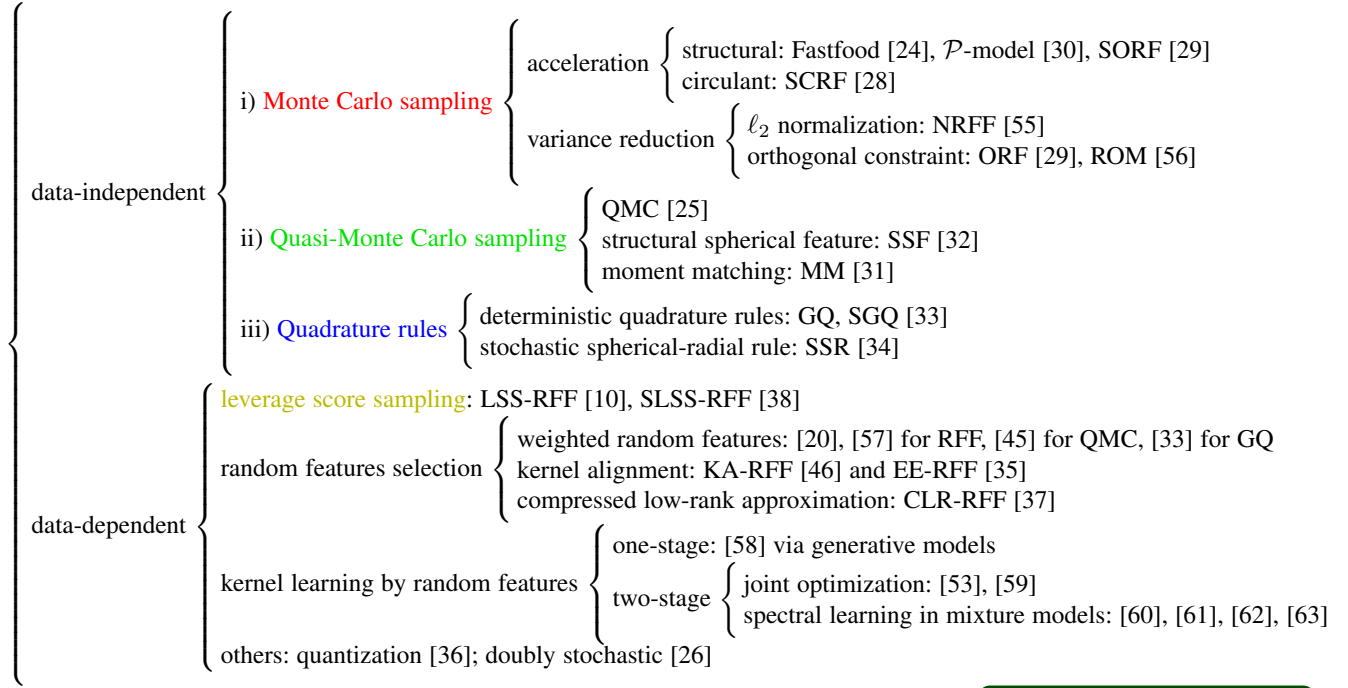


Figure 2. Taxonomy of representative random features based algorithms. Here we put QMC, SSF, and MM together for ease of description due to their same integration representation over the unit cube.

based algorithms. They can be roughly grouped into two categories, one is *data-independent* and the other is *data-dependent*. The former one means that the selection scheme of $\boldsymbol{\omega}_i$ and a_i is *independent* of the training data. In contrast, if $\boldsymbol{\omega}_i$ or a_i depends on the training data, the corresponding methods are *data-dependent*.

According to the sampling strategy, *data-independent* random features based algorithms can be cast into three classes:

i) *Monte Carlo sampling*: The random features are sampled from $p(\boldsymbol{\omega})$ in Eq. (4) (also shown in the red box in Figure 2). In the standard RFF [8], to approximate the Gaussian kernel, $\{\boldsymbol{\omega}_i\}_{i=1}^s$ are randomly sampled from $p(\boldsymbol{\omega}) = \mathcal{N}(0, \sigma^{-2} \mathbf{I}_d)$. The weights are equal, i.e., $a_i \equiv 1$ in Eq. (9). To reduce the store complexity or speed up the construction of random features, one way is to substitute the dense Gaussian matrix in RFF by structural matrices, e.g., Fastfood [24] via Hadamard matrices and its general version \mathcal{P} -model [30]; the other way is using circulant matrices, e.g., Signed Circulant Random Features (SCRf) [28]. To improve the approximation quality, an ℓ_2 -normalization scheme is a simple but effective way, leading to Normalized RFF (NRFF) [55]. Orthogonal Random Features (ORF) [29], which incorporates an orthogonality

constraint to the random Gaussian matrix, is another powerful technique for variance reduction. The feature matrix \mathbf{W} in [29] can be efficiently computed and stored by structural matrices, e.g., Structural ORF (SORF) [29], [64]. Specifically, the structural orthogonal property of random features is further exploited in Random Orthogonal Embeddings (ROM) [56] for rotation-invariant kernels.

ii) *quasi-Monte Carlo sampling*: The convergence of Monte-Carlo used in RFF and ORF can be significantly improved by is Quasi-Monte Carlo sampling (QMC) [45], which uses a low-discrepancy sequence $\mathbf{t}_1, \mathbf{t}_2, \dots, \mathbf{t}_s \in [0, 1]^d$ over the unit cube (see in the green box in Figure 2). Based on such integration representation, Lyu [32] propose Spherical Structural Features (SSF) to generate asymptotically uniformly distributed points on the sphere \mathcal{S}^{d-1} for higher convergence rate and approximation quality. Similarly, according to this integration, the Moment Matching (MM) scheme [31] is used for a d -dimensional refined uniform sampling sequence $\{\mathbf{t}_i\}_{i=1}^s$ instead of a low discrepancy sequence in QMC. Note that SSF and MM do not belong to the quasi-Monte Carlo sampling framework. However, they share the same integration formulation

with QMC over the unit cube and thus we put them here for simplicity.

iii) *quadrature based methods*: The representation in Eq. (4) can be approximated by a numerical integration way to improve the approximation quality. The selection of points and weights can be *deterministic*, e.g., Gaussian Quadrature (GQ) [33] and Sparse Grids Quadrature (SGQ) [33] over each dimension (the integration can be found in blue box in Figure 2). They also can be *randomized*, e.g., Stochastic Spherical-Radial (SSR) rules [34] transforms the d -dimensional integration in Eq. (4) to a double integrals: stochastic radial rules and stochastic spherical rules (see in the blue box in Figure 2).

The above methods are all *data-independent*, i.e., the selection of points and weights is independent of the training data. Another line of work considers *data-dependent* algorithms, which utilize the training data to guide the generation of random features for better approximation quality or generalization performance. According to the scheme of generating random features, we can group data-dependent algorithms into three classes:

i) *leverage score sampling*: It is based on the importance sampling framework (see the yellow box in Figure 2). The original distribution $p(\omega)$ is substituted by a delicately designed distribution $q(\omega)$ via leverage scores [42], [43] for better generalization performance. The typical approach is Leverage Score based RFF (LS-RFF) [10], and it can be further accelerated by Surrogate Leverage Score based RFF (SLS-RFF) [38].

ii) *random features selection*: A simple way in this class is to re-weight random features by solving a constrained optimization problems, including weighted RFF [20], [57], weighted QMC [45], and weighted GQ [33]. Different from directly learning the weights of pre-given random features, another line of this class methods involves two steps: i) ‘‘up-projection’’: begin with generating a large set of random features with $\{\omega_i\}_{i=1}^J$; ii) ‘‘compression’’: reduce them to a small number of weighted features in a data-dependent strategy, including KA-RFF [46] and EE-RFF [35] by kernel alignment, and CLR-RFF [37] by compressed low-rank approximation.

iii) *kernel learning by random features*: Approaches in this class attempt to learn random features in a sophisticated way, e.g., learning the spectral distribution of kernel from the data. From a more general view, the above *random features selection* based algorithms can be regarded in this class. Nevertheless, the key difference between them is that random features in *random features selection* based algorithms are directly generated by RFF, i.e., only learning the weights of these candidate features. Representative approaches in this class can be in an *one-stage* [58] or *two-stage* process [53], [59], [60], [61], [62], [63]. Since this topic actually belongs to kernel learning instead of kernel approximation, we do not detail them in our paper.

Other data-dependent based approaches that does not belong to these three categories mainly include: i) quantization random features [36]: it attempts to quantize RFF with the Gaussian kernel under a memory budget. A new insight demonstrated by this method is that, under the same memory budget, random features based algorithms achieve better generalization performance than Nyström approximation [65]. ii) doubly stochastic random features [26]: one stochasticity comes from sampling data points by stochastic gradient descent (SGD); another source is using RFF to approximate the kernel. This doubly stochastic scheme is further used for KPCA approximation [11], and extended to triply stochastic scheme for multiple kernel approximation [66].

In the following, we will detail the above-mentioned data-independent and data-dependent algorithms. Regarding to the taxonomy of theoretical results on random features, we will discuss them in Section 5.

3 Data-independent ALGORITHMS

We introduce data-independent algorithms in a unified description framework by the transformation matrix \mathbf{W} . It is formulated as $\mathbf{W} = [\omega_1, \omega_2, \dots, \omega_s]^\top \in \mathbb{R}^{s \times d}$, and thus determines how well the estimated kernel converges to the actual kernel. Table 1 reports various random features based algorithms on space and complexities to obtain the feature mapping $\mathbf{W}\mathbf{x}$ for each $\mathbf{x} \in \mathcal{X}$. Specifically, in Table 1, we also summarize the variance reduction property of these approaches and their scope.

3.1 Monte Carlo sampling based approaches

RFF [8]: Its transformation matrix can be written as

$$\mathbf{W}_{\text{RFF}} = \frac{1}{\sigma} \mathbf{G}, \quad (10)$$

where $\mathbf{G} \in \mathbb{R}^{s \times d}$ is a dense random Gaussian matrix, with every entry sampled independently from the standard normal distribution. For the Gaussian kernel, the estimation by RFF is unbiased with $\mathbb{E}(k_{\text{RFF}}(\mathbf{x}, \mathbf{x}')) = \exp\left(-\frac{\|\mathbf{x}-\mathbf{y}\|_2^2}{2\sigma^2}\right)$ and the variance is $\mathbb{V}[\text{RFF}] = \frac{(1-e^{-\tau^2})^2}{2s}$ given by [29], where $\tau = \mathbf{x} - \mathbf{x}'$ and $\tau := \|\tau\|_2$ for notational simplicity.

Fastfood [24]: It attempts to speed up the construction of dense random Gaussian matrices in RFF by Hadamard matrices. The transformation matrix in Eq. (10) can be substituted by

$$\mathbf{W}_{\text{Fastfood}} = \frac{1}{\sigma} \mathbf{B}_1 \mathbf{H} \mathbf{G} \mathbf{T} \mathbf{H} \mathbf{B}_2, \quad (11)$$

where \mathbf{H} is the Walsh-Hadamard matrix which admits fast multiplication in $\mathcal{O}(d \log d)$ time and $\mathbf{T} \in \{0, 1\}^{d \times d}$ is a permutation matrix that decorrelates the eigen-systems of two Hadamard matrices. The three diagonal random matrices \mathbf{B}_1 , \mathbf{G} and \mathbf{B}_2 exhibit different properties: \mathbf{B}_2 has random $\{\pm 1\}$ entries on its main diagonal for binary decorrelation; \mathbf{G} has random Gaussian entries drawn *i.i.d* via $G_{ii} \sim \mathcal{N}(0, 1)$; the random scaling matrix \mathbf{B}_1 encodes the spectral properties of the associated kernel with $(\mathbf{B}_1)_{ii} = \|\omega_i\|_2 / \|\mathbf{G}\|_{\text{F}}$. FastFood generates the unbiased estimation but achieves a large variance at a certain $\mathcal{O}(1/s)$ rate

$$\mathbb{V}[\text{Fastfood}] \leq \mathbb{V}[\text{RFF}] + \frac{6\tau^4}{s} \left(e^{-\tau^2} + \frac{\tau^2}{3} \right).$$

P-model [30]: It is a general version of Fastfood by constructing the transformation matrix as

$$\mathbf{W}_{\mathcal{P}} = [\mathbf{g}^\top \mathbf{P}_1, \mathbf{g}^\top \mathbf{P}_2, \dots, \mathbf{g}^\top \mathbf{P}_s]^\top \in \mathbb{R}^{s \times d},$$

where \mathbf{g} is a Gaussian random vector of length t and $\mathbf{P}_i \in \mathbb{R}^{t \times d}$ with unit ℓ_2 norm columns generates the sequence $\mathcal{P} = \{\mathbf{P}_i\}_{i=1}^s$. According to Eq. (11), the matrix $\mathbf{H}\mathbf{G}$ can be constructed by the \mathcal{P} -model with the fixed budget of randomness \mathbf{g} and each \mathbf{P}_i is a random diagonal matrix with entries on the diagonal of the form: $H_{i,1}, H_{i,2}, \dots, H_{i,d}$. The \mathcal{P} -model is unbiased and its variance is close to that of RFF at the certain $\mathcal{O}(1/d)$ convergence rate with

$$\left| \mathbb{V}[\mathcal{P}\text{-model}] - \mathbb{V}[\text{RFF}] \right| = \mathcal{O}\left(\frac{1}{d}\right).$$

Table 1
Comparison of different kernel approximation methods on space and time complexities to obtain $\mathbf{W}\mathbf{x}$.

Method	kernels	Extra Memory	Time	Lower variance than RFF
Random Fourier Features (RFF) [8]	shift-invariant kernels	$\mathcal{O}(sd)$	$\mathcal{O}(sd)$	-
Quasi-Monte Carlo (QMC) [25]	shift-invariant kernels	$\mathcal{O}(sd)$	$\mathcal{O}(sd)$	Yes
Normalized RFF (NRFF) [55]	Gaussian kernel	$\mathcal{O}(sd)$	$\mathcal{O}(sd)$	Yes
Moment matching (MM) [31]	shift-invariant kernels	$\mathcal{O}(sd)$	$\mathcal{O}(sd)$	Yes
Orthogonal Random Feature (ORF) [29]	Gaussian kernel	$\mathcal{O}(sd)$	$\mathcal{O}(sd)$	Yes
Fastfood [24]	Gaussian kernel	$\mathcal{O}(s)$	$\mathcal{O}(s \log d)$	No
Spherical Structured Features (SSF) [32]	shift and rotation-invariant kernels	$\mathcal{O}(s)$	$\mathcal{O}(s \log d)$	Yes
Structured ORF (SORF) [29], [64]	shift and rotation-invariant kernels	$\mathcal{O}(s)$	$\mathcal{O}(s \log d)$	unknown
Signed Circulant (SCRf) [28]	shift-invariant kernels	$\mathcal{O}(s)$	$\mathcal{O}(s \log d)$	the same
\mathcal{P} -model [30]	shift and rotation-invariant kernels	$\mathcal{O}(s)$	$\mathcal{O}(s \log d)$	No
Random Orthogonal Embeddings (ROM) [56]	rotation-invariant kernels	$\mathcal{O}(d)$	$\mathcal{O}(d \log d)$	Yes
Quadrature based	-	$\mathcal{O}(d)$	$\mathcal{O}(d \log d)$	Yes

SCRf [28]: It accelerates the construction of random features by circulant matrices. The transformation matrix is

$$\mathbf{W}_{\text{SCRf}} = [\boldsymbol{\nu} \otimes \mathcal{C}(\boldsymbol{\omega}_1), \boldsymbol{\nu} \otimes \mathcal{C}(\boldsymbol{\omega}_2), \dots, \boldsymbol{\nu} \otimes \mathcal{C}(\boldsymbol{\omega}_t)]^\top \in \mathbb{R}^{td \times d},$$

where the Rademacher vector $\boldsymbol{\nu} = [\nu_1, \nu_2, \dots, \nu_d]$ satisfies $\mathbb{P}(\nu_i = 1) = \mathbb{P}(\nu_i = -1) = 1/2$. The circulant matrix $\mathcal{C}(\boldsymbol{\omega}_i) \in \mathbb{R}^{d \times d}$ is generated by $\boldsymbol{\omega}_i \sim \mathcal{N}(0, \sigma^{-2} \mathbf{I}_d)$. Hence, we only need $\mathcal{O}(s)$ to store the feature mapping matrix \mathbf{W}_{SCRf} with $s := td$ due to the circulant structure. Note that $\mathcal{C}(\boldsymbol{\omega}_i)$ can be made diagonal by the Discrete Fourier Transform (DFT), regardless of the generating vector $\boldsymbol{\omega}_i$. SCRf is unbiased and outputs the same variance estimation with RFF.

The above approaches attempt to accelerate the computational process for RFF, and in the next we give an overview on representative methods for variance reduction.

NRFF [55]: It normalizes the input data to unit ℓ_2 norm and then conducts RFF. After that, the Gaussian kernel can be reformulated as

$$k(\mathbf{x}, \mathbf{x}') = \exp\left(-\frac{1}{\sigma^2} \left(1 - \frac{\mathbf{x}^\top \mathbf{x}'}{\|\mathbf{x}\|_2 \|\mathbf{x}'\|_2}\right)\right),$$

which is related to the normalized linear kernel [27], [55]. Albeit simple, this scheme is effective with the nice variance reduction property

$$\mathbb{V}[\text{NRFF}] = \mathbb{V}[\text{RFF}] - \frac{1}{4s} e^{-\tau^2} (3 - e^{-2\tau^2}).$$

ORF [29]: It considers the orthogonality on random features, and accordingly the transformation matrix is formulated as

$$\mathbf{W}_{\text{ORF}} = \frac{1}{\sigma} \mathbf{S} \mathbf{Q},$$

where \mathbf{Q} is a uniformly distributed random orthogonal matrix, and \mathbf{S} is a diagonal matrix, of which diagonal entries are sampled *i.i.d* from the χ -distribution with d degrees of freedom. This orthogonality is important to reduce the approximation error in random features, and also is applied to unifying orthogonal Monte Carlo [67]. ORF is unbiased and its variance can be bounded by

$$\mathbb{V}[\text{ORF}] - \mathbb{V}[\text{RFF}] \leq \frac{1}{s} \left(\frac{g(\tau)}{d} - \frac{(d-1)e^{-\tau^2} \tau^4}{2d} \right),$$

where $g(\tau)$ is a function $g(\tau) = e^{\tau^2} (\tau^8 + 6\tau^6 + 7\tau^4 + \tau^2)/4 + e^{\tau^2} \tau^4 (\tau^6 + 2\tau^4)/2d$. Therefore, for a large d , the ratio of the variance of ORF and RFF can be approximated by

$$\frac{\mathbb{V}[\text{ORF}]}{\mathbb{V}[\text{RFF}]} \approx 1 - \frac{(s-1)e^{-\tau^2} \tau^4}{d(1 - e^{-\tau^2})^2}. \quad (12)$$

Accordingly, $\text{Var}[\text{ORF}] < \text{Var}[\text{RFF}]$ holds under some conditions, e.g., a large d and a small τ . Further, Choromanski et al. [68] improve the result as

$$\begin{aligned} \mathbb{V}[\text{RFF}] - \mathbb{V}[\text{ORF}] = & \frac{s-1}{s} \mathbb{E}_{R_1, R_2} \left[\frac{J_{\frac{d}{2}-1}(\sqrt{R_1^2 + R_2^2} \tau) \Gamma(d/2)}{(\sqrt{R_1^2 + R_2^2} \tau/2)^{\frac{d}{2}-1}} \right] - \\ & \frac{s-1}{s} \mathbb{E}_{R_1} \left[\frac{J_{\frac{d}{2}-1}(R_1 \tau) \Gamma(d/2)}{(R_1 \tau/2)^{\frac{d}{2}-1}} \right]^2, \end{aligned} \quad (13)$$

where J_d is the Bessel function of the first kind of degree d . Two independent scalar random variables R_1, R_2 satisfy $\boldsymbol{\omega}_1 = R_1 \mathbf{v}$ and $\boldsymbol{\omega}_2 = R_2 \mathbf{v}$ with $\boldsymbol{\omega}_1, \boldsymbol{\omega}_2 \sim \mathcal{N}(0, \sigma^{-2} \mathbf{I}_d)$ and $\mathbf{v} \sim \text{Unif}(\mathcal{S}^{d-1})$. According to Eq. (13), $\mathbb{V}[\text{ORF}] < \mathbb{V}[\text{RFF}]$ holds for two asymptotic cases: i) for a fixed d and small enough τ if $\mathbb{E}[\|\boldsymbol{\omega}\|_2^4] \leq \infty$; ii) for fixed $\tau < \frac{1}{4\sqrt{c}}$ with some constant c and large d , we have

$$\mathbb{V}[\text{RFF}] - \mathbb{V}[\text{ORF}] = \frac{s-1}{s} \left(\frac{1}{2d} \frac{\tau^4}{\sigma^2} e^{-\frac{\tau^2}{\sigma^2}} + \mathcal{O}\left(\frac{1}{d}\right) \right).$$

SORF [29], [64]: Random orthogonal matrices in ORF are replaced by a class of special structured matrices like Fastfood with

$$\mathbf{W}_{\text{SORF}} = \frac{\sqrt{d}}{\sigma} \mathbf{H} \mathbf{D}_1 \mathbf{H} \mathbf{D}_2 \mathbf{H} \mathbf{D}_3, \quad (14)$$

where \mathbf{H} is the normalized Walsh-Hadamard matrix and $\mathbf{D}_i \in \mathbb{R}^{d \times d}$, $i = 1, 2, 3$ are diagonal sign-flipping matrices, of which each diagonal entry is sampled from the Rademacher distribution. Specifically, Bojarski et al. [64] generalize each block matrix $\mathbf{H} \mathbf{D}_i$ in Eq. (14) in various structures. More importantly, each block matrix has different effects. The first block $\mathbf{H} \mathbf{D}_1$ admits $\Pr\left[\|\mathbf{H} \mathbf{D}_1 \mathbf{x}\|_\infty > \frac{\log d}{\sqrt{d}}\right] \leq 2de^{-\frac{\log^2 d}{8}}$ for any $\mathbf{x} \in \mathbb{R}^d$ with $\|\mathbf{x}\|_2 = 1$, termed as $(\log d, 2de^{-\frac{\log^2 d}{8}})$ -balanced, so that there is no dimension that carries too much of the ℓ_2 -norm of the vector \mathbf{x} .

The second block HD_2 makes vectors close to orthogonal and the third block HD_3 defines the capacity of the entire structured transform by providing a vector of parameters. SORF is not an unbiased estimator of the Gaussian kernel but exhibits the asymptotic unbiased property

$$\left| \mathbb{E}[\text{SORF}] - e^{-\tau^2/2} \right| \leq \frac{6\tau}{\sqrt{d}}.$$

ROM [56]: It generalizes SORF to

$$\mathbf{W}_{\text{ROM}} = \frac{\sqrt{d}}{\sigma} \prod_{i=1}^t \mathbf{H} \mathbf{D}_i,$$

where \mathbf{H} can be the normalized Hadamard matrix or the Walsh matrix, and \mathbf{D}_i is the Rademacher matrix as defined in SORF. Theoretical results demonstrate that the ROM estimator is able to achieve variance reduction of RFF. Interestingly, odd t yields better results than even t . This is the reason why SORF chooses $t = 3$.

3.2 Quasi-Monte Carlo sampling

Here we briefly review the quasi-Monte Carlo sampling (QMC) [25], spherical structured feature (SSF) [32] and moment matching (MM) [31]. These three methods generate lower variance or approximation error than RFF.

The classical Monte Carlo sampling generates a series of independent samples, but this independent sampling would lead to an undesired clustering effect and a consequence empty spaces [69]. Instead, QMC [25] outputs low-discrepancy sequences rather than the fully-random samples of Monte Carlo estimation. A typical QMC sequence has a hierarchical structure: the initial points are sampled from the integrand on a coarse scale while the latter points are sampled more finely. As a result, it provides an asymptotic error of $\epsilon = \mathcal{O}((\log s)^d/s)$, which exhibits a faster convergence than Monte Carlo with $\mathcal{O}(s^{-1/2})$ to approximate the high-dimensional integral. Often it requires s to be exponential in d for the improvement to manifest.

QMC [25]: It assumes that $p(\mathbf{x})$ is separable in each dimension, i.e., $p(\mathbf{x}) = \prod_{j=1}^d p_j(x_j)$, where $p_j(\cdot)$ is a univariate density function. The QMC method is generally applicable to integrals from \mathbb{R}^d to a unit cube $[0, 1]^d$. By generating a low discrepancy sequence² $\mathbf{t}_1, \mathbf{t}_2, \dots, \mathbf{t}_s \in [0, 1]^d$, the random feature can be constructed by $\omega_i = \Phi^{-1}(\mathbf{t}_i)$ for $i \in [s]$. By change of variables between \mathbf{t}_i and ω_i , Eq. (4) can be equivalently written as

$$k(\mathbf{x} - \mathbf{x}') = \int_{[0,1]^d} \exp(i(\mathbf{x} - \mathbf{x}')^\top \Phi^{-1}(\mathbf{t})) d\mathbf{t}, \quad (15)$$

where $\Phi^{-1}(\mathbf{t})$ is defined by

$$\Phi^{-1}(\mathbf{t}) = (\Phi_1^{-1}(t_1), \dots, \Phi_d^{-1}(t_d)) \in \mathbb{R}^d,$$

with Φ_j is the cumulative distribution function (CDF) of p_j , for $j \in [d]$. Accordingly, the transformation matrix by QMC is

$$\mathbf{W}_{\text{QMC}} = [\Phi^{-1}(\mathbf{t}_1), \Phi^{-1}(\mathbf{t}_2), \dots, \Phi^{-1}(\mathbf{t}_s)]^\top \in \mathbb{R}^{s \times d}. \quad (16)$$

SSF [32]: It generates asymptotically uniformly distributed points on the sphere \mathcal{S}^{d-1} to approximate shift and rotation invariant kernels. It can be used to improve QMC in space and time complexities. The feature mapping matrix of SSF is constructed by

$$\mathbf{W}_{\text{SSF}} = [\Phi^{-1}(t)\mathbf{v}_1, \Phi^{-1}(t)\mathbf{v}_2, \dots, \Phi^{-1}(t)\mathbf{v}_s]^\top \in \mathbb{R}^{s \times d},$$

2. There are four sequences: Halton, Sobol', Lattice rules, and digital nets.

where $\Phi^{-1}(t)$ uses the one-dimensional QMC point and $\mathbf{V} = [\mathbf{v}_1, \mathbf{v}_2, \dots, \mathbf{v}_s] \in \mathbb{S}^{d-1 \times s}$ denotes the point set asymptotically uniformly distributed on \mathbb{S}^{d-1} . The structure matrix \mathbf{V} is

$$\mathbf{V} = \frac{1}{\sqrt{d/2}} \begin{bmatrix} \text{Re } \mathbf{F}_\Lambda & -\text{Im } \mathbf{F}_\Lambda \\ \text{Im } \mathbf{F}_\Lambda & \text{Re } \mathbf{F}_\Lambda \end{bmatrix} \in \mathbb{R}^{d \times s}$$

where $\mathbf{F}_\Lambda \in \mathbb{C}^{\frac{d}{2} \times \frac{d}{2}}$ is a subset of the discrete Fourier matrix $\mathbf{F} \in \mathbb{C}^{\frac{d}{2} \times \frac{d}{2}}$. The selection of $\frac{d}{2}$ rows from \mathbf{F} to construct \mathbf{F}_Λ is conducted by minimizing the discrete Riesz 0-energy [70] such that the points spread as evenly as they can on the sphere.

MM [31]: It generates a d -dimensional uniform sampling sequence $\{\mathbf{t}_i\}_{i=1}^s$ in Eq. (16) by a moment matching scheme instead of a low discrepancy sequence in QMC. The transformation matrix of MM is

$$\mathbf{W}_{\text{MM}} = [\tilde{\Phi}^{-1}(\mathbf{t}_1), \tilde{\Phi}^{-1}(\mathbf{t}_2), \dots, \tilde{\Phi}^{-1}(\mathbf{t}_s)]^\top \in \mathbb{R}^{s \times d}, \quad (17)$$

where $\tilde{\Phi}^{-1}(\mathbf{t}_i)$ is constructed by moment matching with

$$\tilde{\Phi}^{-1}(\mathbf{t}_i) = \tilde{\mathbf{A}}^{-1}(\Phi^{-1}(\mathbf{t}_i) - \tilde{\boldsymbol{\mu}}),$$

where $\tilde{\boldsymbol{\mu}} = \frac{1}{s} \sum_{i=1}^s \Phi^{-1}(\mathbf{t}_i)$ is the sample mean value and $\tilde{\mathbf{A}}$ is the square root of the sample covariance matrix satisfying $\tilde{\mathbf{A}}\tilde{\mathbf{A}}^\top = \text{Cov}(\Phi^{-1}(\mathbf{t}_i) - \tilde{\boldsymbol{\mu}})$.

3.3 Quadrature based methods

Quadrature based approaches here take advantage of a long line of work on numerical quadrature for estimating integrals. The equivalence between kernel quadrature and random features is elucidated in [43]. In quadrature rules, the points are usually given by *deterministic* rules and the weights are often not equal, including Gaussian quadrature (GQ) [71] and sparse grids quadrature (SGQ) [33]. Deterministic rules can be extended to a stochastic version, Munkhoeva et al. [34] explore the stochastic spherical-radial (SSR) rule [72] in kernel approximation.

GQ [33]: It assumes that the kernel function k can factor along the dimensions and the distribution $p(\boldsymbol{\omega})$ is sub-gaussian. Thus the integral in Eq. (4) over \mathbb{R}^d can be expressed as

$$k(\mathbf{x} - \mathbf{x}') = \prod_{j=1}^d \left(\int_{-\infty}^{\infty} p_j(\omega^{(j)}) \exp(i\omega^{(j)}(x^{(j)} - x'^{(j)})) d\omega^{(j)} \right), \quad (18)$$

where $\boldsymbol{\omega} = [\omega^{(1)}, \omega^{(2)}, \dots, \omega^{(d)}]^\top$. Since each of the factors is an integral over a single dimension, we can approximate them all with an one-dimensional quadrature rule, e.g., Gaussian quadrature [71] by orthogonal polynomials, i.e.

$$\int_{-\infty}^{\infty} p(\omega) \exp(i\omega(x - x')) d\omega \approx \sum_{j=1}^L a_j \exp(i\gamma_j^\top (x - x')), \quad (19)$$

where L is the accuracy level and the univariate point is γ_j associated with its weight a_j . For a third-point rule with the points $\{-\hat{p}_1, 0, \hat{p}_1\}$ and their associated weights $(\hat{a}_1, \hat{a}_0, \hat{a}_1)$, the transformation matrix $\mathbf{W}_{\text{GQ}} \in \mathbb{R}^{s \times d}$ admits that each entry W_{ij} follows with

$$\Pr(W_{ij} = \pm \hat{p}_1) = \hat{a}_1, \quad \Pr(W_{ij} = 0) = \hat{a}_0, \quad \forall i \in [s], j \in [d].$$

Generally, the univariate Gaussian quadrature with L quadrature points is exact up to the $2L - 1$ th order of polynomials. The multivariate Gaussian quadrature is exact for all polynomials of the form $\omega_1^{i_1} \omega_2^{i_2} \dots \omega_d^{i_d}$ with $1 \leq i_j \leq 2L - 1$. However, the

total number of points $s = L^d$ increases exponentially with the dimension d , which is the curse of dimensionality problem.

SGQ [33]: It is based on the Smolyak rule [73] to decrease the needed number of points, i.e., overcoming the curse of dimensionality in univariate quadrature. Here we consider the third-degree SGQ using the symmetric univariate quadrature point set $\{-\hat{p}_1, 0, \hat{p}_1\}$ with the weight $(\hat{a}_1, \hat{a}_0, \hat{a}_1)$

$$k(\mathbf{x}, \mathbf{x}') \approx (1-d+d\hat{a}_0)g(\mathbf{0}) + \hat{a}_1 \sum_{j=1}^d [g(\hat{p}_1 \mathbf{e}_j) + g(-\hat{p}_1 \mathbf{e}_j)],$$

where the function g is defined in Eq. (8), and \mathbf{e}_i is a d -dimensional unit vector with the i -th element being 1. The corresponding transformation matrix is

$$\mathbf{W}_{\text{SGQ}} = [\mathbf{0}_d, \hat{p}_1 \mathbf{e}_1, \dots, \hat{p}_1 \mathbf{e}_d, -\hat{p}_1 \mathbf{e}_1, \dots, -\hat{p}_1 \mathbf{e}_d]^\top \in \mathbb{R}^{(2d+1) \times d},$$

which leads to the explicit feature mapping

$$\varphi(\mathbf{x}) = [\hat{a}_0 g(\mathbf{0}), \hat{a}_1 g(\mathbf{w}_2^\top \mathbf{x}), \dots, g(\mathbf{w}_{2d+1}^\top \mathbf{x})],$$

where \mathbf{w}_i is the i -th row in \mathbf{W} . Note that, given d , the number of generated points is $2d + 1$. So to obtain *dimension-adaptive* feature mapping, Dao et al. [33] subsample the points according to the distribution determined by their weights such that the mapping feature dimension is equal to s .

SSR [34]: It transforms the \mathbb{R}^d integration in Eq. (8) to a double integral over a hyper-sphere. Let $\boldsymbol{\omega} = r\mathbf{u}$ with $\mathbf{u}^\top \mathbf{u} = r^2$ for $r \in [0, \infty]$, we have

$$k(\mathbf{x} - \mathbf{x}') = \frac{1}{2} \int_{U_d} \int_{-\infty}^{\infty} e^{-\frac{r^2}{2}} |r|^{d-1} g(r\mathbf{u}) dr d\mathbf{u}, \quad (20)$$

where the integrand g is given by Eq. (8) and U_d is a unit d -sphere $U_d = \{\mathbf{u} : \mathbf{u}^\top \mathbf{u} = 1, \mathbf{u} \in \mathbb{R}^d\}$. The inner integral in Eq. (20) can be approximated by stochastic radial rules of degree $2l + 1$ $R(h) = \sum_{i=0}^l \hat{w}_i \frac{g(\rho_i) + g(-\rho_i)}{2}$. The outer integral over the surface of unit d -sphere in Eq. (20) can be approximated by stochastic spherical rules $S_Q(g) = \sum_{j=1}^q \tilde{w}_j g(\mathbf{Q}\mathbf{u}_j)$, where \mathbf{Q} is a random orthogonal matrix and \tilde{w}_j are stochastic with distribution such that the rule is exact for polynomials of degree q and gives unbiased estimate for other functions. Combining the above two rules, we have the SSR rule

$$k(\mathbf{x}, \mathbf{x}') \approx g(\mathbf{0}) \left(1 - \frac{d}{\vartheta^2}\right) + \frac{d}{d+1} \sum_{j=1}^d \frac{g(-\vartheta \mathbf{Q}\mathbf{v}_j) + g(\vartheta \mathbf{Q}\mathbf{v}_j)}{2\vartheta^2},$$

where $\vartheta \sim \chi(d+2)$ and the vertex \mathbf{v}_j is given by the randomly rotated unit vertex regular d -simplex \mathbf{V} . Accordingly, the related transformation matrix is

$$\mathbf{W}_{\text{SSR}} = \boldsymbol{\vartheta} \otimes \begin{bmatrix} (\mathbf{Q}\mathbf{V})^\top \\ -(\mathbf{Q}\mathbf{V})^\top \end{bmatrix} \in \mathbb{R}^{2(d+1) \times d},$$

with $\boldsymbol{\vartheta} = [\vartheta_1, \vartheta_2, \dots, \vartheta_s]$. To get s features, one can stack \mathbf{W} for $s/(2d+3)$ times as indicated by [34]. Finally, the feature mapping by SSR is given by

$$\varphi(\mathbf{x}) = [a_0 g(\mathbf{0}), a_1 g(\mathbf{w}_1^\top \mathbf{x}), \dots, g(\mathbf{w}_s^\top \mathbf{x})],$$

where $a_0 = \sqrt{1 - \frac{j-1}{\sum_{d+1}^j \frac{1}{\rho_j^2}}}$, $a_j = \frac{1}{\rho_j} \sqrt{\frac{d}{2(d+1)}}$ for $j \in [s]$, and \mathbf{w}_j is the j -th of the stacked \mathbf{W} .

4 DATA-DEPENDENT ALGORITHMS

Data-dependent approaches aim to design/learn random features to achieve better approximation quality or generalization performance. According to the scheme of generating random features, we can group data-dependent algorithms into *leverage score sampling*, *random features selection*, and *kernel learning by random features*.

4.1 Leverage score based sampling

Leverage score based approaches [10], [38], [74] are built on *importance sampling* framework. Assume that $\{\mathbf{w}_i\}_{i=1}^s$ are sampled from $q(\mathbf{w})$ that we need to design, the feature mapping in Eq. (5) can be formulated as

$$\varphi_q(\mathbf{x}) = \frac{1}{\sqrt{s}} \left(\sqrt{\frac{p(\mathbf{w}_1)}{q(\mathbf{w}_1)}} e^{-i\mathbf{w}_1^\top \mathbf{x}}, \dots, \sqrt{\frac{p(\mathbf{w}_s)}{q(\mathbf{w}_s)}} e^{-i\mathbf{w}_s^\top \mathbf{x}} \right)^\top. \quad (21)$$

We again have $k(\mathbf{x}, \mathbf{x}') = \mathbb{E}_{\mathbf{w} \sim q} [\varphi_q(\mathbf{x})^\top \varphi_q(\mathbf{x}')] \approx \tilde{k}_q(\mathbf{x}, \mathbf{x}') = \sum_{i=1}^s z_q(\mathbf{w}_i, \mathbf{x}) z_q(\mathbf{w}_i, \mathbf{x}')$, where $z_q(\mathbf{w}_i, \mathbf{x}_j) := \sqrt{p(\mathbf{w}_i)/q(\mathbf{w}_i)} z_p(\mathbf{w}_i, \mathbf{x}_j)$. Accordingly, the kernel matrix \mathbf{K} can be approximated by $\mathbf{K}_q = \mathbf{Z}_q \mathbf{Z}_q^\top$, where $\mathbf{Z}_q := [\varphi_q(\mathbf{x}_1), \dots, \varphi_q(\mathbf{x}_n)]^\top \in \mathbb{R}^{n \times s}$. Denoting by $z_{q, \mathbf{w}_i}(\mathbf{X})$ the i -th column of \mathbf{Z}_q , we have $\mathbf{K} = \mathbb{E}_{\mathbf{w} \sim p} [z_{p, \mathbf{w}}(\mathbf{X}) z_{p, \mathbf{w}}^\top(\mathbf{X})] = \mathbb{E}_{\mathbf{w} \sim q} [z_{q, \mathbf{w}}(\mathbf{X}) z_{q, \mathbf{w}}^\top(\mathbf{X})]$.

In leverage score sampling based approaches, the designed $q(\mathbf{w})$ rely on the ridge leverage function [42], [43] in KRR

$$l_\lambda(\mathbf{w}_i) = p(\mathbf{w}_i) z_{p, \mathbf{w}_i}^\top(\mathbf{X}) (\mathbf{K} + n\lambda \mathbf{I})^{-1} z_{p, \mathbf{w}_i}(\mathbf{X}), \quad (22)$$

where λ is the regularization parameter in KRR. The integral of $l_\lambda(\mathbf{w})$ is

$$\int_{\mathbb{R}^d} l_\lambda(\boldsymbol{\omega}) d\boldsymbol{\omega} = \text{Tr} [\mathbf{K} (\mathbf{K} + n\lambda \mathbf{I})^{-1}] := d_{\mathbf{K}}^\lambda. \quad (23)$$

The quantity $d_{\mathbf{K}}^\lambda \ll n$ determines the number of independent parameters in a learning problem and hence is referred to as the *number of effective degrees of freedom* [75]. Accordingly, the distribution $q(\mathbf{w})$ is designed by [42] with

$$q(\boldsymbol{\omega}) := \frac{l_\lambda(\boldsymbol{\omega})}{\int l_\lambda(\boldsymbol{\omega}) d\boldsymbol{\omega}} = \frac{l_\lambda(\boldsymbol{\omega})}{d_{\mathbf{K}}^\lambda}. \quad (24)$$

Compared to standard Monte Carlo sampling for RFF, $q(\boldsymbol{\omega})$ -based sampling requires fewer Fourier features and enjoys theoretical guarantees [10], [42], and we will detail this in the next section.

LS-RFF [10]: It use the subset of data to approximate \mathbf{K} in Eq. (23)

$$\text{Tr}(\mathbf{K} (\mathbf{K} + n\lambda \mathbf{I}_n)^{-1}) \approx \text{Tr}(\mathbf{Z}_s \mathbf{Z}_s^\top (\mathbf{Z}_s^\top \mathbf{Z}_s + n\lambda \mathbf{I}_s)^{-1}),$$

which needs $\mathcal{O}(ns^2 + s^3)$ time to generate refined random features. Then they can be equipped with KRR [10] and SVM [9] for prediction.

SLS-RFF [38]: To avoid inverting $s \times s$ matrix in LS-RFF, it designs a simple but effective surrogate leverage function

$$L_\lambda(\mathbf{w}) = p(\mathbf{w}) z_{p, \mathbf{w}}^\top(\mathbf{X}) \left(\frac{1}{n^2 \lambda} (\mathbf{y}\mathbf{y}^\top + n\mathbf{I}) \right) z_{p, \mathbf{w}}(\mathbf{X}), \quad (25)$$

where the additional term $n\mathbf{I}$ and the coefficient $1/(n^2 \lambda)$ in Eq. (25) are to ensure, L_λ is a *surrogate* function that upper bounds l_λ in Eq. (22) due to $L_\lambda(\mathbf{w}_i) \geq l_\lambda(\mathbf{w}_i)$. In this way, sampling random features from the *surrogate* distribution $Q(\boldsymbol{\omega}) = \frac{L_\lambda(\boldsymbol{\omega})}{\int L_\lambda(\boldsymbol{\omega}) d\boldsymbol{\omega}}$ achieves the same time complexity $\mathcal{O}(ns^2)$ with RFF, and can be applied to KRR for prediction [38], and Canonical Correlation Analysis [74].

4.2 Random features selection

Here we briefly review three methods including KA-RFF [46] and EE-RFF [35] by kernel alignment, and CLR-RFF [37] by compressed low-rank approximation.

KA-RFF [46]: It beforehand creates a large number of random features that are generated by RFF, and then solves a simple optimization problem based on kernel alignment [76] to select a subset. The corresponding optimization problem is

$$\max_{\mathbf{a} \in \mathcal{P}_J} \sum_{i,j=1}^n y_i y_j \sum_{t=1}^J a_t z_p(\mathbf{x}_i, \boldsymbol{\omega}_t) z_p(\mathbf{x}_j, \boldsymbol{\omega}_t), \quad (26)$$

where J is the number of the candidate random features by RFF satisfying $J > s$, and \mathbf{a} is the weight vector. The set $\mathcal{P}_J := \{\mathbf{a} : D_f(\mathbf{a} \| \mathbf{1}/J) \leq c\}$ with a specified constant $c > 0$ is defined by χ^2 -divergence on the space of probability distributions, i.e., $f(t) = t^2 - 1$. Here the f -divergence between distribution \mathcal{P} and \mathcal{Q} is $D_f(\mathcal{P} \| \mathcal{Q}) = \int f(\frac{d\mathcal{P}}{d\mathcal{Q}}) d\mathcal{Q}$. Essentially, learning the subset of random features in Eq. (26) is actually equivalent to learning the (sparse) weights of these candidate random features. More directly, finding weights \mathbf{a} makes the kernel matrix match the target kernel $\mathbf{y}\mathbf{y}^\top$. Problem (26) can be efficiently solvable via bisection over a scalar dual variable, in which an ϵ -suboptimal solution can be found in $\mathcal{O}(J \log(1/\epsilon))$.

EE-RFF [35]: It firstly generates a large number of random features by RFF and then selects a subset from them in an energy-based scheme, i.e.

$$\tilde{S}(\boldsymbol{\omega}) = \frac{1}{n} \sum_{i=1}^n y_i z_p(\mathbf{x}_i, \boldsymbol{\omega}).$$

Further, $1/J \sum_{i=1}^J \tilde{S}^2(\boldsymbol{\omega}_j)$ can be associated with kernel polarization for $\{\mathbf{w}_i\}_{i=1}^J$ sampling from $p(\boldsymbol{\omega})$. Accordingly, the top s random features with the top $|\tilde{S}(\cdot)|$ values are selected as the refined random features.

CLR-RFF [37]: It firstly generates a large number of random features and then selects a subset from them in an approximation scheme

$$\min_{\mathbf{a} \in \mathbb{R}^J: \|\mathbf{a}\|_0 \leq s} \frac{1}{n^2} \left\| \mathbf{Z}_J \mathbf{Z}_J^\top - \tilde{\mathbf{Z}}_J(\mathbf{a}) \tilde{\mathbf{Z}}_J(\mathbf{a})^\top \right\|_{\text{F}}^2 = \mathbb{E}_{i,j \stackrel{\text{i.i.d.}}{\sim} [J]} \left[\varphi_p(\mathbf{x}_i)^\top \varphi_p(\mathbf{x}_j) - \tilde{\varphi}_p(\mathbf{x}_i)^\top \tilde{\varphi}_p(\mathbf{x}_j) \right], \quad (27)$$

where $\varphi_p(\mathbf{x}) \in \mathbb{R}^J$ due to the using J random features, and $\tilde{\varphi}_p(\mathbf{x})$ is

$$\tilde{\varphi}_p(\mathbf{x}) := \frac{1}{\sqrt{J}} [a_1 \exp(-i\boldsymbol{\omega}_1^\top \mathbf{x}), \dots, a_J \exp(-i\boldsymbol{\omega}_J^\top \mathbf{x})]^\top,$$

which leads to $\tilde{\mathbf{Z}}_J(\mathbf{a}) = [\tilde{\varphi}_p(\mathbf{x}_1), \tilde{\varphi}_p(\mathbf{x}_2), \dots, \tilde{\varphi}_p(\mathbf{x}_n)] \in \mathbb{R}^{n \times J}$. Therefore, we can generate a Monte-Carlo estimate of the optimization objective function in Eq. (27) by sampling some pairs $i, j \stackrel{\text{i.i.d.}}{\sim} [J]$. In this case, this scheme focuses on the subset of pairs instead of the all data pairs to seek a sparse weight vector \mathbf{a} with only s nonzero elements. Such problem build a small, weighted subset of the data that approximates the full dataset, i.e., the *Hilbert coreset construction problem*. It can be approximately solved by greedy iterative geodesic ascent [77] or Frank-Wolfe based methods [78]. Besides, another way to obtain the compact random features is using Johnson-Lindenstrauss random projection [79] instead of the above data-dependent optimization scheme.

4.3 Kernel learning by random features

The other class is *kernel learning by random features*: these approaches attempt to learn random features in a sophisticated way, e.g., learning the spectral distribution of kernel from the data. From a more general view, the above *random features selection* based algorithms can be regarded in this class. Nevertheless, the key difference between them is that random features in *random features selection* based algorithms are directly generated by RFF, i.e., only learning the weights of these candidate features. Since this topic actually belongs to kernel learning instead of kernel approximation, we do not detail them in our paper.

Representative approaches in this class can be in an *one-stage* or *two-stage* process. The *two-stage* scheme is extremely common in random features, i.e., it firstly obtains the random features, and then incorporates them into kernel methods for prediction. Actually, the above-mentioned *leverage sampling* and *random features selection* based algorithms employ this scheme. In terms of kernel learning by random features, a typical method is proposed in [58], that first learns a spectral distribution of a kernel via an implicit generative model, and then trains a linear model by these learned features.

Compared to the *two-stage* scheme, the *one-stage* based algorithms aim to simultaneously learn the spectral distribution of a kernel and the model by solving a single joint optimization problem or a spectral inference scheme, including: Yu et al. [59] attempt to jointly optimize the nonlinear feature mapping matrix \mathbf{W} and the linear model with the hinge loss. The related optimization problem can be solved in an alternating fashion with SGD. In [53], the kernel alignment in the Fourier domain and SVM are incorporated into a unified framework, which can be also solved in an alternating scheme by Langevin dynamics and projection gradient descent. Furthermore, Wilson and Adams [60] construct stationary kernels as the Fourier transform of a Gaussian mixture based on Gaussian process frequency functions and this model can be extended to learning with Fastfood [61], non-stationary spectral kernel generalisation [52], [80], and the harmonizable mixture kernel [62]. Moreover, Oliva et al. [63] propose a nonparametric Bayesian model, of which $p(\boldsymbol{\omega})$ is modeled as a mixture of Gaussians with a Dirichlet process prior. The parameters of the mixtures of Gaussian and the classifier/regressor model parameter are inferred by MCMC.

4.4 Non-stationary kernels

The above methods are usually suitable to shift-invariant and rotation-invariant kernels. Here we briefly review approximation algorithms for non-stationary kernels.

In [22], the author consider a positive definite kernel k follows with $k(\mathbf{x}, \mathbf{x}') = f(\langle \mathbf{x}, \mathbf{x}' \rangle)$, where f admits a Maclaurin expansion. The polynomial kernel $k(\mathbf{x}, \mathbf{x}') = (\langle \mathbf{x}, \mathbf{x}' \rangle)^b$ and the Hellinger's kernel $k(\mathbf{x}, \mathbf{x}') = \sqrt{\langle \mathbf{x}, \mathbf{x}' \rangle}$ [23] are two dot-product kernels admitting this formulation. Hence, the coefficient of the Maclaurin's expansion can be regarded as a positive measure and we sample this distribution to define estimators for each individual term of the expansion. In their algorithmic implementation, an exponential tail distribution is used to entail huge randomness to estimate higher order terms. In [81], a feature hashing technique, i.e., Count Sketch [82], serves as a specific random projection scheme in a high dimensional space by simple independent hash functions. Further, this technique can be accelerated in the Fourier domain achieving $\mathcal{O}(nr(d + s \log s))$ time and $\mathcal{O}(rd \log s)$ space complexity. If polynomial kernels are considered over a unit sphere,

then the positive-definiteness of polynomial kernels do not hold. That means, polynomial kernels on the sphere are indefinite (real, symmetric, but not positive definite), and thus can be approximated by Gaussian mixtures via RFF [27]. Kernel approximation for more general indefinite kernels can be found in [49] by an infinite Gaussian mixtures in a double-variational bayesian framework.

Besides, the premise of shift-invariant kernels is relaxed and generalized to a larger class of group in [21]. Histogram intersection kernels are investigated by [83] and are further generalized to a class of additive homogeneous kernels in [23].

5 THEORETICAL ANALYSIS

This section reviews a branch of theoretical results that address the following two questions mentioned in the introduction:

- 1) how many random features are needed to ensure a high quality estimator in kernel approximation?
- 2) how many random features are needed to incur no loss of empirical risk and expected risk in a learning estimator?

Answering the above questions can help us understand the approximation quality and the generalization properties of RFF. Figure 3 shows the taxonomy of references on these two aspects with more and more refined results. The approximation error for uniform convergence focuses on $\|k - \tilde{k}\|_\infty$ [8], [39], [40], $\|k - \tilde{k}\|_{L^r}$ with $1 \leq r < \infty$ [40], Δ -spectral approximation [42], [68], and (Δ_1, Δ_2) -spectral approximation [36]. Regarding to the empirical risk under the fixed design setting, the expected in-sample prediction error of the KRR estimator can be bounded based on Δ -spectral approximation [42] and (Δ_1, Δ_2) -spectral approximation [36]. For the expected risk, a series of research works investigate the generalization properties of $p(\omega)$ -sampling and $q(\omega)$ -sampling with/without the Lipschitz continuity requirement for loss functions, e.g., KRR [10], [44] and SVM [9], [20], [43] under different assumptions. Rahimi and Recht [20] present the earliest result on learning with RFF under the Lipschitz continuity requirement for loss functions, i.e., a $\Omega(n)$ number of random features are needed to incur no loss of learning accuracy. This result is improved in [10] with $\Omega(\sqrt{n} \log n)$ random features or even less when using the Gaussian kernel. If we consider the data-dependent sampling $\{\omega_i\}_{i=1}^s \sim q(\omega)$, the above theoretical results can be further improved in [9], [10], [43] under different conditions. Since the above analysis requires the Lipschitz continuity of loss functions, which excludes the squared loss in KRR, Rudi et al. [44] demonstrate that $\Omega(\sqrt{n} \log n)$ random features by RFF suffice for an optimal learning rate $\mathcal{O}(1/\sqrt{n})$ in a minimax case. Further, a refined analysis is given in [10] under the $p(\omega)$ -sampling and $q(\omega)$ -sampling settings.

5.1 Approximation error

Table 2 summarizes convergence rates, the upper bound of the growing diameter, and the required sample complexity of various theoretical results under different metrics. Here the sample complexity indicates that when instantiated with s random features, it has maximum error at most ϵ . The earliest work on approximation error is conducted by Rahimi and Recht [8], which provides a covering-number upper bound on the error probability for uniform convergence as follows.

Theorem 3. (Uniform convergence of Fourier features [8], [39]) Let \mathcal{S} be a compact subset of \mathbb{R}^d with diameter $\text{diam}(\mathcal{S})$, denoted

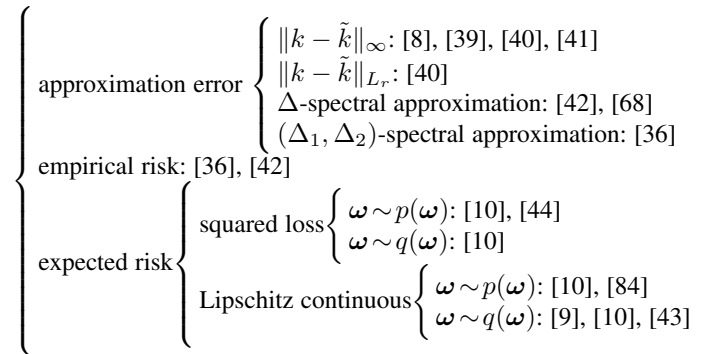


Figure 3. Taxonomy of theoretical results on random features.

as $|\mathcal{S}|$. Then, for the approximated kernel \tilde{k} obtained by RFF, we have

$$\Pr \left[\|k - \tilde{k}\|_\infty \geq \epsilon \right] \leq C_d \left(\frac{\sigma_p |\mathcal{S}|}{\epsilon} \right)^{\frac{2d}{d+2}} \exp \left(-\frac{s\epsilon^2}{4(d+2)} \right)$$

where $\sigma_p^2 = \mathbb{E}_p[\omega^\top \omega] = \text{tr} \nabla^2 k(0) \in \mathcal{O}(d)$ is the second moment of the Fourier transform of k , and $C_d := 2^{\frac{6d+2}{d+2}} \left(\left(\frac{2}{d}\right)^{\frac{d}{d+2}} + \left(\frac{d}{2}\right)^{\frac{2}{d+2}} \right) \leq 256$ in [8] and is further improved to $C_d \leq 66$ in [39].

Based on the above theorem, with $s := \Omega\left(\frac{d}{\epsilon^2} \log\left(\frac{1}{\epsilon\delta}\right)\right)$, one can ensure the same probability greater than $1 - \delta$. The uniform approximation results are also suitable to dot-product kernels by random Maclaurin feature maps (see Theorem 8 in [22]). Further, Sriperumbudur and Szabó [40] revisit the bound by using a Rademacher complexity approach instead of covering numbers using in [8], [39] as follows.

Theorem 4. (Theorem 1 in [40]) Under the same assumption of Theorem 3, we have

$$\Pr \left[\|k - \tilde{k}\|_\infty \geq \frac{h(d, |\mathcal{S}|, \sigma_p) + \sqrt{2}\epsilon}{\sqrt{s}} \right] \leq e^{-\epsilon},$$

where $h(d, |\mathcal{S}|, \sigma_p)$ is a function of d , $|\mathcal{S}|$, and σ_p . Further, for better comparison, the above inequality can be rewritten as [41]

$$\Pr \left[\|k - \tilde{k}\|_\infty \geq \epsilon \right] \leq [(\sigma_p + 1)(2|\mathcal{S}| + 1)]^{1024d} \exp \left(-\frac{s\epsilon^2}{2} + \frac{256d}{\log(2|\mathcal{S}| + 1)} \right)$$

Theorem 4 shows that \tilde{k} is a consistent estimator of k in the topology of compact convergence as $s \rightarrow \infty$ with the convergence rate $\mathcal{O}_p(\sqrt{s^{-1} \log |\mathcal{S}|})$. When compared to the results presented in [8], [39], Theorem 4 requires fewer features to achieve the same approximation accuracy of ϵ . Furthermore, the approximation error can be improved by the following theorem.

Theorem 5. (Theorem 1 in [41]) Under the same assumption of Theorem 3, for the Gaussian kernel k , we have

$$\Pr \left[\|k - \tilde{k}\|_\infty \geq \epsilon \right] \leq \frac{3}{s^{1/3}} \left(\frac{|\mathcal{S}|}{\epsilon} \right)^{2/3} \exp \left(-\frac{s\epsilon^2}{12} \right).$$

Theorem 5 improves the error probability for uniform convergence of [40], which is independent of d , but achieves the same convergence rate. Actually, the above three results elucidate that the sample complexity is required to be $\Omega(n)$, i.e., the needed number

of random features, suffices for approximation. Besides, the order of dependence on $|\mathcal{S}|$ is also important as it determines the number of random features that are needed to achieve a given approximation accuracy. It restricts the increasing rate of $|\mathcal{S}|$ regarding to s , e.g., Theorem 4, 5 ensures consistency even when $|\mathcal{S}|$ grows exponentially in s whereas Theorem 3 requires $|\mathcal{S}|$ does not grow faster than $\sqrt{s/\log s}$ for consistency.

Apart from studying bounds of the maximum approximation error, based on Theorem 4, the approximation error in L^r -norm with $1 \leq r < \infty$ or $2 \leq r < \infty$ over any compact set $\mathcal{S} \subseteq \mathbb{R}^d$ is given by [40], see in Table 2. Here we omit the details for ease of description.

Avron et al. [42] argue that the above point-wise distance $\|k - \tilde{k}\|$ in some metric spaces is not accurate to throughout evaluate the approximation bound, and thus focus on Δ -spectral approximation bounds as follows.

Definition 1. (Δ -spectral approximation [42]) For $0 \leq \Delta < 1$, a symmetric matrix \mathbf{A} is a Δ -spectral approximation of another symmetric matrix \mathbf{B} , if $(1 - \Delta)\mathbf{B} \preceq \mathbf{A} \preceq (1 + \Delta)\mathbf{B}$.

According to this definition, spectral approximation bounds on the entire kernel matrix admits the following form

$$(1 - \Delta)(\mathbf{K} + \lambda\mathbf{I}_n) \preceq \mathbf{Z}\mathbf{Z}^\top + \lambda\mathbf{I}_n \preceq (1 + \Delta)(\mathbf{K} + \lambda\mathbf{I}_n),$$

for some $\Delta < 1$. Hence, the aforementioned approximation question is transformed to: how big should s be so that $\mathbf{Z}\mathbf{Z}^\top$ is Δ -spectral approximation of $\mathbf{K} + \lambda\mathbf{I}_n$? The following spectral approximation results can answer this question.

Theorem 6. (Theorem 7 in [42]) Let $\Delta \leq 1/2$ and $\delta \in (0, 1)$, denote $n_\lambda := n/\lambda$, and assume that $\|\mathbf{K}\|_2 \geq \lambda$ and $\{\omega_i\}_{i=1}^s$ are sampled independently from $p(\omega)$, i.e., obtained by RFF. If the total number of random features satisfies

$$s \geq \frac{8}{3}\Delta^{-2}n_\lambda \log\left(16d_{\mathbf{K}}^\lambda/\delta\right),$$

$\mathbf{Z}\mathbf{Z}^\top$ is Δ -spectral approximation of $\mathbf{K} + \lambda\mathbf{I}_n$

$$\Pr\left[(1 - \Delta)(\mathbf{K} + \lambda\mathbf{I}_n) \preceq \mathbf{Z}\mathbf{Z}^\top + \lambda\mathbf{I}_n \preceq (1 + \Delta)(\mathbf{K} + \lambda\mathbf{I}_n)\right] \leq 16d_{\mathbf{K}}^\lambda \exp\left(\frac{-3s\Delta^2}{8n_\lambda}\right) \leq \delta.$$

Theorem 6 demonstrates that if we use the classic random Fourier features sampling distribution, $\Omega(n)$ random Fourier features suffice for spectral approximation, which attains the similar results with that of using point-wise distance. Further, Choromanski et al. [68] present a non-asymptotic comparison between RFF and ORF based on the spectral approximation.

Theorem 7. (Theorem 5.4 in [68]) For the Gaussian kernel, denote $\tilde{\Delta}$ as the smallest positive number such that $\tilde{\mathbf{K}} + \lambda n\mathbf{I}_n$ is a Δ -spectral approximation of $\mathbf{K} + \lambda n\mathbf{I}_n$, where $\tilde{\mathbf{K}}$ is an approximate kernel matrix obtained by RFF or ORF, then for any $\epsilon > 0$

$$\Pr[\tilde{\Delta} > \epsilon] \leq \frac{B}{\epsilon^2\sigma_{\min}^2},$$

where $B := \mathbb{E}[\|\tilde{\mathbf{K}} - \mathbf{K}\|_F^2]$ and σ_{\min}^2 is the smallest singular value of $\mathbf{K} + \lambda n\mathbf{I}_n$. In particular, if B^{ORF} refers to the value of B for the estimator ORF and B^{RFF} denotes the one for RFF, then

$$B^{\text{RFF}} - B^{\text{ORF}} = \frac{s-1}{s} \left(\frac{1}{2d} \sum_{i,j=1}^n \frac{\|\mathbf{x}_i - \mathbf{x}_j\|_2^4}{\sigma^2} e^{-\frac{\|\mathbf{x}_i - \mathbf{x}_j\|_2^2}{\sigma^2}} + \mathcal{O}\left(\frac{1}{d}\right) \right).$$

Theorem 7 demonstrates that $B^{\text{RFF}} > B^{\text{ORF}}$ exists in any case for the Gaussian kernel. For better understanding the order of the upper bound of $\Pr[\tilde{\Delta} > \epsilon]$, we have $B \in \mathcal{O}(n^2/s)$ due to $\mathbb{V}[\text{RFF}], \mathbb{V}[\text{ORF}] \in \mathcal{O}(1/s)$. Besides, since the Gaussian kernel admits the exponential decay (we detail this in Assumption 4), we have $\sigma_{\min}^2 = \Omega(n^2\lambda^2)$. So the upper bound of $\Pr[\tilde{\Delta} > \epsilon]$ is the order of $\mathcal{O}(\frac{1}{s\lambda^2})$. Accordingly, it suffices to take $s := \Omega(n^{2\alpha})$ with $\alpha \in (0, 1]$ random features to get an upper bound of order $\mathcal{O}(1)$ when n tends to infinity. Based on the results, we find that, the current analysis cannot ensure that less than $\Omega(n)$ random Fourier features is enough for spectral approximation when using RFF or ORF.

If we consider the data-dependent sampling, i.e., $\{\omega_i\}_{i=1}^s$ are sampled independently from the empirical ridge leverage score distribution $q(\omega) = l_\lambda(\omega)/d_{\mathbf{K}}^\lambda$ in Eq. (24) instead of the standard $p(\omega)$, the results in Theorem 6 can be improved by the following theorem.

Theorem 8. (Lemma 6 in [42]) Let $\Delta \leq 1/2$ and $\delta \in (0, 1)$ assume that $\|\mathbf{K}\|_2 \geq \lambda$ and $\{\omega_i\}_{i=1}^s \sim q(\omega)$. If the total number of random features satisfies

$$s \geq \frac{8}{3}\Delta^{-2}d_{\mathbf{K}}^\lambda \log\left(16d_{\mathbf{K}}^\lambda/\delta\right),$$

$\mathbf{Z}\mathbf{Z}^\top$ is Δ -spectral approximation of $\mathbf{K} + \lambda\mathbf{I}_n$

$$\Pr\left[(1 - \Delta)(\mathbf{K} + \lambda\mathbf{I}_n) \preceq \mathbf{Z}\mathbf{Z}^\top + \lambda\mathbf{I}_n \preceq (1 + \Delta)(\mathbf{K} + \lambda\mathbf{I}_n)\right] \leq 16d_{\mathbf{K}}^\lambda \exp\left(\frac{-3s\Delta^2}{8d_{\mathbf{K}}^\lambda}\right) \leq \delta.$$

Theorem 8 shows that if we could sample using the ridge leverage function, then $\Omega(d_{\mathbf{K}}^\lambda \log d_{\mathbf{K}}^\lambda)$ samples, less than $\Omega(n_\lambda \log d_{\mathbf{K}}^\lambda)$, suffice for spectral approximation of \mathbf{K} .

In [36], the authors extend Δ -spectral approximation to (Δ_1, Δ_2) -spectral approximation as Δ_1 and Δ_2 impact generalization differently. The (Δ_1, Δ_2) -spectral approximation is defined as follows.

Definition 2. ((Δ_1, Δ_2) -spectral approximation [36]) For $\Delta_1, \Delta_2 \geq 0$, a symmetric matrix \mathbf{A} is a (Δ_1, Δ_2) -spectral approximation of another symmetric matrix \mathbf{B} , if $(1 - \Delta_1)\mathbf{B} \preceq \mathbf{A} \preceq (1 + \Delta_2)\mathbf{B}$.

According to this definition, Zhang et al. [36] further quantize each random Fourier feature ω_i to a low-precision b -bit representation, thus allowing us to store more features in the same amount of space. The approximation error is given by the following theorem.

Theorem 9. (Theorem 2 in [36]) Let $\tilde{\mathbf{K}}$ be an s -features b -bit LP-RFF approximation of a kernel matrix \mathbf{K} and $\delta \in (0, 1)$ assume that $\|\mathbf{K}\|_2 \geq \lambda \leq \delta_b^2 = 2/(2^b - 1)^2$ and define $a := 8 \text{tr}(\mathbf{K} + \lambda\mathbf{I}_n)^{-1}(\mathbf{K} + \delta_b^2\mathbf{I}_n)$. Assume that $\Delta_1 \leq 3/2$ and $\Delta_2 \in [\frac{\delta_b^2}{\lambda}, \frac{3}{2}]$, If the total number of random features satisfies

$$s \geq \frac{8}{3}n_\lambda \max\left\{\frac{2}{\Delta_1}, \frac{2}{\Delta_2 - \delta_b^2/\lambda}\right\} \log\left(\frac{a}{\delta}\right),$$

$\tilde{\mathbf{K}}$ is (Δ_1, Δ_2) -spectral approximation of $\mathbf{K} + \lambda\mathbf{I}_n$

$$\Pr\left[(1 - \Delta)(\mathbf{K} + \lambda\mathbf{I}_n) \preceq \tilde{\mathbf{K}} + \lambda\mathbf{I}_n \preceq (1 + \Delta)(\mathbf{K} + \lambda\mathbf{I}_n)\right] \leq a \left(\exp\left(\frac{-3s\Delta_1^2}{4n_\lambda(1 + 2/3\Delta_1)}\right) + \exp\left(\frac{-3s(\Delta_2 - \delta_b^2/\lambda)^2}{4n_\lambda(1 + 2/3(\Delta_2 - \delta_b^2/\lambda))}\right) \right).$$

Table 2
Comparison of convergence rates and required random features for kernel approximation error.

Metric	Results	Convergence rate	Upper bound of $ \mathcal{S} $	Required random features s
$\ k - \tilde{k}\ _\infty$	Theorem 3 ([8], [39])	$\mathcal{O}_p\left(\mathcal{S} \sqrt{\frac{\log s}{s}}\right)$	$ \mathcal{S} \leq \Omega\left(\sqrt{\frac{s}{\log s}}\right)$	$s \geq \Omega\left(d\epsilon^{-2} \log \frac{ \mathcal{S} }{\epsilon}\right)$
	Theorem 4 (Theorem 1 in [40])	$\mathcal{O}_p\left(\sqrt{\frac{\log \mathcal{S} }{s}}\right)$	$ \mathcal{S} \leq \Omega(s^c)^1$	$s \geq \Omega(d\epsilon^{-2} \log \mathcal{S})$
	Theorem 5 (Theorem 1 in [41])	$\mathcal{O}_p\left(\sqrt{\frac{\log \mathcal{S} }{s}}\right)$	$ \mathcal{S} \leq \Omega(s^c)$	$s \geq \Omega(\epsilon^{-2} \log \mathcal{S})$
$\ k - \tilde{k}\ _{L^r} (1 \leq r < \infty)$	(Corollary 2 in [40])	$\mathcal{O}_p\left(\mathcal{S} ^{\frac{2d}{r}} \sqrt{\frac{\log \mathcal{S} }{s}}\right)$	$ \mathcal{S} \leq \Omega\left(\left(\frac{s}{\log s}\right)^{\frac{r}{4d}}\right)$	$s \geq \Omega(d\epsilon^{-2} \log \mathcal{S})$
$\ k - \tilde{k}\ _{L^r} (2 \leq r < \infty)$	(Theorem 3 in [40])	$\mathcal{O}_p\left(\mathcal{S} ^{\frac{2d}{r}} \sqrt{\frac{1}{s}}\right)$	$ \mathcal{S} \leq \Omega\left(s^{\frac{r}{4d}}\right)$	$s \geq \Omega(d\epsilon^{-2} \log \mathcal{S})$
Δ -spectral approximation	Theorem 6 (Theorem 7 in [42])	$\mathcal{O}_p\left(\sqrt{\frac{n_\lambda}{s}}\right)$	-	$s \geq \Omega(n_\lambda \log d_\lambda^K)$
	Theorem 7 (Theorem 5.4 in [68])	$\mathcal{O}_{\text{RFF/ORF}}\left(\frac{1}{s\lambda^2}\right)$	-	$s \geq \Omega(n^{2\alpha})$
	Theorem 8 (Lemma 6 in [42])	$\mathcal{O}_q\left(\sqrt{\frac{d_\lambda^K}{s}}\right)$	-	$s \geq \Omega(d_\lambda^K \log d_\lambda^K)$
(Δ_1, Δ_2) -spectral approximation	Theorem 9 (Theorem 2 in [36])	$\mathcal{O}_{\text{LP}}\left(\sqrt{\frac{n_\lambda}{s}}\right)^2$	-	$s \geq \Omega(n_\lambda \log d_\lambda^K)$

¹ c is some constant satisfying $0 < c < 1$.

² LP denotes that $\{\omega_i\}_{i=1}^s$ are obtained by RFF and then are quantized to a Low-Precision b -bit representation, refer to [36].

Theorem 9 shows that when the quantization noise is small relative to the regularization parameter, using low precision has minimal impact on the number of features required for the (Δ_1, Δ_2) -spectral approximation. To be specific, as $s \rightarrow \infty$, Δ_1 converges to zero for any precision b , while Δ_2 converges to a value upper bounded by δ_b^2/λ . If $\delta_b^2/\lambda \ll \Delta_2$, using b -bit precision will have negligible effect on the number of features required to attain this Δ_2 .

5.2 Risk and generalization property

The above studies on approximation error is actually a middle-ground way to an end. The generalization properties of random features based algorithms are more important in theory and we detail them in this section. Regarding to the expected risk, a series of research works investigate the generalization properties of $p(\omega)$ -sampling and $q(\omega)$ -sampling with/without the Lipschitz continuity requirement for loss functions, e.g., KRR [10], [44] and SVM [9], [20], [43] under different assumptions.

5.2.1 Assumptions

Before we detail these theoretical results, here we present the assumptions they needed. Some assumptions are technical and sophisticated, maybe needs specialized knowledge in learning theory. Accordingly, we summarize and re-organize them in four classes as shown in Figure 4, including i) the existence of f_ρ (Assumption 1) and its stronger one (Assumption 8); ii) quality of random features (Assumptions 2, 6, 7); iii) noise condition (Assumptions 3, 9, 10); iv) eigenvalue decays (Assumptions 4, 5).

We first introduce the following three basic assumptions that all of the presented results need.

Assumption 1. We assume throughout that f_ρ exists.

Note that, actually, since we consider a potentially infinite dimensional RKHS \mathcal{H} , possibly universal [85], the existence of the target function f_ρ cannot be guaranteed. However, if we consider

a subspace of \mathcal{H} , i.e., $\mathcal{H}_R = \{f \in \mathcal{H} : \|f\| \leq R\}$, with R fixed a prior. In this case, a minimizer of risk $\mathcal{E}(f)$ always exists, but R needs to be fixed a prior and \mathcal{H}_R cannot be universal. Clearly, assuming f_ρ to exist, implies it belongs to a ball of radius $R_{\rho, \mathcal{H}}$. However, the presented results do not require prior knowledge of $R_{\rho, \mathcal{H}}$ and hold uniformly over all finite radii.

Assumption 2. (random features are bounded and continuous) For the shift-invariant kernel k , we assume that $z(\omega, \mathbf{x})$ in Eq. (6) is continuous in both variables and bounded, i.e., there exists $\kappa \geq 1$ such that $|z(\omega, \mathbf{x})| < \kappa$ for any $\mathbf{x} \in \mathcal{X}$ and $\omega \in \mathbb{R}^d$.

Assumption 3. (output condition on y) For any $\mathbf{x} \in \mathcal{X}$,

$$\mathbb{E}[|y|^t | \mathbf{x}] \leq \frac{1}{2} t! \sigma^2 B^{t-2}, \quad \forall t \geq 2.$$

Note that the above assumption is a natural generalization of the boundedness on y . It is satisfied when y is bounded, sub-Gaussian, or sub-exponential. In particular, if $y \in [-\frac{b}{2}, \frac{b}{2}]$ almost surely, with $b > 0$, then the above assumption is satisfied with $\sigma = B = b$.

The above three assumptions are the most basic ones and thus all of the presented results need them. So we omit them for description simplicity when we introduce their results. In the next, we present some additional/advanced assumptions that some theoretical results need.

Eigenvalue Decay Assumptions: Random features based algorithms often consider the following eigenvalue assumption of the kernel matrix, which is actually related to characterize the ‘‘size of the considered RKHS.

Assumption 4. (Eigenvalue decays [43], [75]) Denote $u_i = \Theta(v_i)$, which means that there exists strictly positive constants A and B such that $Au_i \leq v_i \leq Bu_i$ for all $i = 1, 2, \dots, n$. The eigenvalues of a kernel matrix \mathbf{K} is assumed to be with the form $\Theta(n\mu_i)$, $i = 1, 2, \dots, n$, so that $\text{tr}(\mathbf{K}) = \Theta(n)$. Accordingly, we often consider the following three eigenvalue decays:

- *geometric/exponential decay:* $v_i = \mathcal{O}(\exp(-i^{1/c}))$ indicates $\lambda_i \propto n \exp(-i^{1/c})$, $c > 0$. It holds by the Gaussian

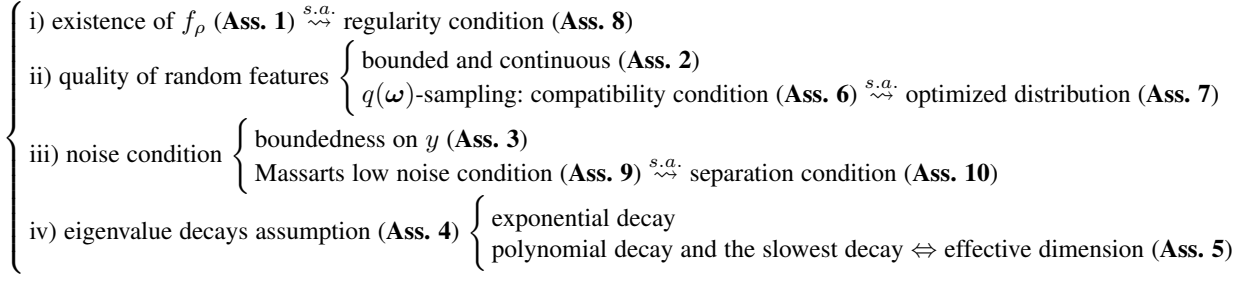


Figure 4. Relationship between the needed assumptions. The notation $A \overset{s.a.}{\rightsquigarrow} B$ means that B is a stronger assumption than A.

kernel with a sub-Gaussian marginal distribution $\rho_{\mathcal{X}}$. In this case, $d_{\mathbf{K}}^{\lambda} \leq \log(R_0/\lambda)$, where R_0 is some constant such that $\mathbb{E}k(\mathbf{x}, \mathbf{x}) = \text{tr}(\Sigma) := R_0^2$.

- *polynomial decay*: $v_i = \mathcal{O}(i^{-2t})$ means $\lambda_i \propto ni^{-2t}$ with $t > \frac{1}{2}$, e.g., \mathcal{H} is a Sobolev space. So we have $d_{\mathbf{K}}^{\lambda} \leq (1/\lambda)^{1/2t}$.
- *slowest polynomial decay*: $v_i = \mathcal{O}(1/i)$ leads to $\lambda_i \propto n/i$. Thus we have $d_{\mathbf{K}}^{\lambda} \leq (1/\lambda)$.

We give some remarks of this assumption here. For shift-invariant kernels, if the RKHS is small, the eigenvalues of the kernel matrix \mathbf{K} often admits a fast decay. Accordingly, functions in the RKHS are potentially smoother than what is necessary so as to obtain a good prediction performance. Instead, if the RKHS is large, the eigenvalue decay does not exhibit fast enough. In other words, functions in the RKHS are not smooth enough, which would lead to a sub-optimal convergence rate for prediction. To make the above description precise, we need a key quantity, i.e., the integral operator [43], [44] defined by the kernel k and the marginal distribution $\rho_{\mathcal{X}}$. Let the integral operator $\Sigma : L_2(d\rho) \rightarrow L_2(d\rho)$ be defined as

$$(\Sigma g)(\mathbf{x}) = \int_{\mathcal{X}} k(\mathbf{x}, \mathbf{x}')g(\mathbf{x}')d\rho_{\mathcal{X}}(\mathbf{x}'), \quad \forall g \in L_2(d\rho).$$

Since $\int_{\mathcal{X}} k(\mathbf{x}, \mathbf{x}) d\rho(\mathbf{x})$ is finite, the operator Σ is self-adjoint, positive definite and trace-class. It can be further represented as $\Sigma = \mathfrak{J}\mathfrak{J}^*$ with the inclusion operator $\mathfrak{J} : \mathcal{H} \rightarrow L_2(d\rho)$, $(\mathfrak{J}f) = f$, $\forall f \in \mathcal{H}$. And \mathfrak{J}^* is the adjoint of \mathfrak{J} [86] is

$$\mathfrak{J}^* : L_2(d\rho) \rightarrow \mathcal{H}, \quad (\mathfrak{J}^*f)(\cdot) = \int_{\mathcal{X}} k(\mathbf{x}, \cdot)f(\mathbf{x})d\rho_{\mathcal{X}},$$

due to the self-adjoint property of the Hilbert spaces $L_2(d\rho)$ and \mathcal{H} . The approximation of the inclusion operator $\mathfrak{J} : \mathcal{H} \rightarrow L_2(d\rho)$ is $\mathfrak{A} : \mathcal{H} \rightarrow L_2(d\rho)$, $(\mathfrak{A}\beta) = \langle \varphi(\cdot), \beta \rangle_{\tilde{\mathcal{H}}}$, $\forall \beta \in \mathbb{R}^s$. Figure 5 presents the relationship between various spaces via different operators.

The integration operator Σ plays a significant role to analysis the hypothesis space in theory. To be specific, the decay rate of the spectrum of Σ characterizes the capacity of the hypothesis space to search for the solution, which further determines the number of random features required in the learning process. Rudi and Rosasco [44] consider the following assumption.

Assumption 5. (effective dimension $\mathcal{N}(\lambda)$). Let $\lambda > 0$, there exists $Q > 0$ and $\gamma \in [0, 1]$ such that for any $\lambda > 0$

$$\begin{aligned} \mathcal{N}(\lambda) &:= \text{tr}((\Sigma + \lambda I)^{-1}\Sigma) = \mathbb{E}_{\omega} \left\| (\Sigma + \lambda I)^{-1/2}\varphi(\mathbf{x}) \right\|_{L_2(d\rho)}^2 \\ &\leq Q^2\lambda^{-\gamma}. \end{aligned} \quad (28)$$

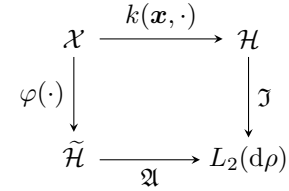


Figure 5. Maps between various spaces.

The effective dimension $\mathcal{N}(\lambda)$ can be regarded as a “measure of size” of the RKHS, and is actually the operator form of $d_{\mathbf{K}}^{\lambda}$ in Eq. (23). In particular, it holds if the eigenvalues λ_i of Σ decay as $i^{-1/\gamma}$, which covers the polynomial decay and the slowest decay in Assumption 4 with $\gamma := 1/2t$. The case $\gamma = 0$ is the more benign situation, whereas $\gamma = 1$ is the worst case.

Quality of Random Features: here we consider some technical assumptions on the quality of random features. The leverage score in Eq. (22) admits an operator form with

$$\mathcal{F}_{\infty}(\lambda) := \sup_{\omega} \left\| (\Sigma + \lambda I)^{-1/2}\varphi(\mathbf{x}) \right\|_{L_2(d\rho)}^2, \quad \lambda > 0,$$

which is also called as the maximum random features dimension [44]. We can directly obtain $\mathcal{N}(\lambda) \leq \mathcal{F}_{\infty}(\lambda)$ based on their definitions. Roughly speaking, when the random features is “good”, it is easy to control its leverage score by the decay of the spectrum of Σ . Further, fast learning rates with fewer random features can be achieved if they are somewhat *compatible* with the data distribution by the compatibility condition.

Assumption 6. (compatibility condition [44]) Define the maximum random features dimension (i.e., the leverage score in Eq. (22)), assume there exists $\varrho \in [0, 1]$, and $F > 0$ such that $\mathcal{F}_{\infty}(\lambda) \leq F\lambda^{-\varrho}$, $\forall \lambda > 0$.

In particular, it always holds by $\mathcal{F}_{\infty}(\lambda) \leq \kappa^2\lambda^{-1}$ when z is uniformly bounded by κ . So $\varrho = 1$ is the worst case, indicating that random features are sampled in an independent way. The favorable situation is $\varrho = \gamma$, which means that $\mathcal{N}(\lambda) \leq \mathcal{F}_{\infty}(\lambda) \leq \mathcal{O}(n^{-\alpha\gamma})$. In [9], the authors consider the following assumption.

Assumption 7. (optimized distribution [9]). The feature mapping $z(\omega, \mathbf{x})$ is called optimized if there is a small constant λ_0 such that for any $\lambda \leq \lambda_0$

$$\mathcal{F}_{\infty}(\lambda) \leq \mathcal{N}(\lambda) = \sum_{i=1}^{\infty} \frac{\lambda_i(\Sigma)}{\lambda_i(\Sigma) + \lambda}.$$

Actually, the above assumption holds only when $\mathcal{F}_{\infty}(\lambda) = \mathcal{N}(\lambda)$, which is a stronger one than compatibility condition

in Assumption 6. Sampling from $q(\boldsymbol{w})$ naturally satisfies this assumption with $\mathcal{F}_\infty(\lambda) = \mathcal{N}(\lambda)$.

Existence of f_ρ : we consider some nice properties on f_ρ by the following assumption.

Assumption 8. (regularity condition in [44]) *There exists $1/2 \leq r \leq 1$ and $g \in L_2(\text{d}\rho)$ such that*

$$f_\rho(\boldsymbol{x}) = (\Sigma^r g)(\boldsymbol{x}) \quad \text{almost surely.}$$

This assumption can be regarded as regularity/sparsity of f_ρ , which requires the expansion of f_ρ on the basis given by the integral operator Σ . Note that this is a more strict assumption than that of the existence of f_ρ . To be specific, the case $r = \frac{1}{2}$ is the worst case (not too much regularity/sparsity), and can be equivalent to assuming f_ρ exists.

Noise Condition: Sun et al. [9] consider the following two assumptions.

Assumption 9. (Massart's low noise condition [9]) *There exists $V \geq 2$ such that*

$$|\mathbb{E}_{(\boldsymbol{x}, y) \sim \rho}[y|\boldsymbol{x}]| \geq 2/V.$$

Assumption 10. (separation condition [9]) *The points in \mathcal{X} can be collected in to two sets according to their labels as follows*

$$\begin{aligned} X_1 &:= \{\boldsymbol{x} \in \mathcal{X} | \mathbb{E}(y|\boldsymbol{x}) > 0\} \\ X_{-1} &:= \{\boldsymbol{x} \in \mathcal{X} | \mathbb{E}(y|\boldsymbol{x}) < 0\} \end{aligned}$$

The distance of a point $\boldsymbol{x} \in X_i$ to the set X_{-i} is denoted by $\Delta(\boldsymbol{x})$. We say that the data distribution satisfies a separation condition if there exists $\Delta > 0$ such that $\rho_{\mathcal{X}}(\Delta(\boldsymbol{x}) < c) = 0$.

The above two assumptions describes the noise level in the labels, and thus can be incorporated into a unified assumption framework [87] as follows. Define the regression function $\eta(\boldsymbol{x}) = \mathbb{E}(y|X = \boldsymbol{x})$ in binary classification problems, suppose there exists $h \in (0, 1]$ such that for any $\boldsymbol{x} \in \mathcal{X}$, the Massart's low noise condition is $|\eta(\boldsymbol{x})| \geq h$, where h characterizes the level of noise in classification problems: for small h , $\eta(\boldsymbol{x})$ is close to zero. In this case, it is difficult to obtain correct classification. To more flexibly describe the level of the noise, the Massart's condition can be extended to the following Tsybakov's low noise assumption. That is, if there exists a constant $C > 0$ such that for all sufficiently small $t > 0$, we have

$$\Pr(\{\boldsymbol{x} \in \mathcal{X} : |2\eta(\boldsymbol{x}) - 1| \leq t\}) \leq C \cdot t^q,$$

for some $q > 0$. The above separation condition in Assumption 10 is an extreme case of the Tsybakov's noise assumption [87] with $q = \infty$. Noise-free distributions admit this, and thus the conditional probability η is bounded away from $1/2$.

5.2.2 Squared loss in KRR

In this section, we review all presented results with the squared loss in KRR. Table 3 summarizes the needed key assumptions, the derived learning rates, and the required number of random features under the *independent/dependent* settings.

A remarkable process in generalization properties of random features is conducted by Rudi and Rosasco [44], which is the first work to show that, for KRR, under some mild assumptions and appropriately chosen parameters, $\Omega(\sqrt{n} \log n)$ random features suffice for minimax optimal rates. Here we summarize them via $p(\boldsymbol{w})$ -sampling and $q(\boldsymbol{w})$ -sampling under different assumptions as follows.

Theorem 10. (Generalization bound: Theorem 3 in [44]) *Suppose that the regularity condition in Assumption 8 holds with $r \in [\frac{1}{2}, 1]$, the compatibility condition in Assumption 6 holds with $\varrho \in [0, 1]$, the effective dimension in Assumption 5 holds with $\gamma \in [0, 1]$. Assuming $n \geq n_0$ and choosing $\lambda := n^{\frac{1}{2r+\gamma}}$, if the number of random features satisfies*

$$s \geq c_0 n^{\frac{\alpha+(2r-1)(1+\gamma-\alpha)}{2r+\gamma}} \log \frac{108\kappa^2}{\lambda\delta},$$

then the excess risk of $\widetilde{f_{\boldsymbol{z}, \lambda}}$ can be upper bounded as

$$\mathcal{E}(\widetilde{f_{\boldsymbol{z}, \lambda}}) - \mathcal{E}(f_\rho) = \left\| \widetilde{f_{\boldsymbol{z}, \lambda}} - f_\rho \right\|_{L_2(\text{d}\rho)} \leq c_1 \log^2 \frac{18}{\delta} n^{-\frac{2r}{2r+\gamma}},$$

where c_0, c_1 are constants independent of n, λ, δ , and n_0 does not depends on n, λ, f_ρ, ρ .

Note that the error is exactly the distance in $L_{\rho_{\boldsymbol{x}}}^2$ due to the strong convexity of the squared loss, where $L_{\rho_{\boldsymbol{x}}}^2$ is a weighted L^2 -space with the norm $\|f\|_{L_{\rho_{\boldsymbol{x}}}^2} = \left(\int_{\mathcal{X}} |f(\boldsymbol{x})|^2 \text{d}\rho_{\boldsymbol{x}}(\boldsymbol{x}) \right)^{1/2}$. Under different assumptions, Theorem 10 presents various results on the convergence rates. Theorem 1 in [44] is the simplest version with minimum number of assumptions. It only requires the aforementioned three basic assumptions, i.e., the existence of f_ρ , $|y| \leq y_0$ almost surely, and z is bounded continuous. So it is the worst case with $\varrho = \gamma = 1$ and $r = 1/2$. By choosing $\lambda := n^{-1/2}$, we requires $\Omega(\sqrt{n} \log n)$ random features to achieve the minimax convergence rate at $\mathcal{O}(n^{-1/2})$, see in Table 3.

Further, Theorem 2 in [44] is more refined, which considers the capacity of the RKHS, evaluated by the effective dimension Assumption 5 with $\gamma \in [0, 1]$ and the regularity condition with $r \in [\frac{1}{2}, 1]$. To be specific, $\gamma = 1$ is the worst case, which indicates that eigenvalues of \boldsymbol{K} satisfy the slowest decay. And $\gamma \in (0, 1)$ means that λ_i follows a polynomial decay, i.e., $\gamma := 1/2t$. By choosing $\lambda := n^{-\frac{1}{2r+\gamma}}$, we requires $\Omega(n^{\frac{1+\gamma(2r-1)}{2r+\gamma}} \log n)$ to achieve the convergence rate at $\mathcal{O}(n^{-\frac{2r}{2r+\gamma}})$. Table 3 present this result where we set $\gamma := 1/2t$ for better comparison.

The above two results consider the standard RFF setting, i.e., a data-independent sampling scheme. If $\{\boldsymbol{\omega}_i\}_{i=1}^s$ are sampled from a data-dependent distribution satisfying the compatibility condition in Assumption 6, we can obtain an improved result as demonstrated by Theorem 3 in [44]. It provides fast learning rates with fewer random features if they are somewhat *compatible* with the data distribution by the compatibility condition with $\varrho \in [0, 1]$. By choosing $\lambda := n^{-\frac{1}{2r+\gamma}}$, we requires $\Omega(n^{\frac{\varrho+(1+\gamma-\varrho)(2r-1)}{2r+\gamma}} \log n)$ to achieve the convergence rate at $\mathcal{O}(n^{-\frac{2r}{2r+\gamma}})$.

If the compatibility condition is substituted by a stronger one, i.e., the optimized distribution in Assumption 7, the current sharpest analysis is presented in [10] as follows.

Theorem 11. (Theorem 1 in [10]) *Suppose that the regularization parameter λ satisfies $0 \leq n\lambda \leq \lambda_1$, $\{\boldsymbol{\omega}_i\}_{i=1}^s \sim q(\boldsymbol{\omega})$, and Assumption 7 holds. If the number of random features satisfies*

$$s \geq 5d_{\boldsymbol{K}}^\lambda \log \left(16d_{\boldsymbol{K}}^\lambda / \delta \right),$$

then for $0 < \delta < 1$, with probability $1 - \delta$, the excess risk of $\widetilde{f_{\boldsymbol{z}, \lambda}}$ can be upper bounded as

$$\left\| \widetilde{f_{\boldsymbol{z}, \lambda}} - f_\rho \right\|_{L_2(\text{d}\rho)} \leq 2\lambda + \mathcal{O}(1/\sqrt{n}) + \mathcal{E}(f_{\boldsymbol{z}, \lambda}) - \mathcal{E}(f_\rho), \quad (29)$$

where $\mathcal{E}(f_{\boldsymbol{z}, \lambda}) - \mathcal{E}(f_\rho)$ is the excess risk for the standard kernel ridge regression estimator.

Table 3
Comparison of learning rates and required random features for expected risk with the squared loss function.

sampling scheme	Results	key assumptions	eigenvalue decays	λ	learning rates	required s
$\{\omega_i\}_{i=1}^s \sim p(\omega)$	Theorem 1 in [44]	-	-	$n^{-\frac{1}{2}}$	$\mathcal{O}_p\left(n^{-\frac{1}{2}}\right)$	$s \geq \Omega(\sqrt{n} \log n)$
	Theorem 2 in [44]	regularity condition	i^{-2t}	$n^{-\frac{2t}{1+4rt}}$	$\mathcal{O}_p\left(n^{-\frac{4rt}{1+4rt}}\right)$	$s \geq \Omega\left(\frac{2t+2r-1}{1+4rt} \log n\right)$
			$1/i$	$n^{-\frac{1}{2r+1}}$	$\mathcal{O}_p\left(n^{-\frac{2r}{2r+1}}\right)$	$s \geq \Omega\left(n^{\frac{2r}{2r+1}} \log n\right)$
	Theorem 3 in [10]	-	$e^{-\frac{1}{c}i}$	$n^{-\frac{1}{2}}$	$\mathcal{O}_p\left(n^{-\frac{1}{2}}\right)$	$s \geq \Omega(\sqrt{n} \log \log n)$
			i^{-2t}	$n^{-\frac{1}{2}}$	$\mathcal{O}_p\left(n^{-\frac{1}{2}}\right)$	$s \geq \Omega(\sqrt{n} \log n)$
	Theorem 3 in [44]	regularity condition; compatibility condition	i^{-2t}	$n^{-\frac{2t}{1+4rt}}$	$\mathcal{O}_q\left(n^{-\frac{4rt}{1+4rt}}\right)$	$s \geq \Omega\left(\frac{e+(2r-1)(2t+1-2te)}{1+4rt} \log n\right)$
$1/i$			$n^{-\frac{1}{2r+1}}$	$\mathcal{O}_q\left(n^{-\frac{2r}{2r+1}}\right)$	$s \geq \Omega\left(n^{\frac{2r}{2r+1}} \log n\right)$	
$e^{-\frac{1}{c}i}$			$n^{-\frac{1}{2}}$	$\mathcal{O}_q\left(n^{-\frac{1}{2}}\right)$	$s \geq \Omega(\log^2 n)$	
$\{\omega_i\}_{i=1}^s \sim q(\omega)$	Theorem 1 in [10]	optimized distribution	i^{-2t}	$n^{-\frac{1}{2}}$	$\mathcal{O}_q\left(n^{-\frac{1}{2}}\right)$	$s \geq \Omega(n^{1/(4t)} \log n)$
			$1/i$	$n^{-\frac{1}{2}}$	$\mathcal{O}_q\left(n^{-\frac{1}{2}}\right)$	$s \geq \Omega(\sqrt{n} \log n)$

Theorem 11 demonstrates that the lower bound of s is proportional to $d_K^\lambda \log d_K^\lambda$, which incurs no loss of expected risk in KRR for a minimax $\mathcal{O}(n^{-1/2})$ learning rate if we choose $\lambda := n^{-1/2}$. Accordingly, the corresponding learning rates with $\lambda \in \mathcal{O}(n^{-1/2})$ are given under three different eigenvalue decays, see in Table 3. It can be found that Theorem 11 in [10] improves the results of [44] under the exponential and polynomial decays. More specifically, if $\{\omega_i\}_{i=1}^s \sim p(\omega)$, the required s in Theorem 11 is proportional to $1/\lambda \log d_K^\lambda$. Accordingly, under the RFF setting, when the eigenvalues admit an exponential decay, Theorem 11 in [10] achieves the same $\mathcal{O}(n^{-1/2})$ learning rate, but only requires $\Omega(\sqrt{n} \log \log n)$ random features, which is an improvement compared to [44] with $\Omega(\sqrt{n} \log n)$ random features.

Besides, Carratino et al. [88] consider the result of [44] in KRR with an SGD solver. They show that, under the basic assumptions (e.g., Assumptions 1, 2, 3) and some mild conditions for batch size, step size, and the number of iterations in SGD, it requires $\Omega(\sqrt{n})$ random features to achieve the minimax $\mathcal{O}(n^{-1/2})$ learning rate, which is the same with the convergence rates of classical KRR [89]. Based on this, using the regularity condition in Assumption 8, the above results can be improved as: $\Omega\left(n^{\frac{1+\alpha(2r-1)}{2r+\alpha}}\right)$ random features are needed to ensure the $\mathcal{O}\left(n^{-\frac{2r}{2r+\alpha}}\right)$ learning rate.

In [90], assuming that the random feature mapping are bounded (which is weaker than Assumption 2), the out-of-sample bound is given by

$$\mathcal{E}(\widetilde{f_{z,\lambda}}) - \mathcal{E}(f_{z,\lambda}) \leq \mathcal{O}\left(\frac{1}{s\lambda}\right),$$

which indicates that $\Omega(n)$ random features are needed to ensure $\mathcal{O}(n^{-1/2})$ learning rates for out-of-sample bound (instead of the excess risk) if we choose $\lambda := n^{-1/2}$.

5.2.3 Lipschitz continuous loss function

In this section, the presented results assume that the loss function ℓ is Lipschitz continuous, e.g., the hinge loss in SVM and the cross-entropy loss in kernel logistic regression. Table 4 summarizes the derived learning rates and the required number of random

features under the *independent/dependent* settings. For the ease of simplicity, we briefly review the presented results but omit the detailed theorems.

If $\{\omega_i\}_{i=1}^s \sim p(\omega)$, i.e., under the standard RFF setting, we conclude as follows.

- In [20] (Theorem 1), the excess risk of $\widetilde{f_{z,\lambda}}$ in Eq. (2) converges at a certain $\mathcal{O}(n^{-1/2})$ learning rate with $\Omega(n \log n)$ random features.
- In [10] (Corollary 4), the required number of random features is decreased to $\Omega(1/\lambda \log d_K^\lambda)$ to attain $\mathcal{O}(n^{-1/2})$ convergence rate if we choose $\lambda \in \mathcal{O}(1/n)$. Note that d_K^λ can be bounded by different values under three eigenvalue decays. Accordingly, the excess risk of $\widetilde{f_{z,\lambda}}$ can be upper bounded by

$$\mathcal{E}(\widetilde{f_{z,\lambda}}) - \mathcal{E}(f_\rho) \leq \mathcal{O}(1/\sqrt{n}) + \mathcal{O}(\sqrt{\lambda}).$$

It can be found that, different from the learning rates with the squared loss in Eq. (29), the expected risk with the Lipschitz continuous loss functions can only be upper bounded by $\sqrt{\lambda}$. Hence, the regularization parameter λ is chosen by $\lambda \in \mathcal{O}(1/n)$ to preserve the convergence properties.

If $\{\omega_i\}_{i=1}^s \sim q(\omega)$, i.e., under the data-dependent sampling setting, the above results can be improved as follows.

- For SVM with random features, under the optimized distribution in Assumption 7 and the low noise condition in Assumption 9, Theorem 1 in [9] presents the learning rates and the required number of random features. Further, the results can be improved by Theorem 2 in [9] if we consider a stronger separation condition in Assumption 10. Details can be found in Table 4.
- In Section 4.5 in [43] or Corollary 3 in [10], if Assumption 7 holds, the excess risk of $\widetilde{f_{z,\lambda}}$ converges at a certain $\mathcal{O}(n^{-1/2})$ learning rate with $\Omega(d_K^\lambda \log d_K^\lambda)$ random features, if we choose $\lambda \in \mathcal{O}(1/n)$.

Table 4
Comparison of learning rates and required random features for expected risk with the Lipschitz continuous loss function.

sampling scheme	Results	key assumptions	eigenvalue decay	λ	learning rates	required s
$\{\omega_i\}_{i=1}^s \sim p(\omega)$	Theorem 1 in [20]	-	-	-	$\mathcal{O}_p\left(n^{-\frac{1}{2}}\right)$	$s \geq \Omega(n \log n)$
	Corollary 4 in [10]	-	$e^{-\frac{1}{c}i}$	$\frac{1}{n}$	$\mathcal{O}_p\left(n^{-\frac{1}{2}}\right)$	$s \geq \Omega(n \log \log n)$
			i^{-2t}	$\frac{1}{n}$	$\mathcal{O}_p\left(n^{-\frac{1}{2}}\right)$	$s \geq \Omega(n \log n)$
			$1/i$	$\frac{1}{n}$	$\mathcal{O}_p\left(n^{-\frac{1}{2}}\right)$	$s \geq \Omega(n \log n)$
$\{\omega_i\}_{i=1}^s \sim q(\omega)$	Theorem 1 in [9]	low noise condition	$e^{-\frac{1}{c}i}$	$\frac{1}{n}$	$\mathcal{O}_q\left(\frac{1}{n} \log^{c+2} n\right)$	$s \geq \Omega(\log^c n \log \log^c n)$
		optimized distribution	i^{-2t}	$n^{-\frac{t}{1+t}}$	$\mathcal{O}_q\left(n^{-\frac{t}{1+t}} \log n\right)$	$s \geq \Omega(n^{\frac{1}{1+t}} \log n)$
	Theorem 2 in [9]	separation condition optimized distribution	$1/i$	$\frac{1}{n}$	$\mathcal{O}_q\left(n^{-\frac{1}{2}}\right)$	$s \geq \Omega(n \log n)$
			$e^{-\frac{1}{c}i}$	n^{-2c^2}	$\mathcal{O}_q\left(\frac{1}{n} \log^{2c+1} n \log \log n\right)$	$s \geq \Omega(\log^{2c} n \log \log n)$
			$e^{-\frac{1}{c}i}$	$\frac{1}{n}$	$\mathcal{O}_q\left(n^{-\frac{1}{2}}\right)$	$s \geq \Omega(\log^2 n)$
			Section 4.5 in [43]; Corollary 3 in [10]	optimized distribution	i^{-2t}	$\frac{1}{n}$
$1/i$	$\frac{1}{n}$	$\mathcal{O}_q\left(n^{-\frac{1}{2}}\right)$	$s \geq \Omega(n \log n)$			

5.3 Results for nonlinear component analysis

Apart from classification and regression with random features in algorithm and theory, the results on supervised learning can be extended to unsupervised learning, e.g., randomized nonlinear component analysis. Here we give an overview on them.

In [12], the kernel matrix in kernel Principal Component Analysis (KPCA) and kernel Canonical Correlation Analysis (KCCA) is approximated by random features, and then it converges to the true kernel matrix in operator norm at a rate of $\mathcal{O}(n\sqrt{\log n/s})$. To be specific, it requires $s := \mathcal{O}((\log n)^2/\epsilon^2)$ to obtain $\|\tilde{\mathbf{K}} - \mathbf{K}\|_2 \leq \epsilon n$ with the probability $1 - 1/n$. This algorithm takes $\mathcal{O}(ns^2 + nsd)$ time complexity to construct feature functions and $\mathcal{O}(s^2 + sd)$ space to store the feature functions and covariance matrix. Further, Ghashami et al. [91] combine random features with matrix sketching for KPCA with the top- ℓ principal components, and accordingly improve the time and space complexity to $\mathcal{O}(nsd + n\ell s)$ and $\mathcal{O}(sd + \ell s)$, respectively. Besides, Xie et al. [11] leverage the doubly stochastic gradients scheme to accelerate KPCA. In [92], the authors investigate the statistical consistency of empirical risk minimization with random features. They show that the top- ℓ eigenspace of the empirical covariance matrix in \mathcal{H} converges to the covariance operator in \mathcal{H} at the rate of $\mathcal{O}(1/\sqrt{n} + 1/\sqrt{s})$. The above methods in essence require $s \geq \Omega(n)$ random features to guarantee a $\mathcal{O}(1/\sqrt{n})$ generalization bound. Instead, Ullah et al. [86] pose KPCA as a stochastic optimization problem and demonstrate that the empirical risk minimizer (ERM) in the random feature space converges in objective as $\mathcal{O}(1/\sqrt{n})$ with $\Omega(\ell\sqrt{n} \log n)$ random features.

6 EXPERIMENTS

In this section, we empirically evaluate the behavior of representative random features on both kernel approximation and prediction for classification on several benchmark datasets. All experiments are implemented in MATLAB and carried out on a PC with Intel[®] i7-8700K CPU (3.70 GHz) and 64 GB RAM.

Table 5
Dataset statistics.

datasets	d	#traing	#test	random split	scaling
<i>ijcnn1</i>	22	49,990	91,701	no	-
<i>EEG</i>	14	7,490	7,490	yes	mapstd
<i>cod-RNA</i>	8	59,535	157,413	no	mapstd
<i>covtype</i>	54	290,506	290,506	yes	minmax
<i>magic04</i>	10	9,510	9,510	yes	minmax
<i>letter</i>	16	12,000	6,000	no	minmax
<i>skin</i>	3	122,529	122,529	yes	minmax
<i>a8a</i>	123	22,696	9,865	no	minmax
<i>mushrooms</i>	112	4062	4062	yes	-
<i>spambase</i>	57	2301	2301	yes	minmax
<i>wilt</i>	5	4399	500	no	minmax
<i>wine-quality</i>	12	3249	3248	yes	mapstd
<i>MNIST</i>	784	60,000	10,000	no	minmax
<i>CIFAR-10</i>	3072	50,000	10,000	no	-

6.1 Experimental settings

We choose the popular Gaussian kernel and the first-order arccosine kernel for experiments, where the kernel width σ in the Gaussian kernel is tuned by five-fold cross validation over a grid of $\{0.01, 0.1, 1, 10\}$. For the subsequent classification task, the random features mappings are embedded with two classifiers, one is the ridge linear regression (short for lr) with the squared loss, and the other is the liblinear [93] (a linear classifier with the hinge loss). The regularization parameter λ in ridge linear regression and the balance parameter in liblinear are tuned via 5-fold inner cross validation on a grid of $\{10^{-8}, 10^{-6}, 10^{-4}, 10^{-3}, 10^{-2}, 0.05, 0.1, 0.5, 1, 5, 10\}$ and $\{0.01, 0.1, 1, 10, 100\}$, respectively. The random features dimension s in our experiments is set to $\{s = 2d, 4d, 8d, 16d, 32d\}$. The used evaluation metric for kernel approximation is error = $\|\mathbf{K} - \tilde{\mathbf{K}}\|_F / \|\mathbf{K}\|_F$. A small error indicates a high approximation quality. We randomly sample 1,000 data points to construct the sub-feature matrix and sub-kernel matrix to compute the approximation error. All experiments are repeated 10 times and

we report the approximation error, average classification accuracy with its deviation as well as the time cost for generating random features.

We evaluate ten representative random features based algorithms on twelve non-image benchmark datasets and two image datasets. Table 5 gives an overview of these datasets including the number of feature dimension, training samples, test data, training/test split, and the normalization scheme. These twelve non-image datasets can be downloaded from <https://www.csie.ntu.edu.tw/~cjlin/libsvmtools/datasets/> or the UCI Machine Learning Repository³. Some datasets have beforehand prepared the given training/test partitions, denoted as “no” in random split. For the remaining datasets, we randomly pick half of the data for training and the rest for testing, termed as “yes” in random split. There are two typical normalization schemes, one is the “mapstd” strategy and the other is “minmax”. The “mapstd” scheme sets each sample’s means to 0 and deviations to 1; while the “minmax” scheme is a standard min and max scaling operation mapped to $[0, 1]^d$. Besides, two representative image datasets are also used for comparison, one is the *MNIST* handwritten digits database [94] and the other is the *CIFAR-10* natural image classification dataset [95], see the last two rows in Table 5. The *MNIST* handwritten digits dataset (from 0 to 9) contains 60,000 training samples and 10,000 test samples, of which each sample is a 28×28 gray-scale image. Here the “minmax” normalization scheme means that the data are directly divided by 255. The *CIFAR10* dataset consists of 60,000 color images with the size of $32 \times 32 \times 3$ in 10 categories (50,000 in training and 10,000 in test).

The compared algorithms include RFF [8], ORF [29], SORF [29], ROM [56], Fastfood [24], SCRf [28], QMC [25], SSF [32], GQ [33], and LS-RFF [10], which covers data-dependent/independent algorithms, Monte Carlo based sampling/QMC/quadrature rules, variance reduction and computational savings by structural/circulant information. In the next, we will present the results of various algorithms on these datasets for the Gaussian kernel and the first-order arc-cosine kernel approximation. Accordingly, we think that experiments under this setting is able to provide a comprehensive comparison of these random features based algorithms.

6.2 Results for the Gaussian Kernel

6.2.1 Classification results on non-image benchmark datasets

Figures 6, 10, and 11 show the approximation error for the Gaussian kernel, the time cost of generating random features mappings, the test accuracy yielded by linear regression and liblinear on these twelve datasets, respectively. For the ease of better presentation, we put Figure 10 and 11 in Appendix A. From the result, as the number of random features increases, almost all algorithms achieve smaller approximation error and higher classification accuracy in such two classifiers. However, there are some abnormal phenomena in low-dimensional (i.e., $s = 2d, 4d$) and high dimensional (i.e., $s = 16d, 32d$), the relations between approximation quality and prediction performance in various algorithms. For example, i) a kernel approximation algorithm cannot always perform better than other approaches. That means, the performing best algorithms are often different in the low-dimensional case and the high dimensional case. ii) various

algorithms achieve different approximation quality, but often obtain the similar prediction performance. To this end, we summarize the best algorithm on each dataset in terms of the approximation quality and classification accuracy in Table 6.

Table 6 presents the best algorithm on each dataset given in two cases: low dimensional (i.e., $s = 2d, s = 4d$) and high dimensional (i.e., $s = 16d, 32d$) according to approximation quality, test accuracy in linear regression or liblinear. The notation “-” means that there is no *statistical significance* between the best algorithms. That is to say, some approaches achieve the similar best approximation quality or prediction performance. Regarding to approximation error, we find that SSF often achieves the best approximation quality in the low-dimensional case on most datasets, while ORF often performs better than other algorithms in the high-dimensional case. This is because, SSF aims to generate asymptotically uniformly distributed points on the sphere \mathcal{S}^{d-1} . It would exhibit the marginal effect, that is, the few sampled data points over \mathcal{S}^{d-1} might be adequate. The increasing sampled data points (i.e., the increase of s) would not result in much variance reduction as the initial ones. So the approximation error of SSF sometimes stays almost unchanged with a large number of random features, which is verified in the *skin*, *spambase*, *wilt*, *magic04* and *ijcnn1* datasets. Instead, the variance formulation of ORF in Eq. (12) theoretically demonstrates that ORF requires a high dimensional feature mapping to achieve a significant variance reduction. The numerical results on these datasets show this consistency with theoretical findings. Actually, random features for the Gaussian kernel is to find a finite-dimensional (embedding) Hilbert space to approximate the original infinite-dimensional RKHS for the preservation of inner product. In this view, both SSF and ORF admit a similar target, i.e., generating random features as independent/completed as possible. This way attempts to use fewer random features that conveys more rich information.

Regarding to prediction performance, there is no distinct difference between most algorithms using lr or liblinear classifiers. That means, a higher kernel approximation quality cannot translate to (or fully define) better classification performance. Instead, some methods, e.g., Fastfood, perform inferior to other algorithms on kernel approximation, but achieve higher classification accuracy. This inconsistency between approximation quality and generalization performance is still an open problem, which has been discussed in [34], [36], [42]. The reason may be that the target of kernel approximation and prediction is different. To be specific, kernel approximation aims to seek for the preservation of inner product between two Hilbert spaces, i.e., $\langle k(\mathbf{x}, \cdot), k(\mathbf{x}', \cdot) \rangle_{\mathcal{H}} \approx \langle \tilde{k}(\mathbf{x}, \cdot), \tilde{k}(\mathbf{x}', \cdot) \rangle_{\tilde{\mathcal{H}}}$. For prediction, we take the least squares as an example, the excess error of $\widetilde{f_{z,\lambda}}$ is bounded by

$$\mathcal{E}(\widetilde{f_{z,\lambda}}) - \mathcal{E}(f_{\rho}) \leq [\mathcal{E}(f_{z,\lambda}) - \mathcal{E}(f_{\rho})] + [\mathcal{E}(\widetilde{f_{z,\lambda}}) - \mathcal{E}(f_{z,\lambda})],$$

where the notations are $\widetilde{f_{z,\lambda}} = \sum_{i=1}^n \widetilde{\alpha}_i \tilde{k}(\mathbf{x}, \cdot) \in \tilde{\mathcal{H}}$ and $f_{z,\lambda} = \sum_{i=1}^n \alpha_i k(\mathbf{x}, \cdot) \in \mathcal{H}$ by their respective representer theorems in RKHSs. The first term in the right hand is the excess error of KRR, which has been investigated before in a series of approximation analysis literature [85], [96], [97]. The second term in the right hand denotes the expected error difference between the original KRR and its random features approximation version. However, the above inner-product preserving operation cannot guarantee $\mathcal{E}(\widetilde{f_{z,\lambda}}) - \mathcal{E}(f_{z,\lambda})$ is small. Actually, there is no distinct relations

3. <https://archive.ics.uci.edu/ml/datasets.html>.

Table 6

Results statistics on twelve classification datasets. The best algorithm on each dataset is given in two cases: low dimensional (i.e., $s = 2d, 4d$) and high dimensional (i.e., $s = 16d, 32d$) according to approximation quality, test accuracy in linear regression or liblinear. The notation “-” means there is no *statistical significance* between most algorithms.

datasets	approximation		lr		liblinear	
	low dim.	high dim.	low dim.	high dim.	low dim.	high dim.
<i>ijcnn1</i>	SSF	SORF/QMC/ORF	QMC	Fastfood	Fastfood	-
<i>EEG</i>	SSF	ORF	-	-	-	-
<i>cod-RNA</i>	SSF	-	-	-	-	-
<i>covtype</i>	54	290,506	290,506	yes	minmax	-
<i>magic04</i>	SSF	SSF/ORF/QMC/ROM	-	-	-	-
<i>letter</i>	SSF	SSF/ORF	-	-	-	-
<i>skin</i>	SSF/ROM	QMC	-	-	-	-
<i>a8a</i>	-	-	SSF	-	SSF	-
<i>mushrooms</i>	-	-	Fastfood	-	fastfood	-
<i>spambase</i>	ORF	ORF	-	-	-	-
<i>wilt</i>	SSF,ROM	ORF	-	SSF	-	-
<i>wine-quality</i>	SSF	SORF/QMC/ORF	-	-	-	-

between these two targets. In most cases, the approximated kernel is not optimal for prediction.

In terms of time cost for generating the random features mapping, some acceleration algorithms using structural/circulant information, e.g., Fastfood, SSF, SORF, ROM, SCRF donot prohibit computational savings in the experiments, which appears contradictory to theoretical findings. This is because, in the implementation, directly sampling $W_{ij} \sim \mathcal{N}(0, \sigma^{-2})$ in RFF is not a time-consuming operation, which is even more efficient than generating a series of Hadamard matrices, the Walsh matrices, and the Rademacher matrices.

6.2.2 Classification results on image datasets

Here we conduct various random features based algorithms except SCRF⁴ on the *MNIST* database [94] and the *CIFAR10* dataset [95] for kernel approximation, and then are equipped with liblinear for classification. In our experiment, we choose the Gaussian kernel for evaluation and its kernel width σ is tuned by 5-fold cross validation on a grid of points, i.e., $\sigma = [0.01, 0.1, 1, 10, 100]$. For the *MNIST* database, we directly use the original 784-dimensional feature as the data; while for better performance on the *CIFAR10* dataset, we use VGG16 with batch normalization [98] pre-trained on ImageNet [99] as a feature extractor. We fine-tune this model on the *CIFAR10* dataset with 240 epochs and a min-batch size 64. The learning rate begins from 0.1 and then is divided by 10 at the 120-th, 160-th, and 200-th epoch. Then, for each color image, a 4096 dimensional feature vector is obtained from the output of the first fully-connected layer in this fine-tuned neural network.

Figure 7(a) shows the tendency of the approximation error, the time cost, and the classification accuracy by liblinear across a range of $s = 1000, 2000, 3000, 4000, 5000$ on the *MNIST* database. We find that ORF yields the best approximation quality. Nevertheless, similar to results on non-image datasets, most algorithms still achieve small approximation error and but no distinct difference on the test accuracy. Such similar results are also displayed on the *CIFAR10* dataset with $s = 5000, 6000, 7000, 8000, 9000$ in Figure 7(b).

6.3 Results for the Arc-cosine Kernel

this section presents a comparison of several algorithms including RFF [8], QMC [25], SSF [32], ROM [56], SSR [34] for the first-order arc-cosine kernel. Note that, several algorithms, e.g., ORF, SORF, and Fastfood, are infeasible to arc-cosine kernels due to the rotation-invariant but shift-variant property of arc-cosine kernels, but the Monte Carlo sampling (i.e., RFF) is still valid.

Figure 8 shows the results of the above five random features based algorithms on four representative datasets including *ijcnn1*, *letter*, *EEG*, and *cod-RNA*. It can be observed that, as s increases, SSF always provides lower approximation error than other approaches, especially when using low dimensional random features. When the number of random features increases to $s = 32d$, SSF, SSR, and QMC achieve similar approximation performance on the *letter*, *cod-RNA* datasets. Generally, we find that approximation performance and time cost of various algorithms on the arc-cosine kernel are similar to that of the Gaussian kernel approximation, but the absolute approximation error is often larger than that of the Gaussian kernel. In terms of classification accuracy, RFF achieves the similar generalization performance with SSR and SSF on the *ijcnn1*, *letter*, and *EEG* datasets. But on the *cod-RNA* dataset, ROM performs significantly better than RFF when using lower dimensional random features. Nevertheless, most algorithms achieve slightly difference on the test accuracy under different approximation quality.

7 TRENDS: RANDOM FEATURES IN DNNs

Aforementioned, we throughout review random features based algorithms and their corresponding theoretical results. It can be found that these approaches are simple in formulation but effective in real-world large problems. More importantly, they prohibit nice theoretical guarantee in kernel approximation and generalization properties. Recently, analysis of over-parameterized neural networks is a popular topic in deep learning theory due to some “abnormal” phenomena, e.g., a good fitness of random labels, strong generalization performance of overfitted classifiers [13] and double curve descent [14], [100]. In particular, Belkin et al. [14], [101] point out that the above phenomena not only

4. It requires s to be exponential order of d in their implementation.

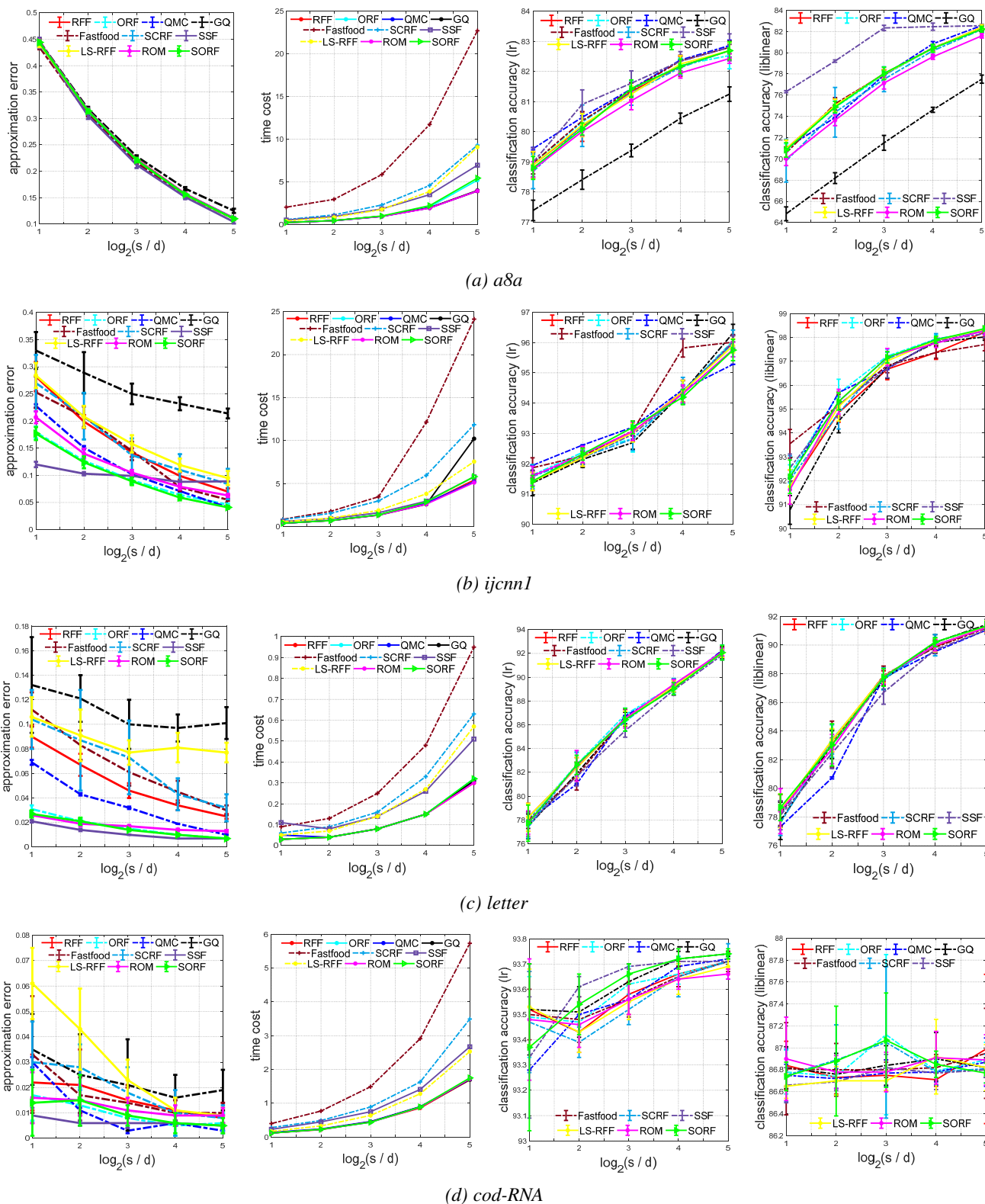


Figure 6. Results of various algorithms for the Gaussian kernel on the *a8a*, *ijcnn1*, *letter*, *cod-RNA* datasets.

are unique to deep networks but also exists in kernel methods. In Figure 9, we report the empirical training error, the test error, and the kernel approximation error of random features regression with $\lambda = 10^{-8}$ as a function of s/n on the *sonar* dataset and the MNIST dataset. For n , d , s only in hundreds, we can still

observe that, as s increases, the training error can reduce to zero, the approximation error monotonously decreases, and the double curve descent phenomenon for the test error exists.

Accordingly, the elegant theory in kernel methods/random features motivates us to extend their results to neural networks

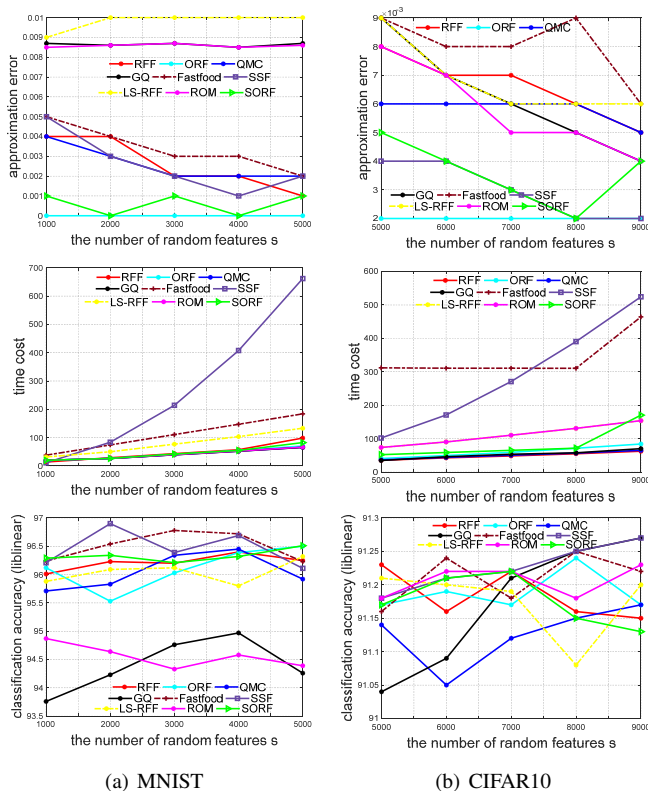


Figure 7. Approximation error, time cost, and test accuracy of random features based algorithms in liblinear on two image classification datasets.

in the over-parameterized regime. We think that it would be a promising research direction for random features and here we give an overview on this topic. In this section, we briefly review the relations between random features and DNNs in Section 7.1, give an overview of its usage for double curve descent and NTK in Section 7.2, and point out the gap between random features and DNNs in Section 7.3.

7.1 Relations between Random Features and DNNs

There is a vast literature showing insightful connections between kernel methods and over-parameterized neural networks, see below.

$$\left\{ \begin{array}{l} \text{weakly trained nets} \\ \text{fully-trained nets: NTK [15], CNTK [19]} \end{array} \right\} \left\{ \begin{array}{l} \text{Gaussian process: [102], [103]} \\ \text{Random features model: [19], [104]} \end{array} \right.$$

The connection is originally pointed out in [102], i.e., a single-layer fully-connected neural network with i.i.d. random parameters is equivalent to a Gaussian process in the infinite-width limit. This equivalence between infinitely wide deep networks with multi-layer and Gaussian process is further explored in [103]. Besides, Daniely et al. [104], [105] demonstrate that, under some conditions, SGD of over-parameterized neural networks is guaranteed to learn any function in the kernel space, which corresponds to the random features model. Note that these correspond to infinitely wide deep nets, of which all parameters are chosen randomly/fixed in a proper scheme, and only the last (classification) layer is optimized, termed as *weakly-trained nets* [19]. These weakly-trained nets with finite or infinite width also define some interesting kernels. If the parameters are well initialized (usually Gaussian), training

the output (classification) layer with the ℓ_2 loss can be equivalent to kernel regression. Further, if we extend these weakly-trained nets to fully-trained nets of which all parameters are trained by gradient descent, they can be still equivalent to a kernel regression predictor with a deterministic kernel called neural tangent kernel (NTK) [15]. If weakly-trained nets use fully-connected layers, they can be regarded as a multi-layer random features model. Similarly, the fully-trained nets with convolutional layers correspond to convolutional neural tangent kernel (CNTK) [19].

Random features in kernel methods (e.g., KRR) can be viewed as linear regression in RKHS, so they can also be interpreted as two-layer weakly-trained nets, i.e., the weights $\{\omega_i\}_{i=1}^s$ in the first layer are chosen randomly/fixed and we just optimize the output layer. As such, two layer neural networks in weakly-trained/fully-trained schemes are far more amenable to theoretical analysis than arbitrary deep networks. The function class of a standard two neural networks (with s neurons, just for the same notation with random features) is defined by [106]

$$\mathcal{F}_{\text{NN},s} = \left\{ f(\mathbf{x}) = c + \sum_{i=1}^s a_i \varphi(\langle \omega_i, \mathbf{x} \rangle) : c, a_i \in \mathbb{R}, \omega_i \in \mathbb{R}^d \right\},$$

where $\varphi(\cdot)$ is the active function, a_i is the weight, and c is the bias term. Jacot et al. [15] point out for highly over-parameterized networks, the network weights barely change from their random initialization. Accordingly, the nonlinear function class $\mathcal{F}_{\text{NN},s}$ can be substituted by its first order Taylor expansion around this initialization, i.e., the lazy regime. That is

$$\mathcal{F}_{\text{NN},s} \approx f_{\text{NN},0}(\mathbf{x}) + \mathcal{F}_{\text{RF},s}(\mathbf{W}) + \mathcal{F}_{\text{NTK},s}(\mathbf{W}),$$

with

$$\mathcal{F}_{\text{RF},s}(\mathbf{W}) = \left\{ f_s(\mathbf{x}) = \sum_{i=1}^s a_i \sigma(\langle \omega_i, \mathbf{x} \rangle) : a_i \in \mathbb{R} \right\},$$

$$\mathcal{F}_{\text{NTK},s}(\mathbf{W}) = \left\{ f_s(\mathbf{x}) = c + \sum_{i=1}^s \sigma'(\langle \omega_i, \mathbf{x} \rangle) \langle \mathbf{a}_i, \mathbf{x} \rangle : \mathbf{a}_i \in \mathbb{R}^d \right\}.$$

Here $\mathcal{F}_{\text{RF},s}(\mathbf{W})$ is referred as the “random features” (RF) model: the first layer is randomly chosen or fixed, and only the second layer is optimized. And $\mathcal{F}_{\text{NTK},s}(\mathbf{W})$ corresponds to the first order Taylor expansion of f_{NN} respect to the first layer weights. Both $\mathcal{F}_{\text{RF},s}(\mathbf{W})$ and $\mathcal{F}_{\text{NTK},s}(\mathbf{W})$ are finite-dimensional linear spaces, and minimizing the empirical risk over these classes can be performed efficiently. More importantly, in a certain over-parameterized regime, $\mathcal{F}_{\text{NN},s}$ with gradient descent will converge to a model in $\mathcal{F}_{\text{RF},s}(\mathbf{W}) \oplus \mathcal{F}_{\text{NTK},s}(\mathbf{W})$.

Albeit simple, the random features model is appealing in deep learning theory with the following aspects. First, it can be regarded as a two-layer weakly-trained neural network, closely relates to the lazy regime of neural networks, and thus allows to freely disentangle the feature dimension d from the number of parameters s . Second, the randomness of the fixed first layer weights mimics the randomness due to weight initialization in neural networks. Last and most importantly, the strong generalization performance of overfitted classifiers and the double descent phenomenology can be observed on random features models, which provides a justification to analysis them due to the solid theoretical foundations of random features.

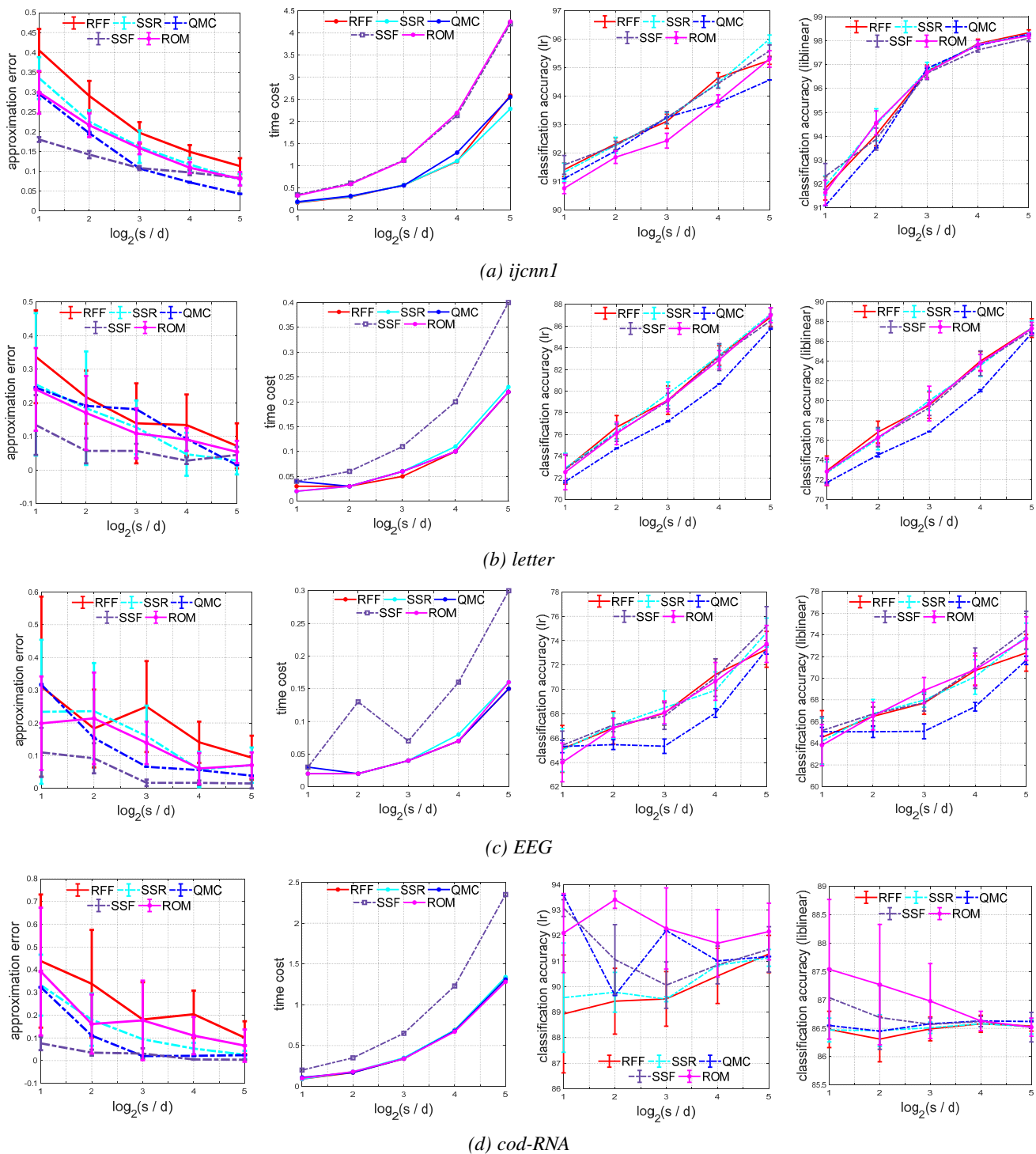


Figure 8. Results of various algorithms for the first-order arc-cosine kernel approximation on the *a8a*, *icnn1*, *letter*, *cod-RNA* datasets.

7.2 Analysis of DNNs by Random Features

Here we give an overview on the usage of random features for analysis of over-parameterized neural networks in the following two aspects.

7.2.1 Random features in double descent

The double descent risk curve [14] is summarized as , i) the training risk monotonically decreases; ii) the test risk first decreases with the model complexity then increases in the under-parameterized regime. Once the model complexity passes a certain threshold, the test risk

decreases in turn over the over-parameterized regime. It is a robust phenomenon in a variety of tasks, architectures, and optimization methods, e.g., random features models, ResNet18 [107], standard 5-layer CNN, and transformers [108] as verified by [14]. Actually, the double descent curve is not a simple phenomenon, e.g., the bias and variance show different tendency in over-parameterized regime [109], it is only a function of model size but also a function of the number of epochs [14], and some models even exhibit multiple-descent shape [110].

The random features model, a weakly-trained two-layer net,

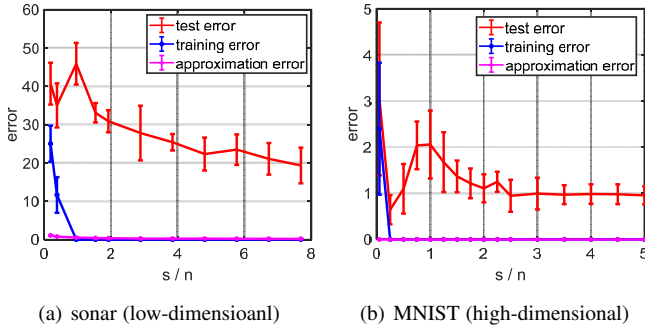


Figure 9. Training error, test error, and approximation error of random features regression with $\lambda = 10^{-8}$ on the *sonar* dataset with $n = 208, d = 60$ and the sub-set of MNIST (class 1 versus class 2) with $n = 200, d = 784$.

admits the double descent phenomenon with theoretical guarantees. Belkin et al. [111] provide a precise analysis for an one-dimensional version of the random features model to explain the double descent phenomenon. Furthermore, Hastie et al. [112] utilize random matrix theory [113], [114], [115], a powerful mathematical tool to study learning problems with $d, n \rightarrow \infty$ and a constant order of n/d , to analysis the risk of ridge regression and minimum norm least-squares regression with random features. They show that, as $n, d, s \rightarrow \infty$ with $s/n \rightarrow \psi_1 \in (0, \infty)$, the limiting variance increases for $\psi_2 \in (0, 1)$, decreases for $\psi_1 \in (1, \infty)$, and diverges with $\psi_1 \rightarrow 1$, confirming the double descent phenomenology. Similarly, in [116], [117], the authors also theoretically validate that the prediction error decreases monotonically with the number of random features in the over-parameterized regime. In [116], the authors consider the random features regression model with a ReLU activation over a sphere, and demonstrate that both bias and variance have a peak at the interpolation threshold $s = n$, diverging there when $\lambda \rightarrow 0$. The above analysis of the random features model with the squared loss is extended to max-margin classifier with random features [117]. Specifically, they show that in the over-parameterized regime, gradient descent with cross-entropy loss converges to the max-margin classifier. Further, a fine-grained analysis of the random features model is provided in [118] to disentangle quantitatively the contributions to the test error: the bias, various sources of variance of estimator, the sampling of the dataset, the additive noise corrupting the labels, and the initialization. The above analysis in random features can be regarded as the first step to further analysis double descent in deep neural networks.

7.2.2 Random features in NTK

The relationship between random features model and the NTK model is not limited to $\mathcal{F}_{\text{NN},s} \approx \mathcal{F}_{\text{RF},s}(\mathbf{W}) \oplus \mathcal{F}_{\text{NTK},s}(\mathbf{W})$ in a certain over-parameterized regime. Actually, random features are used to compute the exact NTK [15] and CNTK [19] in practical attempts due to their infinite limits. Accordingly, recent papers [19], [119] consider a direct way to understand their properties, i.e., using random features as the approximation of the infinite limit kernel. However, empirical evidence [19] indicate that the prediction performance significantly degrades if random features generated from practically sized nets are used. This might be because good approximation cannot guarantee promising prediction performance as we discuss this before. In theoretical aspect, Cao and Gu [18] theoretically point out that the expected 0-1 loss of a wide enough ReLU network with random initialization and SGD

training can be bounded by the training loss of a random features model induced by the network gradient at initialization.

7.3 Discussion: Gap between Random Features and DNNs

Random features models have been fully investigated to analysis the double descent phenomenon. However, these certain models appears non-trivial to be directly transferred to neural networks. The theoretical gap between random features and DNNs still exists. For example, Ghorbani et al. [106] point out, in the random features regression model, under the setting of $n \rightarrow \infty$, if $s = \Omega(d^{\ell+1-\delta})$, then the random features model can only fit the projection of the target function f_d onto degree- ℓ polynomials. More importantly, if the training data $\{\mathbf{x}_i\}_{i=1}^n$ are uniformly distributed over the d -dimensional sphere, and s, d are large with $s = \Omega(d)$, then the functional space associated with $\mathcal{F}_{\text{RF},s}(\mathbf{W})$ can only capture linear functions; while $\mathcal{F}_{\text{NTK},s}(\mathbf{W})$ can only capture quadratic functions. In particular, Yehudai and Shamir [120] show that the random features model cannot efficiently approximate a single ReLU neuron as it requires the number of random features to be an exponential order of the feature dimension d . Actually, under the under-parameterized regime for classical kernel approximation tasks, the random features model requires $s = \Omega(\exp(d))$ to achieve the ϵ approximation error. This claim is suitable to QMC and quadrature based methods as well, i.e., they require s to be exponential in d . Further, Ghorbani et al. [121] throughout prove that both $\mathcal{F}_{\text{RF},s}(\mathbf{W})$ and $\mathcal{F}_{\text{NTK},s}(\mathbf{W})$ have limited approximation power in the lazy training scheme, but significant gain can be achieved by full training.

Admittedly, the above claims on random features for analysis of DNNs appears to be pessimistic. However, the universality of random features still holds [122]. To be specific, the RKHSs induced by a broad class of random features are dense in the space of continuous functions, and thus random features have the capability of strong approximation. Regarding to exponential number of required random features, it does not imply that the random features model fails to grasp the properties of DNNs. This is because, in practical model neural networks, the number of parameters (or neurons) and the number of training data are much larger than the feature dimension d . Hence we can consider the case with $n, s \rightarrow \infty$ while d is finite. We think that this condition is still acceptable or even more reasonable than the case of $n, s, d \rightarrow \infty$. In this case, random matrix theory seems to fail to analysis this situation due to the finite rank of the transformation matrix \mathbf{W} . Actually, if we take a step back, the random features model is still effective to analysis DNNs for pruning. For example, the best paper [123] on *the seventh International Conference on Learning Representations (ICLR2019)* states that a deep neural network with random initialization contains a small sub-network such that, when trained in isolation, the sub-network is able to compete with the performance of the original one. This is termed as *the Lottery Ticket Hypothesis*. Malach et al. [17] provide a stronger claim that a randomly-initialized and sufficiently over-parameterized neural network contains a sub-network with nearly the same accuracy as the original one, without any further training. In their analysis, they demonstrate the equivalence between random features and the neuron-subnetwork model. It means that pruning entire neurons is equivalent to the well known random features model, which validates the feasibility of random features in DNNs. Besides, random features can be also used in two layer network with the

hidden manifold model [124] and Graph Neural Networks (GNNs) [16], which enables GNNs to learn almost optimal polynomial time approximation algorithms in terms of the approximation ratios.

8 CONCLUSION

In this survey, we throughout review random features based algorithms and theoretical results. More importantly, we also give an overview on the relations between random features and DNNs, study the usage of random features in DNNs, and discuss the limitations of random features for neural networks theory. There are still some statements that we need to clarify, and some open problems that could be addressed in the future.

- Experiments show that better kernel approximation cannot translate to lower generalization errors. This is an interesting future issue in theory that deserves further detailed study. Current theoretical results on error bounds of eigenvalues [75], [125] may be not sufficient to explain this phenomenon.
- Kernel learning via the spectral density is a popular direction [60], [62] and it can naturally combined with Generative Adversarial Networks (GANs), see [58] for details. By this scheme, the learned kernel can be associated with an implicit probability density that would be flexible to depict the data-relationships or data-similarities. More work needs to be done in this interesting area.
- The double descent phenomenon cannot be found in any model but always exists in random features models, see a counterexample of two-layer neural networks in [126]. Accordingly, random features provide a justification to theoretically analysis the double descent phenomenon. Current results based on [116] could be extended to data-free distribution for a general analysis. More importantly, a series of work [100], [109] point out that the risk in the double descent is not just a function of s , but also relates to the number of epochs. The bias and variance show different tendencies, and so it needs more further findings and analysis.
- Indeed, there exists gap between the random features model and over-parameterized neural network models. Some empirical evidence [19] indicate that, in NTK and CNTK model, the prediction performance significantly degrades if random features generated from practically sized nets are used. Admittedly, NTK can achieve a zero error with a finite number of neurons while the RF model cannot. However, the comparison between the random features model and the NTK is unfair as NTK has much more parameters to learn than RF.
- In the standard setting, random features, QMC, and quadrature based rules, they often require $s = \Omega(\exp(d))$ to achieve the ϵ approximation error. In over-parameterized regime, random features still follow with this claim but it appears unacceptable as claimed by [120]. Random features with the exponential order $\mathcal{O}(e^d)$ for approximation needs to be carefully considered and investigated.
- Random features models can be still useful to study DNNs, e.g., the equivalence between the RF model and weight pruning in the Lottery Ticket Hypothesis [17] and GNNs [16]. This is a promising direction that deserves further study.

We elaborate the above open problems that need to be carefully considered and we believe that this survey will help readers to gain a thorough understanding of random features.

APPENDIX A

CLASSIFICATION RESULTS FOR THE GAUSSIAN KERNEL

Here we present the compared random features based algorithms on the approximation error for the Gaussian kernel, the time cost, the test accuracy yielded by linear regression and liblinear on the remaining eight classification datasets, see Figure 10 and 11.

REFERENCES

- [1] Bernhard Schölkopf and Alexander J Smola, *Learning with kernels: support vector machines, regularization, optimization, and beyond*, MIT Press, 2003.
- [2] Johan A.K. Suykens, Tony Van Gestel, Jos De Brabanter, Bart De Moor, and Joos Vandewalle, *Least Squares Support Vector Machines*, World Scientific, 2002.
- [3] Mehran Kafai and Kave Eshghi, “CROification: accurate kernel classification with the efficiency of sparse linear SVM,” *IEEE Transactions on Pattern Analysis and Machine Intelligence*, vol. 41, no. 1, pp. 34–48, 2019.
- [4] Ji Zhu and Trevor Hastie, “Kernel logistic regression and the import vector machine,” *Journal of Computational and Graphical Statistics*, vol. 14, no. 1, pp. 185–205, 2002.
- [5] Harris Drucker, Christopher JC Burges, Linda Kaufman, Alex J Smola, and Vladimir Vapnik, “Support vector regression machines,” in *Proceedings of Advances in Neural Information Processing Systems*, 1997, pp. 155–161.
- [6] Sebastian Mika, Bernhard Schölkopf, Alex J Smola, Klaus-Robert Müller, Matthias Scholz, and Gunnar Rätsch, “Kernel PCA and de-noising in feature spaces,” in *Proceedings of Advances in Neural Information Processing Systems*, 1999, pp. 536–542.
- [7] Inderjit S Dhillon, Yuqiang Guan, and Brian Kulis, “Kernel k-means: spectral clustering and normalized cuts,” in *Proceedings of ACM SIGKDD international conference on Knowledge discovery and data mining*. ACM, 2004, pp. 551–556.
- [8] Ali Rahimi and Benjamin Recht, “Random features for large-scale kernel machines,” in *Proceedings of Advances in Neural Information Processing Systems*, 2007, pp. 1177–1184.
- [9] Yitong Sun, Anna Gilbert, and Ambuj Tewari, “But how does it work in theory? Linear SVM with random features,” in *Proceedings of Advances in Neural Information Processing Systems*, 2018, pp. 3383–3392.
- [10] Zhu Li, Jean-Francois Ton, Dino Oglie, and Dino Sejdinovic, “Towards a unified analysis of random Fourier features,” in *Proceedings of the 36th International Conference on Machine Learning*, 2019, pp. 3905–3914.
- [11] Bo Xie, Yingyu Liang, and Le Song, “Scale up nonlinear component analysis with doubly stochastic gradients,” in *Proceedings of Advances in Neural Information Processing Systems*, 2015, pp. 2341–2349.
- [12] David Lopez-Paz, Suvrit Sra, Alex Smola, Zoubin Ghahramani, and Bernhard Schölkopf, “Randomized nonlinear component analysis,” in *Proceedings of the International Conference on Machine Learning*, 2014, pp. 1359–1367.
- [13] Chiyuan Zhang, Samy Bengio, Moritz Hardt, Benjamin Recht, and Oriol Vinyals, “Understanding deep learning requires rethinking generalization,” *arXiv preprint arXiv:1611.03530*, 2016.
- [14] Mikhail Belkin, Daniel Hsu, Siyuan Ma, and Soumik Mandal, “Reconciling modern machine-learning practice and the classical bias-variance trade-off,” *Proceedings of the National Academy of Sciences*, vol. 116, no. 32, pp. 15849–15854, 2019.
- [15] Arthur Jacot, Franck Gabriel, and Clément Hongler, “Neural tangent kernel: Convergence and generalization in neural networks,” in *Advances in neural information processing systems*, 2018, pp. 8571–8580.
- [16] Ryoma Sato, Makoto Yamada, and Hisashi Kashima, “Random features strengthen graph neural networks,” *arXiv preprint arXiv:2002.03155*, 2020.
- [17] Eran Malach, Gilad Yehudai, Shai Shalev-Shwartz, and Ohad Shamir, “Proving the lottery ticket hypothesis: Pruning is all you need,” *arXiv preprint arXiv:2002.00585*, 2020.

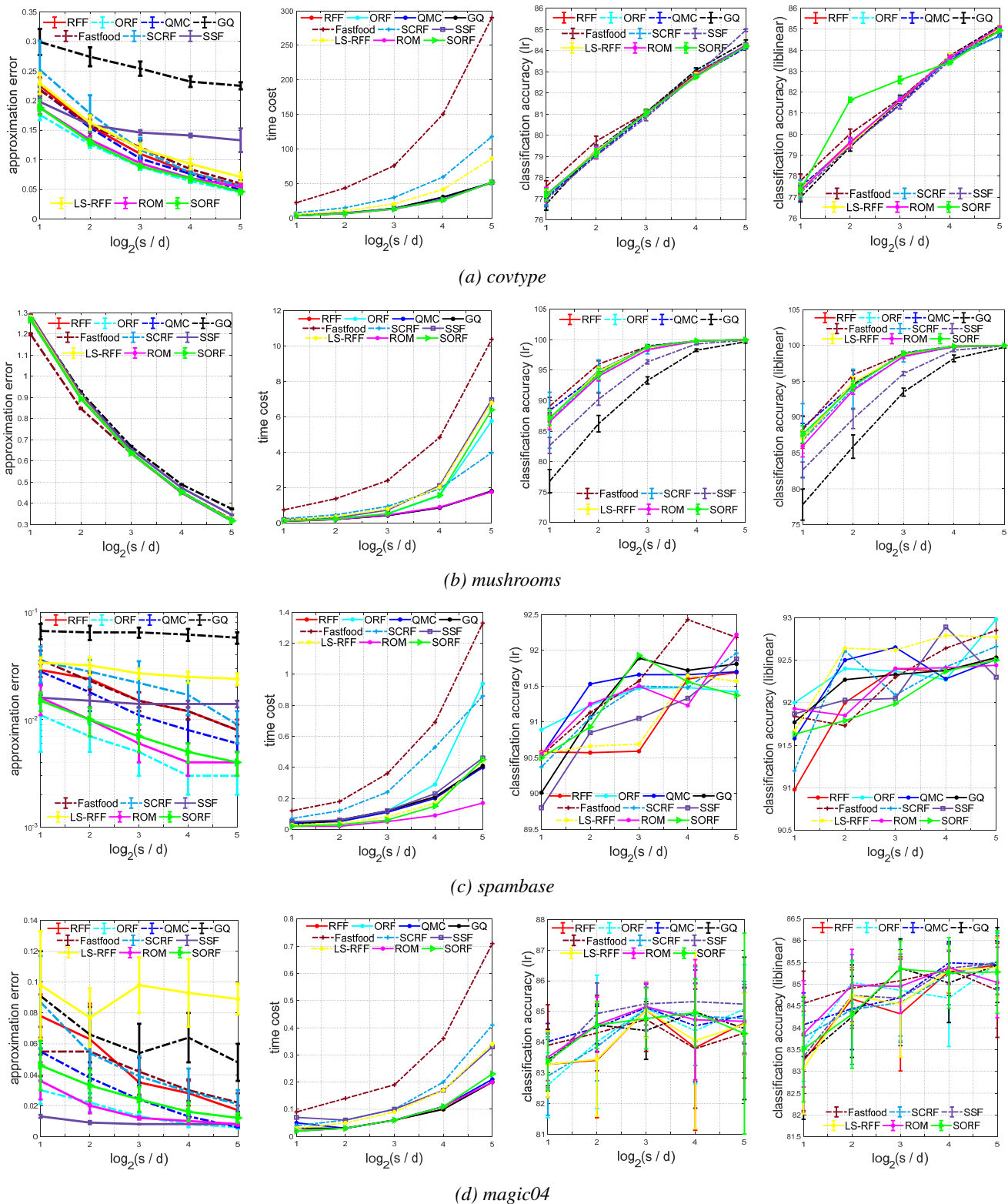


Figure 10. Results of various algorithms for the Gaussian kernel on the *covtype*, *mushrooms*, *spambase*, *magic04* datasets.

- [18] Yuan Cao and Quanquan Gu, “Generalization bounds of stochastic gradient descent for wide and deep neural networks,” in *Proceedings of Advances in Neural Information Processing Systems*, 2019, pp. 10835–10845.
- [19] Sanjeev Arora, Simon S Du, Wei Hu, Zhiyuan Li, Russ R Salakhutdinov, and Ruosong Wang, “On exact computation with an infinitely wide neural net,” in *Proceedings of Advances in Neural Information Processing Systems*, 2019, pp. 8139–8148.
- [20] Ali Rahimi and Benjamin Recht, “Weighted sums of random kitchen sinks: Replacing minimization with randomization in learning,” in *Proceedings of Advances in neural information processing systems*, 2009, pp. 1313–1320.
- [21] Fuxin Li, Catalin Ionescu, and Cristian Sminchisescu, “Random fourier approximations for skewed multiplicative histogram kernels,” in *Proceedings of Joint Pattern Recognition Symposium*. Springer, 2010, pp. 262–271.

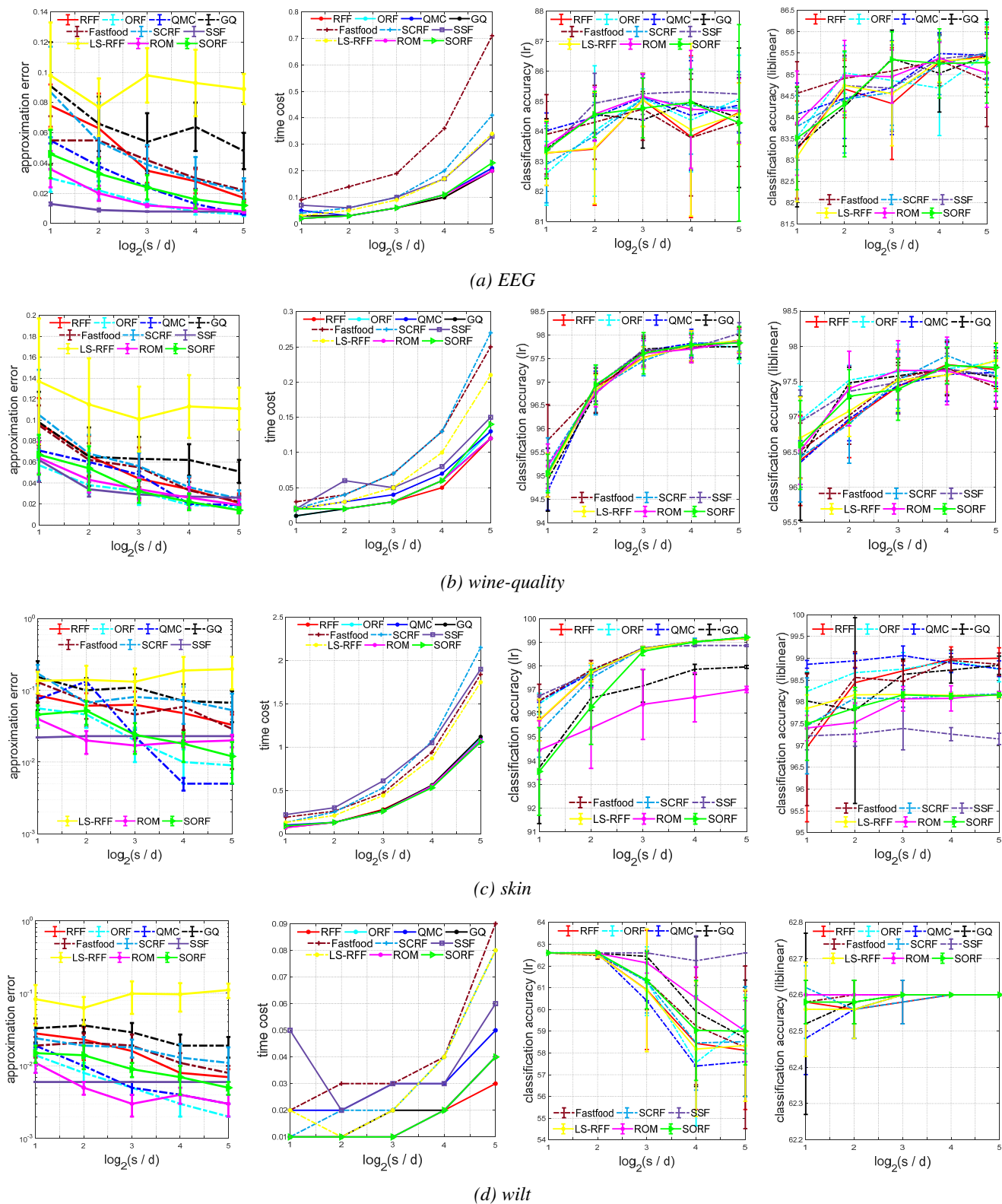


Figure 11. Results of various algorithms for the Gaussian kernel on the *EEG*, *wine-quality*, *skin*, *wilt* datasets.

- [22] Purushottam Kar and Harish Karnick, “Random feature maps for dot product kernels,” in *Proceedings of the International Conference on Artificial Intelligence and Statistics*, 2012, pp. 583–591.
- [23] Andrea Vedaldi and Andrew Zisserman, “Efficient additive kernels via explicit feature maps,” *IEEE Transactions on Pattern Analysis and Machine Intelligence*, vol. 34, no. 3, pp. 480–492, 2012.
- [24] Quoc Le, Tamás Székely, and Alex Smola, “FastFood-approximating kernel expansions in loglinear time,” in *Proceedings of the International Conference on Machine Learning*, 2013, pp. 1–9.
- [25] Jiyan Yang, Vikas Sindhwani, Haim Avron, and Michael Mahoney, “Quasi-Monte Carlo feature maps for shift-invariant kernels,” in *Proceedings of the International Conference on Machine Learning*, 2014, pp. 485–493.
- [26] Bo Dai, Bo Xie, Niao He, Yingyu Liang, Anant Raj, Maria-Florina F

- Balkan, and Le Song, “Scalable kernel methods via doubly stochastic gradients,” in *Proceedings of Advances in Neural Information Processing Systems*, 2014, pp. 3041–3049.
- [27] Jeffrey Pennington, Felix Xinnan X. Yu, and Sanjiv Kumar, “Spherical random features for polynomial kernels,” in *Proceedings of Advances in Neural Information Processing Systems*, 2015, pp. 1846–1854.
- [28] Chang Feng, Qinghua Hu, and Shizhong Liao, “Random feature mapping with signed circulant matrix projection,” in *Proceedings of the Twenty-Fourth International Joint Conference on Artificial Intelligence*, 2015.
- [29] Felix Xinnan Yu, Ananda Theertha Suresh, Krzysztof Choromanski, Daniel Holtmannrice, and Sanjiv Kumar, “Orthogonal random features,” in *Proceedings of Advances in Neural Information Processing Systems*, 2016, pp. 1975–1983.
- [30] Krzysztof Choromanski and Vikas Sindhwani, “Recycling randomness with sublinear time kernel expansions,” in *Proceedings of International Conference on Machine Learning*, 2016, pp. 2502–2510.
- [31] Weiwei Shen, Zhihui Yang, and Jun Wang, “Random features for shift-invariant kernels with moment matching,” in *Proceedings of the Thirty-First AAAI Conference on Artificial Intelligence*, 2017.
- [32] Yueming Lyu, “Spherical structured feature maps for kernel approximation,” in *Proceedings of the 34th International Conference on Machine Learning*. JMLR. org, 2017, pp. 2256–2264.
- [33] Tri Dao, Christopher M De Sa, and Christopher Ré, “Gaussian quadrature for kernel features,” in *Proceedings of Advances in neural information processing systems*, 2017, pp. 6107–6117.
- [34] Marina Munkhoeva, Yermek Kapushev, Evgeny Burnaev, and Ivan Oseledets, “Quadrature-based features for kernel approximation,” in *Proceedings of Advances in Neural Information Processing Systems*, 2018, pp. 9165–9174.
- [35] Shahin Shahrampour, Ahmad Beirami, and Vahid Tarokh, “On data-dependent random features for improved generalization in supervised learning,” in *Proceedings of Thirty-Second AAAI Conference on Artificial Intelligence*, 2018, pp. 4026–4033.
- [36] Jian Zhang, Avner May, Tri Dao, and Christopher Re, “Low-precision random Fourier features for memory-constrained kernel approximation,” in *Proceedings of the 22nd International Conference on Artificial Intelligence and Statistics*, 2019, pp. 1264–1274.
- [37] Raj Agrawal, Trevor Campbell, Jonathan Huggins, and Tamara Broderick, “Data-dependent compression of random features for large-scale kernel approximation,” in *Proceedings of the 22nd International Conference on Artificial Intelligence and Statistics*, 2019, pp. 1822–1831.
- [38] Fanghui Liu, Xiaolin Huang, Yudong Chen, Jie Yang, and Johan A.K. Suykens, “Random fourier features via fast surrogate leverage weighted sampling,” in *Proceedings of Thirty-Fourth AAAI Conference on Artificial Intelligence*, 2020.
- [39] Dougal J Sutherland and Jeff Schneider, “On the error of random Fourier features,” in *Proceedings of the Thirty-First Conference on Uncertainty in Artificial Intelligence*, 2015, pp. 862–871.
- [40] Bharath K. Sriperumbudur and Zoltán Szabó, “Optimal rates for random Fourier features,” in *Proceedings of Advances in Neural Information Processing Systems*, 2015, pp. 1144–1152.
- [41] Jean Honorio and Yu-Jun Li, “The error probability of random fourier features is dimensionality independent,” *arXiv preprint arXiv:1710.09953*, 2017.
- [42] Haim Avron, Michael Kapralov, Cameron Musco, Christopher Musco, Ameya Velingker, and Amir Zandieh, “Random Fourier features for kernel ridge regression: Approximation bounds and statistical guarantees,” in *Proceedings of the 34th International Conference on Machine Learning-Volume 70*, 2017, pp. 253–262.
- [43] Francis Bach, “On the equivalence between kernel quadrature rules and random feature expansions,” *Journal of Machine Learning Research*, vol. 18, no. 1, pp. 714–751, 2017.
- [44] Alessandro Rudi and Lorenzo Rosasco, “Generalization properties of learning with random features,” in *Proceedings of Advances in Neural Information Processing Systems*, 2017, pp. 3215–3225.
- [45] Haim Avron, Vikas Sindhwani, Jiyan Yang, and Michael W. Mahoney, “Quasi-Monte Carlo feature maps for shift-invariant kernels,” *Journal of Machine Learning Research*, vol. 17, no. 1, pp. 4096–4133, 2016.
- [46] Aman Sinha and John C Duchi, “Learning kernels with random features,” in *Proceedings of Advances in Neural Information Processing Systems*, pp. 1298–1306, 2016.
- [47] Youngmin Cho and Lawrence K Saul, “Kernel methods for deep learning,” in *Advances in Neural Information Processing Systems*, 2009, pp. 342–350.
- [48] Subhransu Maji, Alexander C Berg, and Jitendra Malik, “Efficient classification for additive kernel SVMs,” *IEEE Transactions on Pattern Analysis and Machine Intelligence*, vol. 35, no. 1, pp. 66–77, 2013.
- [49] Fanghui Liu, Xiaolin Huang, Lei Shi, Jie Yang, and Johan A.K. Suykens, “A double-variational bayesian framework in random fourier features for indefinite kernels,” *IEEE Transactions on Neural Networks and Learning Systems*, 2019.
- [50] Salomon Bochner, *Harmonic Analysis and the Theory of Probability*, Courier Corporation, 2005.
- [51] Marc G Genton, “Classes of kernels for machine learning: a statistics perspective,” *Journal of machine learning research*, vol. 2, no. Dec, pp. 299–312, 2001.
- [52] Sami Remes, Markus Heinonen, and Samuel Kaski, “Non-stationary spectral kernels,” in *Proceedings of Advances in Neural Information Processing Systems*, 2017, pp. 4645–4654.
- [53] Brian Bullins, Cyril Zhang, and Yi Zhang, “Not-so-random features,” in *Proceedings of International Conference on Learning Representations*, 2018.
- [54] IJ Schoenberg et al., “Positive definite functions on spheres,” *Duke Mathematical Journal*, vol. 9, no. 1, pp. 96–108, 1942.
- [55] Ping Li, “Linearized GMM kernels and normalized random fourier features,” in *Proceedings of the 23rd ACM SIGKDD International Conference on Knowledge Discovery and Data Mining*, 2017, pp. 315–324.
- [56] Krzysztof M Choromanski, Mark Rowland, and Adrian Weller, “The unreasonable effectiveness of structured random orthogonal embeddings,” in *Proceedings of Advances in Neural Information Processing Systems*, 2017, pp. 219–228.
- [57] Wei-Cheng Chang, Chun-Liang Li, Yiming Yang, and Barnabás Póczos, “Data-driven random Fourier features using Stein effect,” in *Proceedings of the 26th International Joint Conference on Artificial Intelligence*, 2017, pp. 1497–1503.
- [58] Chun-Liang Li, Wei-Cheng Chang, Youssef Mroueh, Yiming Yang, and Barnabas Poczos, “Implicit kernel learning,” in *Proceedings of the 22nd International Conference on Artificial Intelligence and Statistics*, 2019, pp. 2007–2016.
- [59] Felix X. Yu, Sanjiv Kumar, Henry Rowley, and Shih Fu Chang, “Compact nonlinear maps and circulant extensions,” *arXiv preprint arXiv:1503.03893*, 2015.
- [60] Andrew Gordon Wilson and Ryan Prescott Adams, “Gaussian process kernels for pattern discovery and extrapolation,” in *Proceedings of the International Conference on Machine Learning*, 2013, pp. 1067–1075.
- [61] Zichao Yang, Andrew Wilson, Alex Smola, and Le Song, “À la carte-learning fast kernels,” in *Proceedings of Artificial Intelligence and Statistics*, 2015, pp. 1098–1106.
- [62] Zheyang Shen, Markus Heinonen, Samuel Kaski, et al., “Harmonizable mixture kernels with variational fourier features,” in *Proceedings of International Conference on Artificial Intelligence and Statistics*. PMLR, 2019.
- [63] Junier B Oliva, Avinava Dubey, Andrew G Wilson, Barnabás Póczos, Jeff Schneider, and Eric P Xing, “Bayesian nonparametric kernel learning,” in *Proceedings of the International Conference on Artificial Intelligence and Statistics*, 2016, pp. 1078–1086.
- [64] Mariusz Bojarski, Anna Choromanska, Krzysztof Choromanski, Francois Fagan, Cedric Gouy-Pailler, Anne Morvan, Nouri Sakr, Tamas Sarlos, and Jamal Atif, “Structured adaptive and random spinners for fast machine learning computations,” in *Proceedings of Artificial Intelligence and Statistics*, 2017, pp. 1020–1029.
- [65] Tianbao Yang, Yu Feng Li, Mehrdad Mahdavi, Rong Jin, and Zhi Hua Zhou, “Nyström method vs random Fourier features: a theoretical and empirical comparison,” in *Proceedings of Advances in Neural Information Processing Systems*, 2012, pp. 476–484.
- [66] Xiang Li, Bin Gu, Shuang Ao, Huaimin Wang, and Charles X Ling, “Triply stochastic gradients on multiple kernel learning,” in *Proceedings of the Conference on Uncertainty in Artificial Intelligence*, 2017, pp. 1–9.
- [67] Krzysztof Choromanski, Mark Rowland, Wenyu Chen, and Adrian Weller, “Unifying orthogonal Monte Carlo methods,” in *Proceedings of International Conference on Machine Learning*, 2019, pp. 1203–1212.
- [68] Krzysztof Choromanski, Mark Rowland, Tamás Sarlós, Vikas Sindhwani, Richard Turner, and Adrian Weller, “The geometry of random features,” in *Proceedings of International Conference on Artificial Intelligence and Statistics*, 2018, pp. 1–9.
- [69] Harald Niederreiter, *Random number generation and quasi-Monte Carlo methods*, vol. 63, SIAM, 1992.
- [70] Johann S Brauchart and Peter J Grabner, “Distributing many points on spheres: minimal energy and designs,” *Journal of Complexity*, vol. 31, no. 3, pp. 293–326, 2015.
- [71] Gwynne Evans, *Practical numerical integration*, Wiley New York, 1993.

- [72] Alan Genz and John Monahan, “Stochastic integration rules for infinite regions,” *SIAM Journal on Scientific Computing*, vol. 19, no. 2, pp. 426–439, 1998.
- [73] Florian Heiss and Viktor Wünschel, “Likelihood approximation by numerical integration on sparse grids,” *Journal of Econometrics*, vol. 144, no. 1, pp. 62–80, 2008.
- [74] Yinsong Wang and Shahin Shahrampour, “A general scoring rule for randomized kernel approximation with application to canonical correlation analysis,” *arXiv preprint arXiv:1910.05384*, 2019.
- [75] Francis Bach, “Sharp analysis of low-rank kernel matrix approximations,” in *Proceedings of Conference on Learning Theory*, 2013, pp. 185–209.
- [76] Corinna Cortes, Mehryar Mohri, and Afshin Rostamizadeh, “Two-stage learning kernel algorithms,” in *Proceedings of the International Conference on Machine Learning*, 2010, pp. 239–246.
- [77] Trevor Campbell and Tamara Broderick, “Bayesian coresets construction via greedy iterative geodesic ascent,” in *Proceedings of International Conference on Machine Learning*, 2018, pp. 698–706.
- [78] Trevor Campbell and Tamara Broderick, “Automated scalable bayesian inference via hilbert coresets,” *The Journal of Machine Learning Research*, vol. 20, no. 1, pp. 551–588, 2019.
- [79] Raffay Hamid, Ying Xiao, Alex Gittens, and Dennis Decoste, “Compact random feature maps,” in *Proceedings of the International Conference on Machine Learning*, 2014, pp. 19–27.
- [80] Jean-Francois Ton, Seth Flaxman, Dino Sejdinovic, and Samir Bhatt, “Spatial mapping with gaussian processes and nonstationary fourier features,” *Spatial statistics*, vol. 28, pp. 59–78, 2018.
- [81] Ninh Pham and Rasmus Pagh, “Fast and scalable polynomial kernels via explicit feature maps,” in *Proceedings of ACM International Conference on Knowledge Discovery and Data Mining*, 2013, pp. 239–247.
- [82] Kilian Weinberger, Anirban Dasgupta, John Langford, Alex Smola, and Josh Attenberg, “Feature hashing for large scale multitask learning,” in *Proceedings of the 26th International Conference on Machine Learning*, 2009, pp. 1113–1120.
- [83] Subhransu Maji and Alexander C Berg, “Max-margin additive classifiers for detection,” in *Proceedings of IEEE International Conference on Computer Vision*. IEEE, 2009, pp. 40–47.
- [84] Ali Rahimi and Benjamin Recht, “Uniform approximation of functions with random bases,” in *Proceedings of the Annual Allerton Conference on Communication, Control, and Computing*. IEEE, 2008, pp. 555–561.
- [85] Ingo Steinwart and Christmann Andreas, *Support Vector Machines*. Springer Science and Business Media, 2008.
- [86] Enayat Ullah, Poorya Mianjy, Teodor Vanislavov Marinov, and Raman Arora, “Streaming kernel PCA with $\tilde{O}(\sqrt{n})$ random features,” in *Proceedings of Advances in Neural Information Processing Systems*, 2018, pp. 7311–7321.
- [87] Vladimir Koltchinskii, *Oracle Inequalities in Empirical Risk Minimization and Sparse Recovery Problems*, vol. 2033, Springer Science & Business Media, 2011.
- [88] Luigi Carratino, Alessandro Rudi, and Lorenzo Rosasco, “Learning with SGD and random features,” in *Proceedings of Advances in Neural Information Processing Systems*, 2018, pp. 10212–10223.
- [89] Ingo Steinwart and Clint Scovel, “Fast rates for support vector machines using Gaussian kernels,” *Annals of Statistics*, vol. 35, no. 2, pp. 575–607, 2007.
- [90] Shusen Wang, “Simple and almost assumption-free out-of-sample bound for random feature mapping,” *arXiv preprint arXiv:1909.11207*, 2019.
- [91] Mina Ghashami, Daniel J Perry, and Jeff Phillips, “Streaming kernel principal component analysis,” in *Proceedings of Artificial intelligence and statistics*, 2016, pp. 1365–1374.
- [92] Bharath Sriperumbudur and Nicholas Sterge, “Statistical consistency of kernel PCA with random features,” *arXiv preprint arXiv:1706.06296*, 2017.
- [93] Rong-En Fan, Kai-Wei Chang, Cho-Jui Hsieh, Xiang-Rui Wang, and Chih-Jen Lin, “LIBLINEAR: a library for large linear classification,” *Journal of Machine Learning Research*, vol. 9, pp. 1871–1874, 2008.
- [94] Yann Lecun, Leon Bottou, Yoshua Bengio, and Patrick Haffner, “Gradient-based learning applied to document recognition,” *Proceedings of the IEEE*, vol. 86, no. 11, pp. 2278–2324, 1998.
- [95] Alex Krizhevsky and Geoffrey Hinton, “Learning multiple layers of features from tiny images,” *Technical report, University of Toronto*, 2009.
- [96] Felipe Cucker and Steve Smale, “On the mathematical foundations of learning,” *Bulletin of the American mathematical society*, vol. 39, no. 1, pp. 1–49, 2002.
- [97] Cheng Wang and Dingxuan Zhou, “Optimal learning rates for least squares regularized regression with unbounded sampling,” *Journal of Complexity*, vol. 27, no. 1, pp. 55–67, 2011.
- [98] Sergey Ioffe and Christian Szegedy, “Batch normalization: accelerating deep network training by reducing internal covariate shift,” in *Proceedings of the International Conference on Machine Learning*, 2015, pp. 448–456.
- [99] Jia Deng, Wei Dong, Richard Socher, Li Jia Li, Kai Li, and Fei Fei Li, “Imagenet: A large-scale hierarchical image database,” in *Proceedings of the IEEE Conference on Computer Vision and Pattern Recognition*, 2009, pp. 248–255.
- [100] Preetum Nakkiran, Gal Kaplun, Yamini Bansal, Tristan Yang, Boaz Barak, and Ilya Sutskever, “Deep double descent: Where bigger models and more data hurt,” in *Proceedings of International Conference on Learning Representations*, 2019.
- [101] Mikhail Belkin, Siyuan Ma, and Soumik Mandal, “To understand deep learning we need to understand kernel learning,” in *Proceedings of International Conference on Machine Learning*, 2018, pp. 541–549.
- [102] Christopher KI Williams, “Computing with infinite networks,” in *Proceedings of Advances in Neural Information Processing Systems*, 1997, pp. 295–301.
- [103] Jaehoon Lee, Yasaman Bahri, Roman Novak, Samuel S Schoenholz, Jeffrey Pennington, and Jascha Sohl-Dickstein, “Deep neural networks as Gaussian Processes,” in *Proceedings of International Conference on Learning Representations*, 2018.
- [104] Amit Daniely, “SGD learns the conjugate kernel class of the network,” in *Proceedings of Advances in Neural Information Processing Systems*, 2017, pp. 2422–2430.
- [105] Amit Daniely, Roy Frostig, and Yoram Singer, “Toward deeper understanding of neural networks: The power of initialization and a dual view on expressivity,” in *Proceedings of Advances In Neural Information Processing Systems*, 2016, pp. 2253–2261.
- [106] Behrooz Ghorbani, Song Mei, Theodor Misiakiewicz, and Andrea Montanari, “Linearized two-layers neural networks in high dimension,” *arXiv preprint arXiv:1904.12191*, 2019.
- [107] Kaiming He, Xiangyu Zhang, Shaoqing Ren, and Jian Sun, “Identity mappings in deep residual networks,” in *Proceedings of European conference on computer vision*. Springer, 2016, pp. 630–645.
- [108] Ashish Vaswani, Noam Shazeer, Niki Parmar, Jakob Uszkoreit, Llion Jones, Aidan N Gomez, Lukasz Kaiser, and Illia Polosukhin, “Attention is all you need,” in *Proceedings of Advances in Neural Information Processing Systems*, 2017, pp. 5998–6008.
- [109] Zitong Yang, Yaodong Yu, Chong You, Jacob Steinhardt, and Yi Ma, “Rethinking bias-variance trade-off for generalization of neural networks,” *arXiv preprint arXiv:2002.11328*, 2020.
- [110] Tengyuan Liang, Alexander Rakhlin, and Xiyu Zhai, “On the risk of minimum-norm interpolants and restricted lower isometry of kernels,” *arXiv preprint arXiv:1908.10292*, 2019.
- [111] Mikhail Belkin, Daniel Hsu, and Ji Xu, “Two models of double descent for weak features,” *arXiv preprint arXiv:1903.07571*, 2019.
- [112] Trevor Hastie, Andrea Montanari, Saharon Rosset, and Ryan J Tibshirani, “Surprises in high-dimensional ridgeless least squares interpolation,” *arXiv preprint arXiv:1903.08560*, 2019.
- [113] Terence Tao, *Topics in random matrix theory*, 2012.
- [114] Cosme Louart, Zhenyu Liao, Romain Couillet, et al., “A random matrix approach to neural networks,” *The Annals of Applied Probability*, vol. 28, no. 2, pp. 1190–1248, 2018.
- [115] Zhenyu Liao and Romain Couillet, “On the spectrum of random features maps of high dimensional data,” in *Proceedings of the International Conference on Machine Learning*, 2018, pp. 3063–3071.
- [116] Song Mei and Andrea Montanari, “The generalization error of random features regression: Precise asymptotics and double descent curve,” *arXiv preprint arXiv:1908.05355*, 2019.
- [117] Andrea Montanari, Feng Ruan, Youngtak Sohn, and Jun Yan, “The generalization error of max-margin linear classifiers: High-dimensional asymptotics in the overparametrized regime,” *arXiv preprint arXiv:1911.01544*, 2019.
- [118] Stéphane d’Ascoli, Maria Refinetti, Giulio Biroli, and Florent Krzakala, “Double trouble in double descent: Bias and variance (s) in the lazy regime,” *arXiv preprint arXiv:2003.01054*, 2020.
- [119] Jaehoon Lee, Lechao Xiao, Samuel Schoenholz, Yasaman Bahri, Roman Novak, Jascha Sohl-Dickstein, and Jeffrey Pennington, “Wide neural networks of any depth evolve as linear models under gradient descent,” in *Proceedings of Advances in Neural Information Processing Systems*, 2019, pp. 8570–8581.
- [120] Gilad Yehudai and Ohad Shamir, “On the power and limitations of random features for understanding neural networks,” in *Proceedings of Advances in Neural Information Processing Systems*, 2019, pp. 6594–6604.

- [121] Behrooz Ghorbani, Song Mei, Theodor Misiakiewicz, and Andrea Montanari, “Limitations of lazy training of two-layers neural network,” in *Proceedings of Advances in Neural Information Processing Systems*, 2019, pp. 9108–9118.
- [122] Yitong Sun, Anna Gilbert, and Ambuj Tewari, “On the approximation properties of random ReLU features,” *arXiv preprint arXiv:1810.04374*, 2018.
- [123] Jonathan Frankle and Michael Carbin, “The lottery ticket hypothesis: Finding sparse, trainable neural networks,” 2019.
- [124] Federica Gerace, Bruno Loureiro, Florent Krzakala, Marc Mézard, and Lenka Zdeborová, “Generalisation error in learning with random features and the hidden manifold model,” *arXiv preprint arXiv:2002.09339*, 2020.
- [125] Mikio L Braun, “Accurate error bounds for the eigenvalues of the kernel matrix,” *Journal of Machine Learning Research*, vol. 7, no. Nov, pp. 2303–2328, 2006.
- [126] Jimmy Ba, Murat A Erdogdu, Taiji Suzuki, Denny Wu, and Tianzong Zhang, “Generalization of two-layer neural networks: an asymptotic viewpoint,” pp. 1–8, 2020.